AD-A120 340 UNITED TECHNOLOGIES RESEARCH CENTER EAST HARTFORD CT F/G 13/10
TWO-PHASE NOZZLE THEORY AND PARAMETRIC ANALYSIS. PHASE II. OFF--ETC(U)
OCT 82 C W OEANE, S C KUO N00014-79-C-0344
UNCLASSIFIED UTRC/R82-955744-4 NL

[redacted]

[redacted]

Phase II – Off-Design Performance Analysis

Final Annual Technical Report
October 1982

[redacted]
[redacted], Principal Investigator

[redacted]

SECURITY CLASSIFICATION OF THIS PAGE (When Data Entered)

REPORT DOCUMENTATION PAGE

READ INSTRUCTIONS BEFORE COMPLETING FORM

1. REPORT NUMBER: UTRC R82-955744-4	2. GOVT ACCESSION NO.: AD-A120 340
3. RECIPIENT'S CATALOG NUMBER:	
4. TITLE (and Subtitle): Two-Phase Nozzle Theory and Parametric Analysis (Phase III - Off-Design Performance Analysis)	5. TYPE OF REPORT & PERIOD COVERED: Final Annual Technical Report July 15, 1981-Sept 30, 1982
	6. PERFORMING ORG. REPORT NUMBER: UTRC R82-955744-4
7. AUTHOR(s): Charles W. Deane Simion C. Kuo, Principal Investigator	8. CONTRACT OR GRANT NUMBER(s): N00014-79-C-0344 Modification No. P00006
9. PERFORMING ORGANIZATION NAME AND ADDRESS: United Technologies Research Center Silver Lane, East Hartford, CT 06108	10. PROGRAM ELEMENT, PROJECT, TASK AREA & WORK UNIT NUMBERS: Program Element: 61153N Project: RRO 24-03 Task Area: RRO 24-03-02 Work Unit: NR 097-411
11. CONTROLLING OFFICE NAME AND ADDRESS: Office of Naval Research 800 North Quincy Street Arlington, VA 22217	12. REPORT DATE: October 1982 13. NUMBER OF PAGES:
14. MONITORING AGENCY NAME & ADDRESS(if different from Controlling Office):	15. SECURITY CLASS. (of this report): Unclassified 15a. DECLASSIFICATION/DOWNGRADING SCHEDULE

16. DISTRIBUTION STATEMENT (of this Report)

Approved for public release; Distribution unlimited

17. DISTRIBUTION STATEMENT (of the abstract entered in Block 20, if different from Report)

Same as block 16

18. SUPPLEMENTARY NOTES

19. KEY WORDS (Continue on reverse side if necessary and identify by block number)

Two-Phase Nozzle
Two-Phase Engine
Off-Design Nozzle Performance
Droplet Heat Transfer

20. ABSTRACT (Continue on reverse side if necessary and identify by block number)

The off-design performance characteristics of two-phase nozzles were investigated and the impact of heat transfer enhancement between the liquid droplets and the suspending gas on the nozzle performance were examined. The problems associated with the integration of two-phase nozzles with the potential heat sources were reviewed. An experimental program formulated to verify the predicted two-phase performance is outlined.

DD FORM 1 JAN 73 1473 EDITION OF 1 NOV 65 IS OBSOLETE
S/N 0102-LF-014-6601

UNCLASSIFIED
SECURITY CLASSIFICATION OF THIS PAGE (When Data Entered)

Typical two-phase nozzle performance maps are presented to show the off-design total mass flow rate and the nozzle efficiency, as a function of loading ratio, inlet pressure and temperature, and exit pressure. The effects of droplet size and secondary injection of hot liquid as well as the effect of using an exponential instead of a linear axial pressure profile on the nozzle performance are discussed. The effects of droplet size and local gas velocity on the level of flow disturbance (shock) in a two-phase nozzle flow are also examined.

R82-955744-4

Two-Phase Nozzle Theory and Parametric Analysis
Phase III - Off-Design Performance Analysis

Final Annual Technical Report

Simion C. Kuo
Principal Investigator
(203) 727-7258

Prepared for:

The Office of Naval Research, Arlington, Virginia
Under Contract No. N00014-79-C-0344
Mr. M. Keith Ellingsworth, Scientific Officer

October 1982

Two-Phase Nozzle Theory and Parametric Analysis
Phase III - Off-Design Performance Analysis

TABLE OF CONTENTS

FOREWORD

The work described in this Final Annual Technical Report was performed at the United Technologies Research Center (UTRC) under Contract N00014-79-C-0344, Modification No. P00006, entitled "Two-Phase Nozzle Theory and Parametric Analysis - Phase III, Off-Design Performance Analysis," for the Office of Naval Research (ONR). This report summarizes results obtained for the Phase III - (third year) study indicated above exclusive of the Task III.3, Heat Transfer Augmentation in Naval Heat Exchangers - A Field Trip to Japan. This field trip has been approved recently and is now scheduled for November 1, 1982 through November 19, 1982. A Special Task Report will be prepared to cover the major findings from this field trip for submission to ONR before the extended contract completion date of January 31, 1983.

The contract program was initiated with ONR on July 15, 1981, and the contract completion date was extended from September 14, 1982 to January 31, 1983 to accommodate the Task III.3 field trip mentioned above. The Scientific Officer for this contract program is Mr. M. Keith Ellingsworth, Mechanics Division, ONR, Arlington, Virginia. Valuable guidance and comments received from Mr. Ellingsworth are gratefully appreciated.

Two-Phase Nozzle Theory and Parametric Analysis
Phase III - Off-Design Performance Analysis

SUMMARY

The objectives of the work presented in this report were to investigate the off-design performance characteristics of selected two-phase nozzles, to examine methods and impact of implementing heat transfer augmentation in two-phase nozzles, to investigate the heat source integration problems, and to recommend an experimental program appropriate for verifying the analytical performance characteristics predicted. The off-design performance characteristics of selected two-phase nozzles were estimated as a function of the governing parameters using isothermal theory.

Typical performance maps for selected two-phase nozzles were constructed, based on the off-design performance characteristics estimated using isothermal theory adapted for these calculations. These maps were constructed to show the total mass flow rate and the nozzle efficiency (two primary performance parameters), as a function of loading ratio, inlet pressure and temperature, and exit pressure (hence pressure ratio). The effects of drop size and secondary injection of hot liquid on heat transfer enhancement and the possibility of shaping the nozzle contour to produce an exponential pressure profile for a fixed nozzle length to improve two-phase nozzle performance were examined. The effects of droplet size and of local gas velocity (relative to both the composite two-phase sonic velocity and the single-phase sonic velocity) on the level of flow disturbance (shock) in a two-phase mixture were also examined.

The characteristics and suitability of integrating the potential heat sources with two-phase nozzles for marine propulsion applications were reviewed, and the system design characteristics and limitations inherent with these heat sources were summarized. Finally an experimental program to verify the predicted nozzle performance characteristics was formulated to outline the nozzle test section designs, the test rig, the type of instrumentation required and its location, and a test plan to identify the effects of the major flow parameters on nozzle performance.

This study program was conducted by the Thermal Engineering Group at UTRC under Contract N00014-79-C-0344, Modification P00006, from the Office of Naval Research, Mechanics Division, Arlington, Virginia.

RESULTS AND CONCLUSIONS

1. Based on isothermal theory, the off-design efficiency of two-phase nozzles using a mixture of steam and Dowtherm A decreases by approximately four percentage points when the nozzle inlet pressure is reduced from 600 psia (typical design point) to 100 psia at a fixed loading ratio and exit pressure. When the pressure ratio is increased from 10 to 50, at a constant inlet pressure, the predicted nozzle efficiency drops by approximately two percentage points or less, depending upon the level of the inlet pressure. When the loading ratio is reduced from 40 to 10, the nozzle efficiency first drops by about one-half percentage point to a minimum at a loading ratio of about 25, and then rises by about the same amount as the loading ratio is further reduced to 10.

2. The off-design performance of a two-phase nozzle predicted based on the isothermal theory agrees well (mean velocity within three percent) with experimental data reported by Elliott for a converging-diverging nozzle using a two-phase mixture of air and water. This nozzle had an exit to inlet area ratio of 0.25 and was tested over a range of loading ratios between approximately 20 and 100, with an inlet pressure of 290 psia and an exhaust pressure of one atmosphere.

3. Enhancement of the heat transfer coefficient between the liquid droplets and the gas would have a relatively small effect on the performance of two-phase nozzles, because the heat transfer that naturally occurs between the very small liquid droplets and the gas is already high. A 50 percent increase in the heat transfer coefficient would result in about a one percentage point increase in nozzle efficiency.

4. The use of a nozzle contour shaped to provide an exponential pressure profile can increase the predicted two-phase nozzle efficiency by three to six percentage points, depending upon the pressure ratio, as compared to a nozzle designed with a linear pressure profile.

5. The composite sonic velocity in a two-phase (gas/liquid) mixture is well below the sonic velocity in a single-phase gas which depends not only on temperature, but also on pressure and loading ratio. The formation and abruptness of the velocity disturbance (shock) depend on droplet size and the local gas velocity relative to both the composite two-phase sonic velocity and the single-phase gas sonic velocity. For very small droplet sizes (less than 2 microns in diameter) where the mixture begins to behave as a continuum, the velocity disturbance is expected to be abrupt in steam/DTA nozzles if the velocity of the gaseous component is above the composite two-phase sonic velocity. While for larger droplets, the velocity disturbance is expected to be gradual unless the gas velocity is above the single-phase gas sonic velocity.

6. The two prime heat sources for mobile two-phase energy conversion systems suitable for marine propulsion applications are fossil-fired and nuclear-fueled heat sources. Further, the availability of thermal energy from either of these heat sources would be able to meet the rapid fluctuations in shaft power required of typical naval propulsion systems. The temperature of the gaseous heat carrier for each of these heat sources would be high enough to make the temperature limits of the two-phase working fluid be one of the crucial design factors.

7. The use of a two-component working fluid would be favored over a one-component working fluid for marine propulsion applications because of flexibility to control the loading ratio of the two-component mixture. Furthermore, a two-component working fluid has the desirable feature of expanding nearly isothermally, while a one-component working fluid will expand along its saturation line with the drop in pressure through the nozzle.

8. An experimental program should be conducted with two-phase nozzles over the range of the governing flow parameters, including operation at sub-atmospheric exit pressures which may be of interest for marine propulsion applications. An air/water nozzle should be tested in unheated experiments, while two different steam/DTA nozzles should be tested using heated DTA to flash water to steam in a mixer to form the two-phase mixture. Nozzles with both linear and exponential pressure profiles provided by appropriate flow area contours should be tested.

INTRODUCTION

Energy conversion systems utilizing two-phase (gas/liquid) working fluids for work extraction offer many desirable features which are attractive for potential marine propulsion applications. First, the presence of the higher-density liquid droplets in the two-phase mixture would yield nozzle exit velocities significantly lower than these attainable with a single-phase gas expanded over a comparable pressure ratio. The lower exit mixture velocities would mean that the turbine shaft speeds can be advantageously lower than those in conventional turbomachinery, hence the generally bulky gearbox between the turbine shaft and the thrustor shaft can be made smaller and lighter because less speed reduction would be required. A second desirable feature of the two-phase nozzle system for marine propulsion applications is that a boiler may not be required because the liquid phase (such as a heat transfer oil with a low vapor pressure) can be heated without boiling under pressure and then combined with the condensate of the gas phase (such as steam) in a mixer where the condensate is flashed into its vapor to form a two-phase mixture of liquid droplets suspended in steam. This two-phase mixture can then be expanded through the nozzle for work extraction in a two-phase turbine.

Another application for two-phase energy conversion systems is hydrothermal geothermal energy, where the working fluid is already available as a two-phase mixture of steam and brine at the wellhead. Geothermal energy is currently receiving increasing attention (Ref. 1) as an attractive heat source for generating electricity in the western USA.

Both energy conversion systems cited above involve flows of a two-phase substance that is a mixture of liquid droplets suspended in a flowing gas. The specific area of concern in this investigation is a two-phase nozzle where a uniform mixture of a liquid and a gas at high pressure and low velocity are expanded through a nozzle to attain high velocities at low pressure. Previous investigations have made important contributions to the understanding of two-phase nozzle flows, but their physical models have generally displayed one of two drawbacks in terms of conducting parametric analyses of nozzles. The first limitation is that only some of the significant interphase effects of momentum and heat transfer were considered (for example, Refs. 2 to 8). The second limitation is that, although these interphase effects were considered, the model (Ref. 9 and 10) was formulated essentially for the purpose of detailed theoretical computations and not for the purpose of conducting parametric analyses and optimization where many cases must be calculated with reasonable accuracy and within a reasonable period of time.

Hence, to circumvent these drawbacks, a more practical working theory of two-component two-phase (gas/liquid) nozzles was formulated during Phase I of this program (Ref. 11). This working theory includes droplet breakup and interphase transport of momentum and thermal energy but excludes mass transfer and frictional losses. In a subsequent Phase II study on this program (Ref. 12), the working theory was used to conduct parametric analyses of two-phase nozzle performance over a wide range of flow conditions and fluid properties. The sensitivity of the nozzle performance predictions to the assumptions concerning droplet characteristics (droplet drag, heat transfer, and breakup) was examined, and criteria were developed for optimized nozzle designs based on the results of parametric analyses.

The objectives of the Phase III - Two-Phase Nozzle study program described herein were to investigate the off-design performance characteristics of selected two-phase nozzles, to examine methods and impact of heat transfer augmentation in two-phase nozzles, to investigate the heat source integration problems, and to recommend an experimental program to verify the performance predictions. The results of this Phase III study program are presented herein The off-design performance characteristics of selected two-phase nozzles were estimated in Task III.1 as a function of the governing parameters. Then methods to enhance heat transfer from the liquid droplets to the gas were investigated in Task III.2 as a possible means of improving two-phase nozzle performance. In Task III.4, the thermodynamic and gas dynamic behavior of two-phase nozzle flows was examined briefly in terms of possible Mach number effects. Then the characteristics and problems of integrating the two-phase nozzle with potential heat sources for the energy conversion system were investigated in Task III.5, including consideration of heat sources for systems with both one-component and two-component working fluids. Finally, in Task III.6, an experimental program is outlined to verify the analytical results obtained from the working theory developed in the Phase I study (Ref. 11) and the results of parametric performance analyses conducted during Phase II of this program (Ref. 12).

REFERENCES (FOR INTRODUCTION)

1. Kestin, J., R. DiPippo, H. E. Khalifa, and D. J. Ryley, eds.: Sourcebook on the Production of Electricity from Geothermal Energy. DOE Report DOE/RA/4051-1, 1980.

2. Tangren, R. F., C. H. Dodge and H. S. Siefert: Compressibility Effects in Two-Phase Flow. J. Appl. Phys., Vol. 20, No. 7, pp. 637-645, 1949.

3. Kliegel, J. R.: One Dimensional Flow of a Gas-Particle System. Report No. TR-59-0000-00746, Space Technology Laboratories, Los Angeles, 1959.

4. Rudinger, G.: "Relaxation in Gas-Particle Flow," Chapter in Nonequilibrium Flows -- Part I, P. P. Wegener, ed., pp. 119-161. Marcel Dekker, Inc., 1969.

5. Netzer, D. W.: Calculations of Flow Characteristics for Two-Phase Flow in Annular Converging-Diverging Nozzles. Report No. TM-62-3, Jet Propulsion Center, School of Mechanical Engineering, Purdue University, 1962.

6. Hultberg, J. A. and S. L. Soo: Two-Phase Flow Through a Nozzle. Astronautics Acta, Vol. 11, No. 3, pp. 207-216, 1965.

7. Crowe, C. T., M. P. Sharma and D. E. Stock: The Particle-Source-In Cell (PSI-Cell) Model for Gas Droplet Flows. ASME J. of Fluids Eng'g., pp. 325-332, 1977.

8. Comfort, W. J., T. W. Alger, W. H. Giedt and C. T. Crowe: Calculation of Two-Phase Dispersed Droplet-in-Vapor Flows Including Normal Shock Waves. ASME J. of Fluids Eng'g., pp. 355-362, 1978.

9. Elliott, D. G.: "Theoretical and Experimental Investigation of a Gas-Driven Jet Pump for Rocket Engines", in Liquid Rockets and Propellants, Progress in Astronautics and Rocketry - Vol. 2, pp. 497-541. Academic Press, 1960.

10. Elliott, D. G. and E. Weinberg: Acceleration of Liquids in Two-Phase Nozzles. JPL Report 32-987, 1968.

11. Deane, C. W. and S. C. Kuo: Two-Phase Nozzle Theory and Parametric Analysis: Phase I - Two-Phase Nozzle Theory. UTRC Report R80-954624-2, 1980.

12. Deane, C. W. and S. C. Kuo: Two-Phase Nozzle Theory and Parametric Analysis: Phase II - Parametric Analysis and Optimization. UTRC Report R81-955229-4, 1981.

R82-955744-4

Two-Phase Nozzle Theory and Parametric Analysis
Phase III - Off-Design Performance Analysis

The overall objective of this analytical study program was to advance the basic understanding of two-phase nozzles, particularly from the energy conversion point of view. To meet this overall objective, the specific objectives of the Phase III work which are described herein were: to investigate the off-design performance characteristics of selected two-phase nozzles; to examine methods and impact of heat transfer augmentation in two-phase nozzles; to investigate the heat source integration problems; and to recommend an experimental program to verify the performance predictions. As part of the earlier Phase I work (which is described in detail in Ref. 1), a working theory of two-component two-phase (gas-liquid) nozzles, identified as the Model with Droplet Heat Transfer, was developed. This model includes droplet breakup and the interphase transport of momentum and thermal energy but excludes mass transfer and frictional losses. This working theory was computerized in a form suitable for parametric and optimization analyses of these two-phase nozzles. As part of the earlier Phase II work (which is described in detail in Ref. 2), this working theory was used to conduct parametric analyses of two-phase nozzle performance over a wide range of flow conditions and fluid properties. The sensitivity of the predicted nozzle performance to the assumptions concerning the droplet characteristics was examined, and criteria were developed for optimum nozzle designs based on the parametric analyses.

The Phase III work described herein consists of results obtained from five of the six study tasks: III.1) Off-Design Performance; III.2) Heat Transfer Enhancement; III.4) Flow Dynamic Considerations; III.5) Heat Source Integration; and III.6) Experimental Program Recommendation. The major findings from the yet to be completed Task III.3) Heat Transfer Augmentation in Naval Heat Exchangers - A Field Trip to Japan, will be reported in a later report.

III.1 Off-Design Performance

The off-design performance characteristics of selected two-phase nozzles were estimated as a function of the governing parameters. Because such energy system components as two-phase nozzles will undoubtedly have to operate at off-design conditions, the off-design performance characteristics are important in assessing the attractiveness of the two-phase nozzle over the entire range of expected operating conditions. As described below, isothermal theory was adapted for the calculation of off-design nozzle performance characteristics because

numerical instabilities in the numerical solution technique occurred when the working theory for the design of nozzles (Model with Droplet Heat Transfer) was used in reversed steps to calculate the nozzle performance.

III.1.1 Model of Off-Design Performance

The original intention during this present study was to convert the two-phase nozzle design theory developed in the Phase I study into a theory of off-design performance of two-phase nozzles by inverting the logic of the design theory. In principle, this conversion of the numerical marching-type procedure would appear to be relatively straightforward, but in practice, numerical instabilities in the results were encountered in the vicinity of the throat for certain operating conditions. The numerical instabilities in the marching-type solution occur because of the sensitivity of the variables in the equation which governs the change in velocity, to the operating conditions at the throat. The rate of change of velocity with respect to nozzle flow area must undergo a change from a negative relationship in the converging section to exactly zero at the nozzle throat, then to a positive relationship in the diverging section (if the two-phase flow is to be accelerated in the diverging section of the nozzle). Perhaps this numerical problem can be overcome by using a completely different solution procedure--namely by a simultaneous solution of the matrix of the N sets of governing equations for each node, where N is the number of nodes.

For the method of off-design performance calculation that inverts the Model with Droplet Heat Transfer, the linearized continuity and momentum equations developed during Phase I of this program were combined, and this combination is examined here to determine the cause of the numerical problems.

Continuity holds at any location throughout the nozzle and at a given nozzle cross-section, the total flow area (A) can be considered as the sum of the liquid flow area (A_ℓ) and the gas flow area (A_g):

$$A = A_\ell + A_g \tag{III.1}$$

For one-dimensional flow through a cross-section, the continuity equations for each of the two components are:

$$A_g = \frac{\dot{m}_g}{\rho_g V_g} \; ; \; A_\ell = \frac{\dot{m}_\ell}{\rho_\ell V_\ell} \tag{III.2}$$

From the definition of the loading ratio, $r \equiv \dot{m}_\ell / \dot{m}_g$, then the expressions in Eq. III.2 can be substituted into Eq. III.1 to produce:

$$A = \dot{m}_g \left(\frac{1}{\rho_g V_g} + \frac{r}{\rho_\ell V_\ell} \right) \tag{III.3}$$

As previously developed in Ref. 1 and elsewhere, the local phase velocities can be represented in terms of the local velocity ratio ($K \equiv V_f / V_g$) and the local mean velocity, $\bar{V}$, as:

$$V_\ell = \left(\frac{1 + r}{1 + rK} \right) K \bar{V} \equiv L \bar{V} \tag{III.4}$$

$$V_g = \left(\frac{1 + r}{1 + rK} \right) \bar{V} \equiv G \bar{V} \tag{III.5}$$

The quantities L and G are assumed to be constant over each small increment of axial length along the nozzle, ΔX. The perfect gas law is assumed for the density of the gas phase, $\rho_g = PM_g/RT_g$, where M_g is the molecular weight of the gas and R is the universal gas constant. By substituting the perfect gas law and Eqs. III.4 and III.5 into Eq. III.3, the following expression results:

$$\bar{V}A = \dot{m}_g \left(\frac{RT_g}{PG} + \frac{r}{\rho_\ell L} \right) \tag{III.6}$$

By taking the logarithm of each side of Eq. III.6 and then the first differential, the linearized version of Eq. III.6 becomes:

$$\frac{\Delta \bar{V}}{\bar{V}} + \frac{\Delta A}{A} = -\left(\frac{1}{\left(\frac{RT_g}{PG} + \frac{r}{\rho_\ell L} \right)} \right) \frac{RT_g \Delta P}{G P^2} \tag{III.7}$$

The linearized version of the momentum equation needed for the off-design performance analysis was already developed from a differential force balance on a control volume during Phase I of this program (Eq. I.34 in Ref. 1):

$$\Delta \bar{V}^2 = - \left(\frac{2}{1 + r} \right) \left\{ \frac{RT_g}{G M_g} \ell n \left(\frac{P + \Delta P}{P} \right) + \frac{r \Delta P}{\rho_\ell L} \right\} \tag{III.8}$$

With the assumption that $\Delta P/P \ll 1$, which is valid for very small nodes with a small pressure drop over that node, then the logarithm in Eq. III.8 becomes: $\ell n(1+\Delta P/P) \simeq \Delta P/P$. With this simplification, Eq. III.8 can be solved explicitly for ΔP:

$$\Delta P = - \frac{\Delta \bar{V}^2}{\left(\frac{2}{1+r}\right)\left[\frac{RT_g}{PG} + \frac{r}{\rho_\ell L}\right]} \qquad \text{(III.9)}$$

Substituting Eq. III.9 into Eq. III.7 and noting that $\Delta \bar{V}^2 = 2\bar{V}\Delta V$, the result is:

$$\Delta \bar{V}^2 = \frac{-\frac{\Delta A}{A}}{\frac{1}{2\bar{V}^2} - \frac{1}{P\left(1 + \frac{rGP}{\rho_\ell L RT}\right)\left(\frac{2}{1+r}\right)\left(\frac{RT_g}{PG} + \frac{r}{\rho_\ell L}\right)}} \qquad \text{(III.10)}$$

In the examination of Eq. III.10, the following points can be observed. In the converging section of the nozzle (where ΔA is negative), the value of $\Delta \bar{V}^2$ is positive when the denominator of the right-hand side is positive. However, in the diverging section of the nozzle (where ΔA is positive), for $\Delta \bar{V}^2$ to be positive which must be the case for acceleration of the two-phase mixture, the denominator of the right-hand side of Eq. III.10 must become negative.

If the denominator of Eq. III.10 remains positive, then the value of $\Delta \bar{V}^2$ is negative, and the two-phase mixture decelerates. In other words, the diverging section of the nozzle acts as a diffuser with pressure recovery downstream of the nozzle throat. Figure III.1 illustrates such conditions where the converging-diverging nozzle acts as a venturi. As the flow rate is increased at a constant loading ratio, the exit pressure gradually decreases until the flow rate reaches a point (maximum) beyond which both the calculated results and the computer run would indicate a region of flow instability. As shown in Fig. III.1, the pressure profile for the case with the largest flow rates (labelled $\dot{m}_g/(\dot{m}_g)_{Des}$) are very similar in shape to the pressure profile for the classical subsonic nozzle flow of a single-phase gas at expansion ratios just before shock would occur in the diverging section of the nozzle. Figure III.2 shows results of an off-design calculation using the two-phase model with droplet heat transfer for a loading ratio equal to zero, (i.e., an all-gas flow) and expanded over a calculated pressure ratio of 0.1481. The the corresponding gas exit velocity calculated with the model is 3046 ft/sec and exit temperature is 765 R. In comparison, the gas exit temperature calculated using classical gas dynamics for an adiabatic gas expansion is 767 R, and the gas exit velocity calculated with the same theory is 3092 ft/sec. Both of these values (from classical gas dynamics) compare quite

closely with the off-design model at all-gas conditions. The axial profile of the nozzle flow area shown at the top of Fig. III.2 is a third-order polynomial curvefit which matches the flow area of the specified nozzle at three axial locations (inlet, throat, and exit areas) and the axial slope of the flow area at the throat (dA/dX = 0).

For the high loading ratios expected for marine propulsion applications, the calculated temperature drop of the gas is often relatively small because of heat transfer from the liquid droplets, as seen earlier in the parametric studies conducted during Phase II (Ref. 2) with the Model with Droplet Heat Transfer, so the two-phase flow can be nearly isothermal under many flow conditions. Furthermore, because of the numerical instability problems discussed above, it was decided to use isothermal theory for the calculation of off-design nozzle characteristics. The main drawback for using isothermal theory is that the velocity ratio is assumed constant throughout the nozzle and must be known beforehand as an input to the calculations. However, reasonable estimates of this velocity ratio can be obtained from the parametric design results and then used to calculate the off-design performance characteristics of two-phase nozzles.

As noted in the preceding discussion, the continuity equation and the momentum equations are the governing relationships used to estimate the off-design performance characteristics. At a given set of operating conditions, the continuity equation for the gas flow can be written for flow conditions anywhere in the nozzle:

$$\dot{m}_g = (1 - \varepsilon_{in})\, \rho_{g,in}\, V_{g,in}\, A_{in} = (1 - \varepsilon)\, \rho_g\, V_g A \qquad \text{(III.11)}$$

where ε is the local liquid volume fraction which is calculated using the expression:

$$\varepsilon = \frac{1}{1 + \dfrac{K\, \rho_\ell}{r\, \rho_g}} \qquad \text{(III.12)}$$

Here, K is the velocity ratio, (V_ℓ/V_g), which is assumed to be constant throughout the nozzle for a given set of operating conditions. This is the assumption that Rudinger (Ref. 3) made to obtain the version of the momentum equation that is discussed next.

The expression for gas velocity at any location in the nozzle where the local pressure is P was obtained from momentum considerations by Rudinger (Ref. 3) for isothermal flow conditions. This expression is:

$$V_g^2 = V_{g,in}^2 + \frac{2\, RT_g}{1 + rK} \left[\ell n \left(\frac{P_{in}}{P} \right) + \left(\frac{\varepsilon_{in}}{1 - \varepsilon_{in}} \right) \left(1 - \frac{P}{P_{in}} \right) \right] \qquad \text{(III.13)}$$

where R is the perfect gas constant.

For a given set of operating conditions, the gas velocity at any location (V_g) is related to the inlet gas velocity ($V_{g,in}$) by the continuity relationship of Eq. III.11. Using the perfect gas law to convert density into pressure at specific locations, Eq. III.11 can be substituted into Eq. III.13 to obtain the result:

$$V_{g,in}^2 = \frac{\frac{2\,RT_g}{1+rK}\left[\ell n\left(\frac{P_{in}}{P}\right) + \left(\frac{\epsilon_{in}}{1-\epsilon_{in}}\right)\left(1-\frac{P}{P_{in}}\right)\right]}{\left(\frac{P_{in}}{P}\,\frac{A_{in}}{A}\,\frac{1-\epsilon_{in}}{1-\epsilon}\right)^2 - 1} \qquad \text{(III.14)}$$

Hence, with fixed inlet and exit areas and with the assumed inlet conditions of pressure, pressure ratio, temperature, loading ratio, and velocity ratio, the inlet gas velocity at off-design conditions that satisfies both continuity and momentum in the isothermal theory can be calculated with Eq. III.14, and the exit gas velocity at off-design conditions can be calculated with Eq. III.13.

It can be observed, by examination of Eq. III.14, that for the left-hand side of this equation to be positive (and hence the calculated value of $V_{g,in}$ to be a real number, in contrast to an imaginary number), the denominator of the right-hand side must be positive, so that the following inequality must hold:

$$PR\left(\frac{1-\epsilon_{in}}{1-\epsilon_{exit}}\right) > \frac{A_{exit}}{A_{in}} \qquad \text{(III.14a)}$$

where PR is the overall pressure ratio. In other words, there is a minimum pressure ratio based on the ratio of inlet to exit areas below which the nozzle cannot be operated, according to the isothermal theory. The term ϵ is the liquid volume fraction, and ϵ_{in} is larger than ϵ_{exit} because of the pressure drop through the nozzle. Hence, while the value of the minimum pressure ratio will be only several times the exit area ratio, it will not represent a limitation for the pressure ratios in excess of 40 that are of interest for marine propulsion applications.

From the continuity equation, the total mass flow through the nozzle is the sum of the gas and the liquid mass flow rates:

$$\dot{m}_{Tot} = \dot{m}_g + \dot{m}_\ell = \dot{m}_g\,(1+r) \qquad \text{(III.15)}$$

where r is the loading ratio ($\dot{m}_\ell/\dot{m}_g$). The gas flow rate ($\dot{m}_g$) is calculated from the continuity relationship, Eq. III.11, once the off-design gas velocities are known.

The isentropic efficiency is a measure of nozzle performance and is defined as:

$$\eta \equiv \frac{\frac{1}{2}\,\dot{m}\left(\bar{V}^2_{exit} - \bar{V}^2_{in}\right)}{\dot{m}\,\Delta h)_{max}} = \frac{\bar{V}^2_{exit} - \bar{V}^2_{in}}{2\,\Delta h)_{max}} \qquad \text{(III.16)}$$

This efficiency is the ratio of the change in kinetic energy per unit mass of the mixture to the ideal change of enthalpy (into kinetic energy) for the isentropic expansion of a homogeneous two-phase mixture. The maximum enthalpy change through the nozzle, $\Delta h)_{max}$, is given by the expression:

$$\Delta h)_{max} = \left\{\left(\frac{1}{1+r}\right) C_{pg}\left[T_g)_{inlet} - T_{exit}\right]\right\} + \left\{\left(\frac{r}{1+r}\right)\left(C\left[T_\ell)_{inlet} - T_{exit}\right] + \frac{\Delta P}{\rho_\ell}\right)\right\} \qquad \text{(III.17)}$$

The $(\Delta P/\rho_\ell)$ term in the second brackets is included in the liquid enthalpy contribution because the process does not occur at a constant pressure. Although the temperatures of the gas and of the liquid could differ at the nozzle inlet, there exists a common exit temperature for the homogeneous mixture, T_{exit}. This exit temperature is calculated by using the expression for an isentropic expansion of a homogeneous mixture, as discussed in Ref. 1.

III.1.2 Off-Design Performance of Two-Phase Nozzles

Off-design performance characteristics of two-phase nozzles were estimated as a function of the governing parameters using the isothermal procedure developed in the preceding section, which were then used to construct typical performance maps for a two-phase nozzle. These performance maps can be used to judge nozzle performance in conjunction with the other components of a two-phase work extraction system.

The off-design performance of a two-phase nozzle having fixed values of inlet temperature and pressure ratio are shown in Fig. III.3 as a function of nozzle inlet pressure and pressure ratio. For a given pressure ratio, as the inlet pressure is reduced, the total mass flow decreases. This decrease in mass flow can be attributed to the fact that the level of gas density decreases as the pressure is reduced. It can also be seen from the same figure that for a given exit pressure, the total mass flow rate increases as the nozzle inlet pressure is increased. This flow rate increase is the same trend as reported by Toner (Ref. 4) in his nozzle experiments with a two-phase mixture of air and water. Further, for a fixed inlet pressure, the total mass flow rate decreases as the pressure ratio is increased; increased pressure ratio at fixed inlet pressure corresponds to a reduced exit pressure. This trend is shown in more

detail in Fig. III.4 where the total mass flow rate is plotted as a function of exit pressure for a fixed inlet pressure condition. The off-design inlet and exit velocities were calculated using Eqs. III.14 and III.13, and the mass flow rates were calculated using Eqs. III.15 and III.11. As the exit pressure is reduced, the total mass flow rate decreases also. As discussed earlier in connection with the derivation of Eq. III.14a, the minimum pressure ratio that yields a real number in the isothermal off-design theory for this area ratio of 2.37 (see Fig. III.3) is approximately 4.3, which corresponds to an exit pressure of approximately 140 psia for an inlet pressure of 600 psia. This minimum pressure ratio is well below the pressure ratios of 40 and higher that are interest for marine propulsion applications. For nozzles with smaller exit area ratios, the minimum pressure ratio is even lower. As can be seen from the curves of exit gas density and exit gas velocity in Fig. III-4, the gas density decreases faster than the gas velocity increases for this range of exit pressure operation, and as a result, the multiplicative combination (Eq. III.11) of these effects causes the total mass flow to decrease when the nozzle exit pressure is reduced. The expected range of pressure ratios for two-phase nozzles used in a marine propulsion application would be larger than ten, which would correspond to nozzle exit pressures below 60 psia for the conditions of Fig. III.4.

Figure III.5 shows the corresponding results for an exit area ratio much smaller than 2.37, which results in a much lower value (below 4.3) of the minimum pressure ratio. As the exit pressure is reduced, the total mass flow rate begins to increase, as expected. A maximum flow rate is reached at an exit pressure of approximately 325 psia, and below this value, the flow rate decreases as the exit pressure is reduced further. As can be seen from the accompanying curves of exit gas density and exit gas velocity in Fig. III.5, the gas density decreases faster than the gas velocity increases in this operating range (again similar to that for the larger area ratio of 2.37) and the combination of these effects causes the total mass flow rate to decrease when the nozzle exit pressure is reduced.

The effect of nozzle inlet pressure and pressure ratio on estimated nozzle efficiency is shown in Fig. III.6, where the efficiency generally decreases when the pressure ratio increases (which increase corresponds to a lower exit pressure) or as the nozzle inlet pressure decreases. When the nozzle inlet pressure is reduced from 600 psia to 100 psia at constant values of the loading ratio and exit pressure, the predicted nozzle efficiency drops by approximately four percentage points. When the pressure ratio is increased from 10 to 50, at a constant value of the inlet pressure, the predicted nozzle efficiency drops by approximately two percentage points or less, depending upon the level of the inlet pressure.

Figure III.7 shows the effect of loading ratio on off-design nozzle performance. As the loading ratio is increased, the total mass flow increases because the average density of the two-phase mixture increases. Also shown in this figure is the relationship that as pressure ratio increases at a fixed inlet pressure, the total mass flow decreases. The effect of loading ratio on nozzle efficiency is

shown in Fig. III.8. As the loading ratio decreases from 40 to 10 (at fixed pressure ratio), the nozzle efficiency gradually decreases by approximately one-half percentage point to a minimum (at a loading ratio in the range of 25 to 40, depending upon pressure ratio), whereafter it increases by approximately the same amount as the loading ratio is reduced further to 10. The expected range of loading ratio for marine propulsion applications is generally from ten to forty.

Figure III.9 shows experimental data reported recently by Elliott (Ref. 5) for the off-design performance of a two-phase (air/water) nozzle as a function of loading ratio at a pressure ratio of 20.28. Also shown in the figure is the isothermal prediction for the off-design performance of this nozzle using the isothermal theory described in this section with a velocity ratio of 0.7. Elliott's performance predictions for the actual nozzle contour are also shown. Both of his predictions are based on models that include velocity slip, droplet breakup, and heat transfer; while one model includes wall friction, and the other model omits it. As can be seen, the isothermal prediction of off-design performance compares well with this off-design experimental data of Elliott.

Shown in Fig. III.10 is the effect of inlet temperature on total mass flow rate. As the inlet temperature increases, the total mass flow rate decreases, primarily because the density of the gas phase is lower at the higher temperature levels. When the inlet temperature is increased to 1060 R from 960 R, the nozzle efficiency decreases negligibly by less than one-half percentage point.

As a possible useful representation of the off-design performance in two-phase flow, use of a velocity parameter was explored. Such a parameter would be analogous to the velocity parameter, $\dot{m}\sqrt{T}/P$, developed in classical gas dynamics which is used to scale the data. Accordingly, at large values of the pressure ratio, the expression given in Eq. III.14 can be simplified by the assumptions that:

$$PR >> 1; \quad \left(PR \frac{A_{in}}{A} \frac{1 - \epsilon_{in}}{1 - \epsilon}\right) >> 1 \tag{III.18}$$

The resulting simplified version of Eq. III.14 can be rewritten as:

$$V_{g,in} PR \sqrt{\frac{1 + rK}{T_g}} = \frac{\sqrt{2R'}\left[\ell n\ PR + \frac{\epsilon_{in}}{1 - \epsilon_{in}}\right]}{\left(\frac{A_{in}}{A} \frac{1 - \epsilon_{in}}{1 - \epsilon}\right)} \tag{III.19}$$

Figure III.11 shows velocity data calculated using the off-design isothermal theory and presented in terms of the velocity parameter defined by Eq. III.19. For this range of pressure ratio (20 to 50), the calculated data collapses into a band that is approximately ± 7%.

Overall, within the assumptions and limitations of the calculation method described above, the off-design performance of two-phase nozzles can be estimated with a reasonable degree of accuracy. Generally, the value of the loading ratio will have a large effect on the exit velocities and the total mass flow rates but a small effect on the nozzle efficiency. Increasing the nozzle pressure ratio will result in slightly smaller nozzle efficiencies, as will decreasing the nozzle inlet pressure. As the nozzle inlet pressure increases at constant exit pressure, the mass flow rates increase. But, as the nozzle exit pressure decreases at constant inlet pressure (for pressure ratios greater than about ten, depending upon the exit/inlet area ratio), the total mass flow rate decreases, because the exit density decreases faster than the exit velocity increases.

III.2 Heat Transfer Enhancement

Methods which could enhance the rate of heat transfer from the liquid droplets to the gas were investigated to determine whether they offer the potential of improving two-phase nozzle performance. The effects of drop size and of secondary injection of hot liquid on heat transfer enhancement were examined, and the effect of shaping the nozzle contour on nozzle performance to produce an exponential pressure profile for a fixed axial length was also investigated.

III.2.1 Effect of Droplet Size

The effect of droplet size on nozzle performance was investigated as a possible means to improve two-phase nozzle performance. Droplet diameter has an obvious large effect on the heat transfer area of a droplet that is exposed to the surrounding gas, as well as a secondary effect on the heat transfer coefficient between the liquid droplets and the gas.

To examine this effect, droplet size in the calculations was varied by changing the maximum allowable Weber number. The Weber number governs droplet breakup in the calculations and hence the maximum droplet size for a given set of operating conditions. Figure III.12 shows the results of design-point calculations, undertaken using the Model with Droplet Heat Transfer at a loading ratio of ten, for a wide range of pressure ratios, and two values of the maximum allowable Weber Number of six and three. When the value of the maximum Weber Number is reduced from six to three, the maximum allowable droplet size decreases by approximately 30 percent, and the calculated nozzle efficiency increases by approximately four percentage points because the smaller droplet size results in better heat transfer from the liquid droplets to the gas and better momentum transfer from the gas to the liquid droplets. Figure III.13 shows the comparable results calculated for a loading ratio of 40. Here the same effects occur at this new loading ratio - a 50 percent decrease in droplet size results in an increase in calculated nozzle efficiency of approximately four percentage points.

The Weber Number breakup criterion is a simplified representation of the conditions under which droplet breakup occurs. Droplet breakup in a two-phase mixture can be represented by the ratio of two forces: the aerodynamic pressure forces and the surface tension forces. The critical value of the Weber number, determined experimentally, can be used to estimate the maximum droplet size, D_{MAX}, that can exist at the local flow conditions in a two-phase flow:

$$D_{MAX} = \frac{2\sigma\, We)_{crit}}{\rho_g V_{slip}^2} \qquad \text{(III.20)}$$

where ρ_g is the gas density, V_{slip} is the slip velocity ($V_{slip} \equiv V_\ell - V_g$), and σ is the surface tension of the liquid. Droplet sizes that are much smaller than the value of D_{MAX} predicted by Eq. III.20 could possibly be produced by mechanical or acoustic means, but presumably these smaller-size droplets would tend to agglomerate as the two-phase mixture flowed downstream through the nozzle, with the droplets thereby increasing in size back to the size predicted by Eq. III.20 for the local flow conditions.

According to Eq. III.20, increased velocity slip would result in a condition where smaller droplets are produced. However, increased slip also implies reduced nozzle efficiencies because of the reduced momentum transfer between the phases. Because gas density is set by the operating conditions, Eq. III.20 indicates that the liquid surface tension becomes an important factor in the estimation of droplet size. Possibly, an additive which would reduce the surface tension could be identified and added to the liquid phase to reduce the maximum droplet size. However for this additive to be of value, it would have to be effective at the operating temperatures of the system during its entire lifetime without adversely interacting with the system components.

III.2.2 Effect of Heat Transfer Enhancement

The effects of enhancing the heat transfer between the liquid droplets and the gas on nozzle performance were explored as a possible way to improve nozzle efficiency. As seen in previous figures (for example, Fig. III.13), the droplet diameters are typically very small, and therefore, the calculated local heat transfer coefficients between the droplets and the gas are very high (often in the range of 3000 BTU/hr-ft^2-F). Figure III.14 shows the effect of droplet heat transfer enhancement on nozzle performance as a function of pressure ratio, as calculated with the working theory (the Model with Droplet Heat Transfer). The baseline case in this figure is the droplet heat transfer coefficient (HTC) without enhancement (or 100% HTC), while the enhanced case (150% HTC) assumes a 50 percent increase in the heat transfer coefficient over the base case. As seen, a 50 percent increase in the heat transfer coefficient results in an increase in nozzle efficiency of approximately one percentage point. This relatively small increase in nozzle efficiency is attributed to the fact that the value of the heat transfer coefficient in the absence of heat transfer enhancement is already quite high.

In contrast, if the liquid droplets were abiabatic (as represented analytically by a zero heat transfer coefficient between the liquid and the gas) without transferring heat to the gas, then the calculated nozzle performance would be quite different, as seen in Fig. III.15. For a hypothetical case of adiabatic droplets, the calculated temperature of the liquid droplets does not decrease as the two-phase mixture flows through the nozzle with the gas expanding adiabatically to a temperature well below the inlet temperature, but the transfer of momentum

from the gas to the liquid droplets does occur. Here, the difference between the results for the case using the normal (baseline) droplet heat transfer coefficient and that which assumes a heat transfer coefficient of zero is an approximately 15 percentage point reduction in nozzle efficiency. Thus, the level of droplet heat transfer that occurs naturally is important to achieve good nozzle performance, but droplet heat transfer coefficient enhancement beyond the baseline levels has only a small effect for these operating conditions of interest for marine propulsion applications.

Hence, based on these considerations and the fact that the addition of heat transfer enhancement devices (such as turbulators upstream of, or in the nozzle) would only add complication to the system, it does not appear that heat transfer enhancement is particularly advantageous for the improvement of nozzle performance.

III.2.3 Effect of Secondary Injection

The secondary injection of hot liquid into the two-phase nozzle was examined to determine its possible effect on the enhancement of heat transfer between the liquid droplets and the gas in the nozzle. Generally, secondary injection in gas turbines is used to provide either more cooling or additional thrust. In the case of a two-phase nozzle, the secondary injection of hot liquid may be for improving the nozzle performance or for increasing the energy flux through the nozzle, or both. However, as seen earlier in Fig. III.14, the net effect of droplet heat transfer enhancement, hence performance improvement, is small because the level of droplet heat transfer is already very high. In terms of additional energy flux, if this additional hot liquid is available, then the preferred location for using this liquid would seem to be at the nozzle inlet, where the nozzle residence time of this additional liquid would be the largest relative to injection at other axial locations along the nozzle.

Figures III.16 and III.17 show the calculated values of the gas and liquid temperatures and velocities at the nozzle throat and at the nozzle exit, for values of the loading ratio equal to 10 and 40, respectively. As seen in these figures, the temperature of the liquid droplets has decreased less than 10 R between the nozzle inlet and the throat. Therefore, injecting additional liquid (assumed to be at the temperature of the nozzle inlet liquid) at the nozzle throat, for example, would only increase the bulk liquid temperature by a maximum of 10 R. Further, the liquid would have to be injected at a velocity of approximately 400 ft/sec in order to avoid reducing the velocity of the primary liquid already in the nozzle; a reduction in the bulk liquid velocity would be disadvantageous to nozzle efficiency because there already is velocity slip between the gas and the primary liquid.

An estimate of the effect of secondary injection on nozzle efficiency can be made by reviewing Fig. III.8 and using as an example, the assumption of a primary loading ratio (at the nozzle inlet) of 36, and the addition of sufficient liquid (secondary injection) at some location downstream of the inlet to provide an overall loading ratio of 40. If the pressure ratio were 40, the nozzle efficiency for a loading ratio of 36 would be 0.884 from Fig. III.8, and the efficiency for a loading ratio of 40 would be 0.886. This is a minor increase in nozzle efficiency, because nozzle efficiency is nearly independent of loading ratio in this range. Actually, even this small increase in nozzle efficiency might not materialize because the injected liquid would probably require some residence time to get up to speed.

A significantly additional amount of mechanical complexity would be required to provide secondary injection, because there is a probability that the secondary injection would have to be properly distributed over the cross-sectional flow area (as opposed to wall injection) in order to provide a uniform distribution of small liquid droplets. If wall injection were used, the injected liquid would tend to remain on the nozzle wall and not be mixed homogeneously with the gas, and without thorough mixing, the transfer of heat and momentum between the two phases would be poor, and the nozzle efficiency would not be improved. Furthermore, the presence of secondary injection hardware could even cause in a reduction of nozzle efficiency because liquid from upstream would tend to collide with, and hence be collected on, any injection configuration that was placed in the cross-sectional flow area of the nozzle. If some liquid were collected on the upstream side of the injection hardware, it would probably be torn off irregularly by the high-velocity flowing gas. The irregular packets of liquid would presumably break up, probably to the maximum diameter predicted by the critical Weber Number. It is therefore difficult to envision that this complicated sequence of events associated with the secondary injection would indeed increase nozzle efficiency.

III.2.4 Impact of Nozzle Contour on Nozzle Performance

As an alternative to providing heat transfer enhancement for the improvement of nozzle performance, the effect of nozzle contour on estimated nozzle efficiency was investigated as a method to improve the transfer of heat and momentum between the two phases. The axial pressure profile used in the parametric design analyses of the Phase II studies during this program (Ref. 2) was directly proportional to nozzle axial length; however other profiles can also be considered. In this section, the use of a pressure profile that varies exponentially with axial length is discussed.

The exponential pressure profile is one where the local value of the expansion ratio (P_{in}/P_{out} for small increments of axial length) is constant throughout

the nozzle. The mathematical representation of this exponential profile is $(dP/P)/dX$ = constant, and at a given axial location the difference in pressure level between the linear and exponential pressure profiles is shown in Fig. III.18. Figure III.19 shows the effects of an exponential pressure profile on nozzle exit velocities, exit temperatures, and efficiency over a wide range of loading ratio; all values were calculated using the design working theory (Model with Droplet Heat Transfer). These results show that use of a nozzle capable of generating an exponential pressure profile can increase the predicted nozzle efficiency by three to six percentage points, depending upon pressure ratio, when compared to use of a nozzle designed with a pressure profile that is linear with nozzle axial length. This increase in nozzle efficiency occurs because, under the condition of constant expansion over the nozzle length, the level of velocity slip is reduced and the amount of heat transferred from the liquid to the gas is increased. The reductions in velocity slip and the higher gas temperature, and hence the higher nozzle efficiency, are especially apparent at the higher values of the nozzle pressure ratio.

The effect of an exponential pressure profile on the nozzle diameter profile is shown in Fig. III.20 for a pressure ratio of 50. Because the condition of constant expansion exists, the location of the throat is closer to the inlet with the exponential pressure profile than with the linear profile, and the diverging section has a more gradual angle of divergence. This gradual divergence is more preferable because it reduces the likelihood of flow separation in the diverging section. As discussed in Ref. 6, the half-angle of divergence of a single-phase diffuser should be less than about five degrees, depending upon such factors as configuration type (straight-wall or conical) and the length-to-diameter ratio of the diffuser. The divergence half-angle is equally important in the design of the diverging section of a two-phase nozzle. For example, the diverging section of Elliott's nozzle (Ref. 5) has a half-angle of 2.5 degrees.

As also seen in Fig. III.20, the exit diameter for the nozzle with the exponential pressure profile is larger than that for a nozzle with a linear pressure profile because the exit gas velocity is lower (see Fig. III.19), and hence more exit flow area is required (primarily for the gas phase which occupies most of the exit flow area).

Changes in the shape of the diameter profile for a nozzle with an exponential pressure profile, as shown in Fig. III.21, are more pronounced at a pressure ratio of 400 than they were at a pressure ratio of 40. As seen in Fig. III.19, the possible increase in nozzle efficiency by using an exponential instead of a linear pressure profile is larger at the higher pressure ratios, because the local value of $\Delta P/P$ near the exit of a nozzle is increasing more rapidly in a linear pressure profile (hence the expansion is far from being constant) compared to a nozzle with an exponential pressure profile which is designed for a high pressure ratio application.

III.4 Flow Dynamic Considerations

The thermodynamic and gas dynamic behavior of two-phase nozzle flows was examined briefly in terms of Mach number effects. For single-phase gas flows, the sonic velocity and the local gas velocities have long been recognized as key parameters. For two-phase systems, however, the concept of a two-phase sonic velocity is more complicated because of the various possible flow regimes (such as slug, stratified, bubbly, and droplet flows) and because of the presence of both gas and liquid through which the infinitesimal pressure disturbance (or sound wave) must pass in succession.

III.4.1 Sonic Velocity of Two-Phase Mixtures

Analyses can be undertaken for certain two-phase flow regimes to calculate a sonic velocity of the two-phase mixture. For the two-phase nozzle flows considered in this study for possible marine propulsion applications, the flow is expected to be in the droplet, or mist flow regime where the very small liquid droplets are suspended uniformly in the flowing gas. The sonic velocity of this type of mixture can be estimated by treating the interface of one phase as the elastic boundary of the other phase, and by assuming that the two-phase flow system is confined overall by a rigid wall (Ref. 7). This model for two-phase sonic velocity is based on the fact that the sonic velocity of a single-phase fluid in a tube with an elastic wall depends on the bulk modulus of the tube wall, namely that the sonic velocity of this single-phase system decreases with increasing elasticity of the wall material. Nguyen et al. (Ref. 7) used this physical behavior to develop an expression for the composite sonic velocity ($C_{2\phi}$) in a homogeneous two-phase flow, assuming that the pressure wave front successively passes through a liquid zone and then through a gas zone. The expression obtained is:

$$C_{2\phi} = \frac{1}{(1-\alpha)\sqrt{\frac{(1-\alpha)}{C_\ell^2} + \frac{\alpha\rho_\ell}{C_g^2\rho_g}} + \alpha\sqrt{\frac{\alpha}{C_g^2} + \frac{(1-\alpha)\rho_g}{C_\ell^2\rho_\ell}}} \qquad \text{(III.21)}$$

where α is the void fraction ($\alpha \cong 1-\varepsilon$), C_g is the sonic velocity of the single-phase gas in a system with rigid walls, and C_ℓ is the sonic velocity of the single-phase liquid in a system with rigid walls. The term, ε, is the liquid volume fraction, defined in Eq. III.12, which relates the loading ratio,

velocity ratio, and the gas and liquid densities to the liquid volume fraction and hence to the void fraction. To obtain Eq. III.21, it was assumed that no phase change occurs during the propagation of the pressure disturbance. Very good comparisons were found by Nguyen, et al. between the theoretical predictions of Eq. III.21 and experimental data obtained by four other investigators for water/steam systems and water/air systems.

The sonic velocity which was calculated using Eq. III.21 for two-phase mixtures of steam and Dowtherm A (DTA) is shown in Fig. III.22 as a function of loading ratio and pressure. By comparison, the sonic velocity in single-phase steam at 1060 R is 1944 ft/sec, a value much higher than the calculated composite sonic velocity in two-phase mixtures with a loading ratio in the range of 10 to 50. In the absence of experimental data for the sonic velocity (C_ℓ) in single-phase liquid DTA, the value of C_ℓ was assumed to be 4000 ft/sec. However, its exact value has only a minor effect on the results of calculations using Eq. III.21 because of the high value of the liquid density relative to the gas density. As a point of comparison, the sonic velocity in water is approximately 4600 ft/sec. For an inlet pressure of 600 psia, the practical pressure ratio would be approximately 40 if the gas is expanded to the atmospheric pressure of 14.7 psia. The values of sonic velocity in a two-phase mixture are shown in Fig. III.22 as a function of loading ratio for the above inlet/exit pressure levels (or a pressure ratio of 40). For a loading ratio of less than 50 (which is typical for marine propulsion applications), the sonic velocity at the nozzle exit will be larger because the liquid volume fraction of the mixture at the exit will be lower than that at the nozzle inlet. The reason the liquid volume fraction is lower at the exit is because of its lower pressure, and lower gas density.

Wallis (Ref. 8) described a simple expression for the sonic velocity of a two-phase mixture which is based on the assumption of a homogeneous equilibrium flow model where the mass of the liquid droplets adds to the pseudo density of the two-phase mixture. The resulting equations are similar to the classical one-dimensional compressible flow sonic velocity equations except that the properties of the pseudo gas replace the single-phase gas properties. This model was originally developed for suspensions of dispersed (solid) particles in a gas, but can be applied to two-phase droplet flows where the liquid droplets replace the solid particles. The resulting sonic velocity for the two-phase mixture at temperature T is less than the sonic velocity in the gas alone, and the homogeneous equilibrium sonic velocity (C_{HE}) can be calculated with the expression:

$$C_{HE} = \sqrt{\alpha' R' T} \qquad \text{(III.22)}$$

where the isentropic constant for the pseudo gas is:

$$\gamma' = \frac{C_{pg} + rC_{\ell}}{C_{vg} + rC_{\ell}} \qquad \text{(III.23)}$$

and the pseudo gas constant is:

$$R' = \frac{R}{(1+r)} \qquad \text{(III.24)}$$

Here, R is the gas constant for the pure gas, and r is the loading ratio. The terms C_{pg} and C_{vg} are the specific heats of the gas at constant pressure and at constant volume, respectively, and C_{ℓ} is the specific heat of the liquid.

One obvious problem with the homogeneous equilibrium model is that the results are virtually independent of pressure, whereas pressure will certainly have an important effect on void fraction for a mixture with a fixed value of the loading ratio. Figure III.23 shows that the sonic velocities calculated with this homogeneous equilibrium model are substantially lower than the values calculated with the two-phase model proposed by Nguyen, et al. (Ref. 7). Furthermore, as mentioned above, results from the Nguyen model have compared well with the experimental results of four other investigators for two-phase gas-liquid mixtures.

III.4.2 Mach Number in Two-Phase Nozzles

As discussed above, the sonic velocity of a two-phase mixture in the droplet flow regime can be calculated from the Nguyen elasticity model for two-phase sonic velocity using Eq. III.21. Therefore, it is possible to express a two-phase Mach Number ($M_{2\phi}$) as the ratio of the local gas velocity (V_g) to the two-phase sonic velocity ($C_{2\phi}$) calculated at the local conditions of temperature, pressure, loading ratio, and velocity ratio (required to estimate the local void fraction):

$$M_{2\phi} = V_g/C_{2\phi} \qquad \text{(III.25)}$$

Figure III.24 shows the results of design-point calculations for a six-inch nozzle operating with a mixture of steam and DTA at a loading ratio of 40 and a pressure ratio of 40. Also shown are the two-phase sonic velocity ($C_{2\phi}$) (calculated with Eq. III.21) and the sonic velocity in single-phase steam for the local conditions (pressure, temperature, and velocity ratio) as a function of the axial distance through the nozzle. The two-phase sonic velocity, as expected, is much lower than the sonic velocity in single-phase steam. At the inlet, the two-phase sonic velocity is approximately 630 ft/sec, which decreases gradually to a minimum of approximately 560 ft/sec at a location that is nearly 75% along the nozzle axis, and then this velocity increases to a value of about 700 ft/sec at the nozzle exit. The gas velocity, even at the nozzle exit, is well below the sonic velocity of single-phase steam at these operating conditions. The top curve in the figure shows the two-phase Mach Number ($M_{2\phi}$), which is based on the local gas velocity and the local two-phase sonic velocity ($C_{2\phi}$). At the inlet, the two-phase Mach Number is approximately 0.2, which increases gradually to a value of about 1.7 at the nozzle exit. At the nozzle throat, the two-phase Mach Number is approximately 0.75. Thus, at the operating conditions of Fig. III.24, the exit gas velocity of the two-phase mixture is well above the two-phase sonic velocity but well below the single-phase sonic velocity for pure steam at the nozzle exit conditions.

The local maximum droplet diameters and velocities are shown in Fig. III.25 for a pressure ratio of 40, an inlet pressure of 600 psia, and loading ratios of 40 and 10. For a loading ratio of 40, the maximum droplet diameter decreases from a value of approximately 2×10^{-4} ft at the nozzle inlet to a value of approximately 6.3×10^{-5} ft near the nozzle exit, primarily because of the larger values of the slip velocity ($V_{Slip} \cong V_g - V_\ell$) near the nozzle exit. For a loading ratio of 10, the maximum droplet diameter near the nozzle exit is about 3.5×10^{-5} (or about 11 microns in diameter). Comfort and Crowe (Ref. 9) have analytically investigated the dependence of shock characteristics on liquid droplet sizes in two-phase (water/steam) mixtures flowing through converging-diverging nozzles. They found that the formation and abruptness of normal shock waves in two-phase mixtures depend strongly on the coupling between the phases, particularly on droplet size. As droplet diameters become small, the mixture otherwise behaves as a continuum, and sharp discontinuities can occur at gas velocities that are above the two-phase sonic velocity but are below the sonic velocity in single-phase gas (steam in their case). The droplet size where continuum behavior is approached (based on the Ref. 9 calculations for a steam/water expansion) occurs at droplet diameters between 3.3×10^{-6} ft (1 micron) and 6.6×10^{-6} ft (2 microns). However, for droplet diameters above two microns, the flow disturbance caused by a shock in the diverging section of a nozzle is much less pronounced, and the velocity profile through the nozzle is relatively smooth, in contrast to the discontinuity in velocity that occurs for droplet diameters between one and two microns. For flow conditions with large diameters, the continuum behavior no

longer applies, and the downstream conditions of the two-phase flow are then carried upstream by the sonic velocity of the single-phase vapor, as is the case in classical gas dynamics.

For flow conditions where the gas velocity is higher than both the sonic velocity in single-phase steam and the two-phase sonic velocity, Comfort and Crowe found a sharp discontinuity in velocity when a shock occurs, even for droplet diameters as large as ten microns. When the sonic velocity of the single-phase gas was exceeded, then the shock conditions were not carried upstream, and the shock occurred rather abruptly, which is consistent with supersonic flow behavior. For these velocity conditions, the shock is not significantly affected by the size of the droplets, except that the relaxation region downstream of the sharp discontinuity is broader for large droplet sizes. Thus, for gas velocities that are above the two-phase sonic velocity but below the sonic velocity of single-phase steam, as is the case for the conditions illustrated in Fig. III.25, the flow disturbance caused by a shock is expected to be rather gradual for droplet diameters larger than two microns.

Figure III.26 shows the local maximum droplet diameters and velocities for a pressure ratio of 100, an inlet pressure of 600 psia, and loading ratios of 40 and 10. At this pressure ratio and at a loading ratio of 10, the gas velocity of 2000 ft/sec. at the nozzle exit exceeds the sonic velocity of single-phase steam (which is calculated to be 1584 ft/sec at the exit gas temperature of 704 R). The droplet diameters at the nozzle exit are approximately 3.5×10^{-5} ft (11 microns), which suggests that at this high pressure ratio the shock disturbance will be sharp because the gas velocity exceeds the sonic velocity of single-phase steam. At a pressure ratio of 100 and an inlet pressure of 600 psia, it is only above the loading ratios of approximately 40 that the exit gas velocity falls below the sonic velocity of single-phase steam, as can be inferred by inspection of Fig. III.26.

III.5 Heat Source Integration

In this section, the characteristics and problems of integrating the two-phase nozzle with potential heat sources for the work extraction system are discussed. Included are considerations of heat sources for systems with one-component working fluids as well as those for systems with two-component working fluids. If the gas phase is the vapor of the liquid phase, then the working fluid is a "one-component" fluid. If the gas phase is of a different chemical composition from the liquid, then the working fluid is a "two-component" fluid. Cycle configurations for both types of systems were identified, and the system design characteristics and limitations of both types of configurations are summarized.

III.5.1 Heat Source Characteristics

There are a number of possible heat sources that could be used to supply thermal energy to an energy conversion system using two-phase (gas-liquid) working fluids. These would include: fossil fuels, nuclear energy, solar energy, geothermal energy, and waste heat. Fossil fuels, nuclear energy, and solar energy are all high-temperature heat sources, while geothermal energy is a relatively low-temperature heat source. The temperature of the waste heat could be high, medium, or low, depending upon its origin. Table III.1 summarizes the characteristics of all these heat sources which are discussed in more detail in the following sections.

Fossil fuels, nuclear energy, and solar energy, all being high-temperature heat sources, would therefore produce a large temperature differential in the two-phase turbine system. A heat exchanger would be used to transfer the thermal energy of the heat source to the working fluid (liquid or gas or mixture) of the energy conversion system which would apparently include a two-phase turbine for work extraction.

III.5.1.1 Fossil-Fired Heat Source

In the case of fossil fuels (such as diesel fuel, commercial liquified natural gas, and even coal), the combustion gases would pass over the tubes of the heat exchanger that contain the working fluid of the two-phase system. Figure III.27 is a schematic of a fossil-fired two-phase turbine system containing such components. The hot combustion gases heat the liquid (which can be a substance like DTA) in the heat exchanger, and then the liquid DTA is combined with the condensate water in a mixer that is located between the heat exchanger and the two-phase nozzle. The water flashes to steam in the mixer, and the two-phase mixture of liquid DTA droplets and steam is thereby formed. This mixture is expanded through the nozzle whereupon the steam is separated, and either delivered to a steam turbine and then condensed, or condensed directly. The liquid DTA passes through the two-phase turbine and is then returned to the waste heat exchanger to be heated again to repeat the above processes in a closed cycle operation.

For the combustion of marine diesel fuel, the maximum temperature rise is approximately 3150 R at stoichiometric conditions. The hot gas can always be diluted with fresh air to lower its temperature if necessary, but the higher combustion gas temperatures will result in smaller heat exchanger designs for a given thermal capacity. Kuo et. al. (Ref. 10) conducted a comprehensive survey to identify the technical status of fossil-fuelled air and helium heater designs and technologies, with particular attention to candidate systems suitable for lightweight ship propulsion with closed-cycle gas turbines (CCGT). Based on their observations for CCGT systems, combustion chambers developed for open-cycle gas turbine engines could likely be modified to provide thermal energy for work extraction systems using a two-phase turbine. If natural gas or liquid distillate fuels were specified, then only minor modifications of the combustion chambers used in open-cycle aircraft gas turbine engines would be required. If residual oils were specified, then single or multiple combustors developed for industrial gas turbines would have to be adapted. The differences in combustor design occur because residual fuels have a higher carbon-to-hydrogen ratio, higher viscosity, and a higher carbon content than do distillate fuels.

Attention must also be given to the usual erosion and corrosion problems of a fossil-fired system.

For marine applications, where ceramic-core heat exchangers may not be able to withstand the high shock and vibration that could occur during naval operations, a superalloy metal heat exchanger will likely be required, with maximum metal temperatures limited to about 2260 R.

In a two-component system that uses a mixture of steam and DTA as the working fluid, the usual boiler can be eliminated if the DTA alone is heated (without phase change because of its low vapor pressure) in the fossil-fired heater and then mixed with water in its liquid state (from the condenser) in the mixer as illustrated in Fig. III.27. The water flashes into steam to form the two-phase mixture of steam and DTA. As discussed in Ref. 2, the maximum allowable operating temperature of the DTA heat transfer oil is approximately 1060 R, because above this level it begins to break down chemically. The pressure level of the two-phase mixture at the nozzle inlet is expected to be in the range of 600 psi. A two-component system will be desirable for independent control of the loading ratio ($\dot{m}_\ell/\dot{m}_g$), because each flow rate can be set individually. In contrast, the loading ratio in a one-component system would be set by the thermodynamic condition of the fluid which is determined by the rate of heat transfer and flow rate of the working fluid, and therefore provides little flexibility for control.

III.5.1.2 Solar Heat Source

Depending upon the type of collectors employed, solar energy can also be a high-temperature heat source. For example, a solar receiver with metal tubes and gas coolant exit temperatures of 1960 R has been built, and other

collectors with ceramic tubes have been designed for gas coolant exit temperatures of 2410 R. In the metallic unit and the ceramic design, the operating pressure level is 130 psia. The receiver coolant can be a clean gas, most likely air, in contrast to the emission-laden combustion gases in fossil-fired systems. The solar receiver system would substitute directly for the combustors of a fossil-fueled system, so that the schematic diagram illustrated in Fig. III.28 reflects only this change. Because of the lower heat source temperatures in the solar system, its heat exchanger could be larger than the exchanger for the fossil-fired system.

A limiting characteristic of any solar system is the intermittent availability of solar energy. Therefore, to avoid interruptions in power generation, thermal energy storage is usually included as part of a solar system to avoid powerplant fluctuations and/or shutdown. Furthermore, a solar-powered system is not mobile because of the fields of mirrors that are necessary to focus the solar energy into the central gas-heating receiver.

III.5.1.3 Nuclear Heat Source

A nuclear reactor is also a high-temperature heat source, with the temperature of the gas coolant exiting the reactor reaching a level as high as 1840 R at a pressure of 30 psia (Ref. 12). This is the design exit temperature of the helium coolant in the DRAGON gas-cooled reactor, but the design exit temperature of the helium in other reactors such as the ORNL gas-cooled reactor is only 1460 R. Except for the type of heat source and its coolant exit temperature, the schematic of a nuclear-heated two-phase work extraction system as shown in Fig. III.29 is identical to the schematic of the fossil-fired system. The heat exchanger will transfer heat from the reactor coolant (such as helium) to the liquid DTA which will then be mixed with water (in its liquid state) downstream of the heat exchanger to flash the water into steam and thereby form the two-phase mixture of steam and DTA. The temperature levels of the DTA at the exit of the heater will again be limited to 1060 R, and the pressure level is expected to be in the range of 600 psia.

The supply of the nuclear heat source can be considered to be continuous, and the load demand can be met by the control of the reactor. If the reactor is relatively compact after including the necessary shielding, then the nuclear-powered two-phase system can be mobile.

III.5.1.4 Geothermal Heat Source

Geothermal heat sources consist of a flow of brine whose maximum temperature is generally between 760 and 960 R, and whose wellhead pressure levels are typically between 100 and 400 psia (Ref. 13). This brine, which is comprised of water and dissolved salts, is used directly in the work extraction system, and a geothermal system is a one-component system because the steam and brine are of one chemical species (water), except for the salt content.

Geothermal power plants using steam flashed from the hot brine have been in operation for many years, with a separate drum being used to separate the steam and the brine. The steam is then delivered to a turbine, while the residual brine is either discarded or flashed to a lower pressure to produce steam for a separate turbine or for secondary admission to the same machine.

More recently, a rotary separator turbine (Ref. 14) has been proposed for power production from geothermal brine, using a two-phase nozzle expansion to replace the flash process. In the nozzle of such a system, the thermal energy of the brine, possibly with a slight inlet quality, is converted to kinetic energy by accelerating the mixture of steam and brine droplets instead of being dissipated as heat in the flash process. Figure III.30 is a schematic of a geothermal power system using a two-phase nozzle and turbine. The system is definitely not mobile because of its fixed source of geothermal energy; however, the availability of thermal energy is generally continuous. Because the brine is used directly in the work extraction system, no heat exchanger is needed between the heat source and the two-phase system. Although salt scaling and corrosion problems are critical in the design of the geothermal two-phase system, the problem of calcite scaling at some geothermal sites was completely eliminated by the injection of from two to ten ppm of an organic phosphate.

III.5.1.5 Waste Heat Sources

Waste heat can be defined as that portion of energy which is rejected from a process at a temperature that is still high enough to extract additional work or to provide process heat for another application. Sources of waste heat are generally categorized into three temperature ranges: a high-temperature range, with temperatures above 1660 R; a medium-temperature range, with temperatures between 910 R and 1660 R; and a low-temperature range, with temperatures below 910 R.

The combustion of hydrocarbon fuels for various industrial processes produces gases in the high-temperature range. Secondary air is often admitted to the combustor to lower the temperature of the products to the required process temperature and/or to protect equipment. The upper section of Table III.2 shows high-temperature waste heat sources of various industrial processes, and the range of gas exit temperatures for each. These waste heat sources result from processes which use the direct firing of fossil fuels. The middle section of Table III.2 shows waste heat sources with exit gas temperatures are in the medium temperature range; most of these heat sources are also the exhaust gases of direct fossil-fuel-fired processes. Generally, the pressure level of these waste heat gases in the medium- and high-temperature ranges are at levels less than 45 psia, and most often nearly at atmospheric pressure. The lower section of Table III.2 presents a representative list of waste heat sources in the low-temperature range. Generally, the temperature levels of such systems are too low for use in work extraction systems, but the production of low-pressure process steam may still be economical.

Except for the exhausts of mobile steam boilers or mobile gas turbines, waste heat sources generally offer no significant interest for marine propulsion applications, because the location of the waste heat source is fixed. Furthermore, the availability of waste heat is dependent on the time cycle of the primary process. However, auxiliary fossil heat, if economical, could be supplied in some applications to augment the waste-heat supply. A further consideration is that direct fossil-fired sources of waste heat also contain combustion products that must be taken into consideration in the design of the system.

As was the case with the fossil-fired heat sources, a heat exchanger would also be required for a two-phase work extraction system that uses waste heat as its energy source. A typical arrangement for such a system is shown in Fig. III.31 for a two-component working fluid, although a one-component working fluid could be incorporated, depending in part on temperature and pressure levels. If DTA were used, the temperature level of this two-component system would be limited to 1060 R because of DTA degradation characteristics, although a lower maximum design temperature may be necessary because of limitation by the temperature of the waste heat. If a one-component, two-phase system were envisioned where an organic fluid is the working fluid (as shown in Fig. III.32), then the maximum operating temperature would be lower and would depend on the temperature capabilities of the chosen organic. At the exit of the heat exchanger, the one-component working fluid will have been heated nearly to its saturation level, or even possibly to a very low quality, and then expanded through the nozzle to the two-phase turbine. The separated vapor would be directed to a vapor turbine and then condensed before its return to the waste heat exchanger. The liquid would pass through a two-phase turbine and then be rejoined with the condensate from the vapor turbine.

II.5.2 System Design Characteristics and Limitations

Heat sources consistent with both one- and two-component, two-phase work extraction systems have been discussed, and the concomitant cycle configurations have also been identified. Accordingly, the design characteristics and limitations of these systems are discussed in this section.

The use of a one-component working fluid is inherent for geothermal two-phase work extraction systems, because the heat is already carried in a working fluid that is suitable for a two-phase turbine and because the addition of a heat exchanger would add unnecessary mechanical complication and increase the temperature loss (through the heat exchanger). In addition, sites of geothermal wells are limited to regions where geothermal sources exist - namely areas of geologically recent volcanic activity.

However, other two-phase systems could incorporate either one- or two-component working fluids because the heat carrier would generally be a gas -

either as a coolant (for the nuclear reactor or the solar receiver) or as a combustion exhaust (from a fossil-fired heat source or from most of the waste-heat sources of interest).

With a two-component working fluid, the loading ratio can be independently fixed by setting the individual flow rates of the liquid and the gas. The liquid selected should have a low vapor pressure and so it will not contribute to the mass flow of the gas phase. In contrast, the loading ratio at the exit of the two-phase nozzle in a one-component system will be determined by thermodynamic conditions of the fluid as related to the heat transfer rate and flow rate, because the gas phase is the vapor of the liquid phase. Furthermore, the expansion of a one-component working fluid occurs along its saturation line, while the expansion of a two-component working fluid can be nearly isothermal if the loading ratio is sufficiently high. A nearly isothermal nozzle expansion is advantageous for a two-phase work extraction system, because this type of expansion process increases the amount of work that can be extracted as represented by the amount of heat contained in the integral of TdS for the temperature-entropy representation of the two-phase work extraction cycle.

When compared with a single-phase gas, the presence of the dispersed liquid droplets means that a given level of momentum flux can be obtained at a much lower gas velocity, because the average density of the two-phase mixture is higher than that of a single-phase gas at the same conditions of pressure and temperature. Because the gas velocities of the two-phase mixture are lower, a two-phase turbine can be operated at much lower rotor speeds than a turbine using a single-phase gas as the working fluid. The lower rotor speeds of a two-phase turbine are particularly attractive for marine applications because they offer the possibility that either a smaller gear box or even no gearbox at all would be required between the turbine and the thruster. Furthermore, with a two-component working fluid, the loading ratio can be varied independently as a means of controlling the nozzle exit velocity, with the consequence that the turbine speed can be varied to provide a nearly constant efficiency of the work extraction system (Ref. 15). In contrast, the loading ratio of a one-component working fluid undergoes a large decrease, from nearly all liquid (or zero quality) at the nozzle inlet to a two-phase mixture at the nozzle exit where the loading ratio, for example, could be as low as two (which corresponds to a quality of 33%). The exit value of the loading ratio, which is a primary factor in the determination of exit gas velocities, is highly dependent on nozzle inlet conditions which are set, in part, by the flow rate of the working fluid and the heat transfer rate from the heat source. Hence, at part-load conditions, where the turbine rotor speed is more easily controlled when a two-component working fluid is used, the efficiency of a two-phase turbine cycle can be higher than that of either a single-phase turbine or a two-phase turbine with a one-component working fluid.

Another design consideration is that, for a one-component working fluid, the thermodynamic condition of the working fluid at the exit of the heat-source

heat exchanger can vary widely, from an all-liquid to a low-quality two-phase mixture containing both liquid and vapor, especially if the work extraction system is designed to provide a wide range of power output. In contrast, for a two-component working fluid, the heat transfer in the heat source heat exchanger would involve only the liquid component because the liquid (such as DTA, for example) would have a low vapor pressure and because the gas component would be introduced and mixed with the hot liquid DTA in a mixer downstream of the heat-source heat exchanger.

Except for the geothermal heat sources, the choice between one-component and two-component working fluids for a two-phase work extraction system would not be restricted and therefore could be based on overall system considerations for a specific application. As summarized in Table III.1, the primary heat sources of interest would generally incorporate working fluids that are single-phase gases. The receiver coolant of a solar heat source would probably be air; the reactor coolant for a nuclear heat source would be a gas such as helium, or possibly carbon dioxide; while the working fluids for the fossil-fired heat sources and most of the waste heat sources would be combustion gases. With the combustion gases, precautions must be taken in the design of the heat source heat exchanger to minimize and/or avoid corrosion, and even erosion problems must be expected if the fossil-fuel selected were coal. In geothermal systems, scaling problems with the salt in the brine would have to be considered, as was previously mentioned. Furthermore, as summarized in Tables III.1 and III.2, the maximum temperature limits of the work extraction system depend on the heat source and/or on the maximum temperature capability of the working fluid (1060 R if the liquid selected is DTA).

The availability of energy from the potential heat sources also varies. The fossil-fired heat source and the nuclear-fueled heat source should be able to meet the variable power demands, if sized properly, required for marine propulsion systems. However,the intermittent nature of solar energy limits the use unless a bulky thermal energy storage system is included, as is generally envisioned for solar-powered electricity-generation systems. The availability of geothermal energy will be relatively steady,depending upon the characteristics of the geothermal well, but it is unlikely that this type of system would be able to meet sudden demands for extra thermal energy. The availability of energy in the form of waste heat depends on the cyclic nature of the industrial process with which it is associated, and this may also be subject to seasonal variations and/or current demand for the primary product; thermal energy storage could be included with this system to smooth the possible variations in waste-heat supply, however.

The mobility of a two-phase work extraction system depends almost entirely on the characteristics of the heat source. A fossil-fired, two-phase work extraction system will be very mobile because of the high energy densities of the transportable fossil-fuels. In contrast, a solar-powered two-phase work

extraction system will generally be stationary because of the bulky collector mirrors required to concentrate the solar insolation into the solar receiver. The nuclear-powered two-phase work extraction systems could be mobile, within the limits of the required reactor shielding, because of the high energy density of the nuclear fuel. Geothermal-powered two-phase work extraction systems will be stationary because the location of geothermal heat sources are fixed. Likewise, waste-heat-powered two-phase work extraction systems will be stationary because the waste heat sources will generally be associated with various industrial processes.

It can be concluded that the two candidate prime heat sources for mobile, two-phase work extraction systems available for applications such as marine propulsion, will be either fossil-fired or nuclear-fueled. Furthermore, the availability of thermal energy from either a fossil-fired source or a nuclear reactor should give a system incorporating these sources the capability to meet the rapid fluctuations in shaft power that would be necessary for naval propulsion applications. However, the temperatures of the working fluids in each of these heat sources will be sufficiently high that the temperature limits of the two-phase working fluid may become a deciding design factor. Because control of the loading ratio is desirable in a marine propulsion application, use of a two-component working fluid would be favored over the use of a one-component working fluid. The thermodynamic characteristic of a two-component working fluid which allows it to be expanded in a nearly isothermal manner through the nozzle is also an attractive feature. For two-phase work extraction systems using either solar or waste-heat sources, systems studies should be undertaken for each particular application to determine the economic merits of a choice between a one-component working fluid and a two-component working fluid.

III.6 Experimental Program Recommendation

In this section, an experimental program is outlined to verify the performance predictions obtained from the working theory developed in Phase I of this program (Ref. 1) and from the parametric analyses conducted during Phase II of this program (Ref. 2). As part of this experimental program, the test sections have been defined to explore the range of parameters expected for a two-phase nozzle to be used in a two-phase turbine for work extraction. The design of a test section for unheated experiments using air and water as the two-component two-phase mixture is presented, as is the design of two additional test sections for experiments using heated Dowtherm A (DTA) heat transfer oil and steam as the two-component two-phase mixture. The test rig and the type of location of instrumentation to acquire the pertinent data are identified, and a test plan directed toward the exploration of the effects of the major flow parameters on two-phase nozzle performance is presented.

III.6.1 Experimental Test Sections

Based on the discussion above in Section III.5, it appears likely that the working fluid for a two-phase turbine suitable for marine propulsion applications will be a two-component working fluid. Hence experimental test sections using a two-component working fluid were designed. A nozzle using an unheated two-phase mixture of air and water was designed, for use in a simpler set of experiments where no heating of the liquid phase is required. Then two nozzles using a heated mixture of steam and DTA heat transfer oil were designed, where the liquid DTA is heated alone and then mixed with (liquid) water which flashes into steam to form the two-phase mixture of steam and DTA at the nozzle inlet. It is proposed that these nozzles then be tested over a wide range of operating conditions, including those where the nozzle exhausts to pressures lower than atmospheric. Previous experiments (for example, see Refs. 4, 5, and 16) have generally been conducted (for convenience) with the nozzle being exhausted to atmospheric pressure, but marine propulsion applications could well require nozzle exit pressures which are lower than atmospheric.

III.6.1.1 Air/Water Nozzle

Calculated results from the working theory (Model with Droplet Heat Transfer) developed during Phase I of this program (Ref. 1) were used to guide the design of the nozzle for the air/water experiments. For this design, the air and water are assumed to be at ambient temperature at the nozzle inlet (nominally 520 R), the inlet pressure was selected to be 150 psia, the loading ratio was 40, and the pressure ratio at the design point was ten. Exercising the working theory computer model at these design conditions for a linear pressure profile, a one-inch nozzle inlet diameter, and a six-inch nozzle length, resulted in the calculation of a throat diameter of 0.74 inches and an exit diameter of 1.03 inches. With the theory, the axial throat location was

calculated to be 2.9 inches from the nozzle inlet which in turn, produces a half-angle of 2.6 degrees for the conical diverging segment if a flat section is faired smoothly into the nozzle throat from the nozzle exit. Figure III.33 shows the nozzle design, drawn to scale, for the air/water experiments. A mixer located upstream from the nozzle and not shown in Fig. III.33 would combine the air and water flow streams to form the two-phase mixture of liquid droplets suspended uniformly in the gas.

Obviously in the experimental test plan, the air/water nozzle will be tested at off-design conditions as well as design conditions, so the off-design performance of this nozzle was estimated using the isothermal off-design theory discussed above in Section III.1. As presently contemplated, an experimental test plan for the air/water nozzle would involve ambient inlet temperatures and relatively low nozzle inlet pressures (150 psia maximum, although higher pressures could be tested), in addition to nozzle exit pressures which should range from 1 atmosphere down to approximately 5 psia. Shown in Fig. III.34 are the estimated effects of loading ratio and pressure ratio (for constant inlet pressure) on total mass flow rate and nozzle efficiency. The mass flow rate increases as the loading ratio increases, because the two-phase mixture contains relatively more liquid.

Figure III.35 shows the estimated effect of inlet pressure on nozzle performance (total mass flow rate and nozzle efficiency) at constant exit pressure of 15 psia. Nozzle testing at constant exit pressure has been the manner by which most testing has been conducted by previous investigators. As expected, for a fixed value of the loading ratio and exit pressure, the total mass flow through the nozzle increases as the nozzle inlet pressure increases.

III.6.1.2 Steam/DTA Nozzles

In parallel with the above nozzle, calculated results from the working theory (Model with Droplet Heat Transfer) were used to guide the design of the nozzles for the steam/DTA experiments. During the testing of these nozzles, a heater would be used to increase the temperature of the liquid DTA so when it is mixed with the liquid water just upstream of the nozzle inlet, the water will flash into steam and thereby form the two-phase mixture. The design point of the steam/DTA nozzles corresponds to conditions where the inlet temperature is 960 R, the inlet pressure is 600 psia, the loading ratio is 40, the pressure ratio is 40, and the nozzle exit pressure is 15 psia.

The working theory computer model was exercised for a linear pressure profile with a one-inch nozzle inlet diameter and a six-inch nozzle length. At these conditions the throat diameter was calculated to be 0.56 inches and the exit diameter, 1.22 inches. Based on this theory, the axial throat location was estimated to be 3.0 inches from the nozzle inlet, a location which produces a large half-angle in the diverging section of the nozzle. In single-phase diffusers, large half-angles can lead to flow separation (Ref. 6), and the same

type of flow problems could possibly occur in the diverging section of a two-phase nozzle, even though the flow is accelerated for most operating conditions in the diverging section. If the location of the nozzle throat were not moved toward the nozzle inlet (for an overall nozzle length of six inches), then the half-angle of divergence would be significantly larger than the 2.5 to 3.5 degrees that was generally the maximum used in experiments by Elliot (Refs. 5 and 16) and by Toner (Ref. 4). However, Alger (Ref. 17) tested two-phase nozzles with mixtures of water and steam for geothermal applications. The nozzle half-angles were as much as 11 degrees, and flow separation problems were not observed. Hence, based on these latter data the throat location from the theory was not changed. The maximum half-angle in the diverging section of the steam/DTA nozzle was allowed to be nine degrees, and the diverging section was connected to the throat by fairing a smooth curve from the throat to the point where the divergence with the half-angle commences. For the converging portion of the nozzle, the profile calculated with the working theory was used. Figure III.36 shows a scale drawing of the steam/DTA nozzle which has an exit flow area to inlet flow area ratio of 1.50. The heated DTA would be added to (liquid) water in a section located upstream from the nozzle so the two-phase mixture would be allowed to form before entering the nozzle.

The expected off-design performance of this steam/DTA nozzle was also estimated using the isothermal off-design performance theory. In contrast to the air/water nozzle experiments using unheated air and water as the two-phase mixture, the experiments with the steam/DTA nozzles will be more complex because the DTA heat transfer oil must be heated, and nozzle inlet pressures as high as 600 psia would be necessary. At several values of the pressure ratio (for constant inlet pressure of 600 psia), Fig. III.37 shows the effect of the loading ratio on the total mass flow rate and the nozzle efficiency, indicating that the total mass flow rate through the nozzle increases when the loading ratio is increased. Shown in Fig. III.38 is the effect of nozzle inlet and exit pressures on the total mass flow rate, at a loading ratio of 40. At a constant value of the nozzle exit pressure, as the nozzle inlet pressure is increased the total mass flow rate increases. At a constant value of the nozzle inlet pressure, as the nozzle exit pressure is decreased, total mass flow rate through the nozzle decreases. This effect of nozzle exit pressure is explored in more detail in Fig. III.39 where the calculated values of gas velocity, gas density, and void fraction $(1-\varepsilon)$ at the nozzle exit are shown. These three factors combine together to govern the continuity equation which determines the gas flow rate, and the liquid flow rate in turn directly related through the loading ratio ($r = \dot{m}_\ell/\dot{m}_g$), and hence the expression for the total mass flow rate: $\dot{m}_{TOT} = \dot{m}_g\ (1+r)$. Basically, as the exit pressure is reduced, the density of the exit gas decreases linearly, while the exit gas velocity is increasing only gradually with the void fraction already close to unity (and hardly increasing).

In addition to the steam/DTA nozzle design of Fig. III.36 which was designed with a linear pressure profile, a steam/DTA nozzle design with an exponential pressure profile was prepared as shown in Fig. III.40. The design conditions for both nozzles are the same: inlet temperature of 960 R, inlet pressure of 600 psia, loading ratio of 40, and a pressure ratio of 40. The same nozzle inlet diameter of one inch and nozzle length of six inches were also considered. The nozzle resulting from the exponential profile has a maximum half-angle of 7.7 degrees, and the nozzle throat is closer to the nozzle inlet as it should be to provide the constant expansion of the exponential pressure profile. The ratio of exit flow area to inlet flow area of this nozzle is 1.81.

The predicted off-design performance of the exponential steam/DTA nozzle was also estimated with the isothermal off-design theory discussed in Section III.1. Figure III.41 shows the effect of loading ratio on the total mass flow rate and the nozzle efficiency, at a constant inlet pressure of 600 psia and variable pressure ratios. Shown in Fig. III.42 is the effect of nozzle inlet and exit pressures on the total mass flow rate, at a loading ratio of 40.

III.6.2 Test Rig and Instrumentation

In this section, the test rig required for the experiments with the two-phase nozzle designs is identified, along with the pertinent instrumentation (and its location) to measure the parameters which can be used to check the predicitions of nozzle performance. Figure III.43 is a schematic of the test rig proposed to test the air/water nozzle. The separate air and water flow streams are combined in a mixer just upstream of the two-phase nozzle to form a two-phase mixture of liquid water droplets suspended in air. A water pump, an air compressor, a flow meter, and a control valve for each of the two flow streams, are provided so that the loading ratio of the two-phase mixture can be established and the nozzle inlet pressure can be controlled. The vacuum pump downstream of the nozzle is provided to control the exit pressure of the two-phase mixture.

Thermocouples are placed at the inlet and exit of the nozzle to measure the bulk temperature of the two-phase mixture and also of each of the two flow streams before they are mixed. Pressure taps are included for measurement of the wall static pressures at the nozzle inlet and exit and also along the length of the nozzle. In order to calculate the nozzle efficiency, the nozzle thrust must be measured. Elliot and Weinberg (Ref. 16) measured the nozzle thrust with a strain-gauge force transducer mounted between the nozzle and a rigid support, with the nozzle attached to a parallelogram thrust stand. Toner (Ref. 4) measured the nozzle thrust with a strain-gauge load cell connected to a rigid point and to a nearly friction-free trolley on which the nozzle was mounted. In both cases, the two flow streams were connected to the mixer with flexible lines. These flexible connections are critical if the thrust measurements are to be accurate.

Figure III.44 is a schematic of the test rig proposed for the tests with the steam/DTA nozzle. The streams of heated DTA and (liquid) water are combined in a mixer immediately upstream of the nozzle, where the water flashes into steam to form the two-phase mixture of DTA droplets suspended in steam. In the liquid DTA stream, there is a DTA pump, a control valve, a turbine flowmeter, and heat exchanger (probably heated by diluted combustion gases from a fossil-fired combustor). Thermocouples would be used to measure the bulk temperatures of the liquid DTA at the heat exchanger inlet and exit, the latter being the DTA temperature at the inlet to the mixer. In the "gas" stream, there is a water pump, a control valve, and a turbine flowmeter. A thermocouple would be used to measure the temperature of the water stream at the inlet to the mixer. After the mixer, the pressure and bulk temperature of the two-phase mixture would be measured at the inlet to the nozzle, and also at the exit of the nozzle. Pressure taps would also be included for measurement of the static pressure along the length of the nozzle.

A vacuum pump would be attached to the nozzle exit to provide sub-atmospheric exit pressures for some of the tests. The liquid DTA would be collected from the two-phase mixture and then cooled before its return to the DTA supply tank. The steam would be either released directly to the atmosphere or condensed first and then released. Again provisions are made to measure the nozzle thrust in a manner similar to that provided for the air/water nozzle tests. Additionally, because the DTA flow circuit is closed, flexible lines must be carefully included to return the DTA to the DTA supply tank.

III.6.3 Experiment Test Plan

An experimental test plan prepared for the air/water nozzle and the steam/DTA nozzles includes the major flow parameters that should be varied such that their effect on nozzle performance (mass flow rates and nozzle efficiency) can be determined. Based on the analyses of off-design performance developed in Section III.1 and also on the parametric analyses of Phase II of this program (Ref. 2), the key parameters that should be varied during the testing are: loading ratio; inlet pressure; exit pressure (and hence pressure ratio); and inlet temperature. For the unheated air/water nozzle tests, the inlet temperature would vary only if changes in the temperature of the water supply occur, but these changes are expected to be very small. The basic approach for the testing of each nozzle would be to vary the major parameters one at a time in relationship to the design-point conditions which would be treated as the baseline case for each nozzle.

III.6.3.1 Air/Water Nozzle Tests

The baseline case for the air/water nozzle has a loading ratio of 40, an inlet pressure of 150 psia, an exit pressure of 15 psia (or a design-point pressure ratio of ten), and an inlet temperature of 520 R. The nozzle inlet

temperature would not be varied during the air/water nozzle tests. The total mass flow rate and the nozzle efficiency would be the measured performance characteristics of major interest.

The loading ratio will be varied from ten to forty in increments of ten, which is the range of interest for marine propulsion applications. The nozzle inlet and exit pressures will be held constant at their baseline values. Then the nozzle inlet pressure should be changed from the baseline value of 150 psia, to values of 120, 80, and 60 psia, with the loading ratio and the exit pressure held constant at their baseline values. These values of inlet pressure should cover the nozzle pressure ratio of from four to ten, typical of the range covered by previous investigators.

The next parameter that should be varied is the nozzle exit pressure which should be reduced from the baseline value of 15 psia, to values of 10,7.5, 5, and 3 psia, while maintaining the loading ratio and inlet pressure at their baseline values. These values of the nozzle exit pressure would result in nozzle pressure ratios in the range of from ten to fifty. This same variation of nozzle exit pressure should be repeated at a loading ratio of ten.

Selected operating conditions should be repeated to verify the consistency and repeatability of the data, and the calibrations of the measuring equipment should be checked both before and after the nozzle tests.

Overall, this test program would cover the important ranges of the pertinent parameters that are possible in the overall test matrix. Table III.3 summarizes the test matrix proposed for the air/water nozzle. If anomalies or interesting operating conditions are discovered during the experiments, the testing can be expanded in that region of operation.

III.6.3.2 Steam/DTA Nozzle Tests

The baseline case for both of the steam/DTA nozzles has a loading ratio of 40, an inlet pressure of 600 psia, an exit pressure of 15 psia, and an inlet temperature of 960 R. The total mass flow rates and the nozzle efficiency are again the measured performance characteristics of major interest. Two nozzle designs for the steam/DTA tests were discussed earlier in this section: one is based on a linear pressure profile (Fig. III.36), and the other is based on an exponential pressure profile (Fig. III.40). The same test plan will be used for both nozzles because the operating region of interest for marine propulsion applications is the same for both nozzles.

The loading ratio will be varied from ten to forty, in increments of ten, which is the loading range of interest for marine propulsion applications. The nozzle inlet and exit pressures and the inlet temperature would be held

constant at their baseline values. The nozzle inlet pressure would then be changed from its baseline value of 600 psia, to values of 500, 400, and 300 psia, with the loading ratio, exit pressure, and inlet temperature all held constant at their baseline values. These values of nozzle inlet pressure would also cover the range of interest for marine propulsion applications and correspond to a range in pressure ratio of from 40 to 20.

The next parameter to be varied should be the nozzle exit pressure which should be reduced from the baseline value of 15 psia, to values of 10, 7.5, 5, and 3 psia, while the loading ratio, inlet pressure, and inlet temperature are held constant at their respective baseline values. The corresponding values of the nozzle pressure ratio would range from 40 to 200. Then this same variation of nozzle exit pressure should be repeated at a loading ratio of ten.

The final parameter to be varied in the steam/DTA nozzle tests should be the nozzle inlet temperature. The variation in loading ratio (from ten to forty) should be repeated with the inlet temperature increased to 1060 R, while the nozzle inlet and exit pressures are held constant at their respective baseline values.

Again, data points should be repeated to verify the consistency and repeatability of the data, and the calibrations of the measuring equipment will be checked both before and after the steam/DTA nozzle tests.

As mentioned above, both steam/DTA nozzles should be tested according to the test plan outlined because it covers the range of parameters anticipated for marine propulsion applications. Table III.4 summarizes the test matrix proposed for the tests of the two steam/DTA nozzles. The scope of the experiments could be expanded and/or modified to cover any changes in the expected ranges of interest for these parameters, and if anomalies or operating conditions of particular interest are found during the experiments, the tests can be expanded in that operating region.

REFERENCES

1. Deane, C. W. and S. C. Kuo: Two-Phase Nozzle Theory and Parametric Analysis: Phase I - Two-Phase Nozzle Theory. UTRC Report R80-954624-2, 1980.

2. Deane, C. W. and S. C. Kuo: Two-Phase Nozzle Theory and Parametric Analysis: Phase II - Parametric Analysis and Optimization. UTRC Report R81-955229-4, 1981.

3. Rudinger, G.: "Relaxation in Gas-Particle Flow", Chapter in Non-Equilibrium Flow - Part I, P. O. Wegener, ed., pp. 119-161. Marcel Dekker, Inc., 1969.

4. Toner, S. J.: Two-Phase Flow Research. Phase I. Two-Phase Nozzle Research. Doe Report DOE/ER/10687-T1, 1981.

5. Elliott, D. G.: Theory and Tests of Two-Phase Turbines. DOE Report DOE/ER-10614-1, 1982.

6. Reneau, L. R., J. P. Johnston, and S. J. Kline: Performance and Design of Straight, Two-Dimensional Diffusers. ASME J. of Basic Engineering, March, 1967, pp. 141-150.

7. Nguyen, D. L., E. R. Winter, and M. Greiner: Sonic Velocity in Two-Phase Systems. Int. J. of Multiphase Flow, Vol. 7., 1981, pp. 311-320.

8. Wallis, G. B.: One-Dimensional Two-Phase Flow. McGraw-Hill, 1969.

9. Comfort, W. J., and C. T. Crowe: Dependence of Shock Characteristics on Droplet Size in Supersonic Two-Phase Mixtures. Paper in "Polyphase Flow in Turbomachinery", ASME Publication, 1978.

10. Kuo, S. C., T. L. O. Horton, H. T. Shu, C. W. Deane, and E. R. Fisher: Lightweight Propulsion Systems for Advanced Naval Ship Applications Part II - Conceptual Design and Reliability Analysis. UTRC Report R78-952979-4, 1978.

11. Kuo, S. C., T. L. O. Horton, H. T. Shu, and E. R. Fisher: Systems Scoping Study of a 200-kWe Solar-Powered Gas Turbine Experiment. UTRC Report R80-954718, 1980.

12. Shu, H. T. and C. Hsu: Dynamic and System Analysis for Liquid-Metal MHD Power Systems. New Technology, Inc. Report T1069F on ONR Contract N00014-74-C-0195, 1974.

REFERENCES (Cont'd)

13. Kestin, J., R. DiPippo, H. E. Khalifa, and D. J. Ryley, eds.: Sourcebook on the Production of Electricity from Geothermal Energy. DOE Report DOE/RA/4051-1, 1980.

14. Cerini, D. J., and L. G. Hays: Power Production from Geothermal Brine with the Rotary Separator Turbine. Proceedings of the 15th IECEC, Seattle, 1980, pp. 788-797.

15. Elliott, D. G. and L. G. Hays: Two-Phase Turbine Engines. Proceedings of the 11th IECEC, 1976, pp. 222-228.

16. Elliot, D. G. and E. Weinberg: Acceleration of Liquids in Two-Phase Nozzles. JPL Report 32-987, 1968.

17. Alger, T. W.: Droplet Phase Characteristics in Liquid-Dominated Steam-Water Nozzle Flow. Lawrence Livermore Laboratory Report UCRL-52534, 1978.

TABLE III.1

SUMMARY OF POSSIBLE HEAT SOURCES

Type	Heat Carrier	Maximum Temperature Level of Heat Carrier	Energy Availability	Mobile
Fossil-Fired	Combustion Gases	~ 3670 R	Is Able to Meet Demand	Yes
Solar	Air Coolant	~ 2410 R	Intermittent	No
Nuclear	Gas Coolant	~ 1840 R	Is Able to Meet Demand	Yes
Geothermal	Brine	~ 920 R	Steady	No
Waste Heat	Generally Combustion Gases	Wide Range - See *Table III.2 for* Breakdown	Variable and Dependent on Process Cycle	Generally No

TABLE III.2

WASTE HEAT TEMPERATURE LEVELS

Source	Temperature Range of Waste Heat
A. High-Temperature Waste Heat	
Nickel Refining Furnace	3000-3500 R
Aluminum Refining Furnace	1700-1900 R
Zinc Refining Furnace	1900-2500 R
Copper Refining Furnace	1900-2000 R
Steel Heating Furnace	2200-2400 R
Open Hearth Furnace	1700-1800 R
Cement Kiln (Dry Process)	1600-1700 R
Glass Melting Furnace	2300-3300 R
Solid Waste Incinerators	1700-2300 R
Fume Incinerators	1700-3100 R
B. Medium-Temperature Waste Heat	
Gas Turbine Exhausts	1200-1500 R
Steam Boiler Exhausts	900-1400 R
Reciprocating Engine Exhausts	1100-1600 R
Heat Treating Furnaces	1300-1700 R
Drying and Baking Ovens	900-1600 R
Catalytic Crackers	1300-1700 R
Annealing Furnace Cooling Systems	1300-1700 R
C. Low-Temperature Waste Heat	
Process Steam Condensate	590-650 R
Cooling Water From Various Equipment	550-710 R
Liquid Still Condensers	550-650 R
Drying, Baking and Curing Ovens	660-910 R
Hot Processed Liquids and Solids	550-910 R

TABLE III.3

TEST PLAN MATRIX FOR AIR/WATER NOZZLE TESTS

Loading Ratio	Nozzle Inlet Pressure (psia)	Nozzle Exit Pressure (psia)	
A. Variation of Loading Ratio			
40	150	15	- Baseline Conditions
30	↓	↓	
20			
10			
B. Variation of Nozzle Inlet Pressure			
40	120	15	
↓	80	↓	
	60		
C. Variation of Nozzle Exit pressure			
40	150	10	
↓	↓	7.5	
		5	
		3	
10		10	
↓		7.5	
		5	
		3	

TABLE III.4

TEST PLAN MATRIX FOR STEAM/DTA NOZZLE TESTS

Loading Ratio	Nozzle Inlet Pressure (psia)	Nozzle Exit Pressure (psia)	Nozzle Inlet Temperature (R)	
A. Variation of Loading Ratio				
40	600	15	960	- Baseline Conditions
30	↓	↓	↓	
20				
10				
B. Variation of Nozzle Inlet Pressure				
40	500	15	960	
↓	400	↓	↓	
	300			
C. Variation of Nozzle Exit pressure				
40	600	10	960	
↓	↓	7.5	↓	
		5		
		3		
10		10		
↓		7.5		
		5		
		3		
D. Variation of Nozzle Inlet Temperature				
40	600	15	1060	
30	↓	↓	↓	
20				
10				

NOZZLE PERFORMANCE WITH OFF-DESIGN CODE

EFFECT OF FLOW RATE

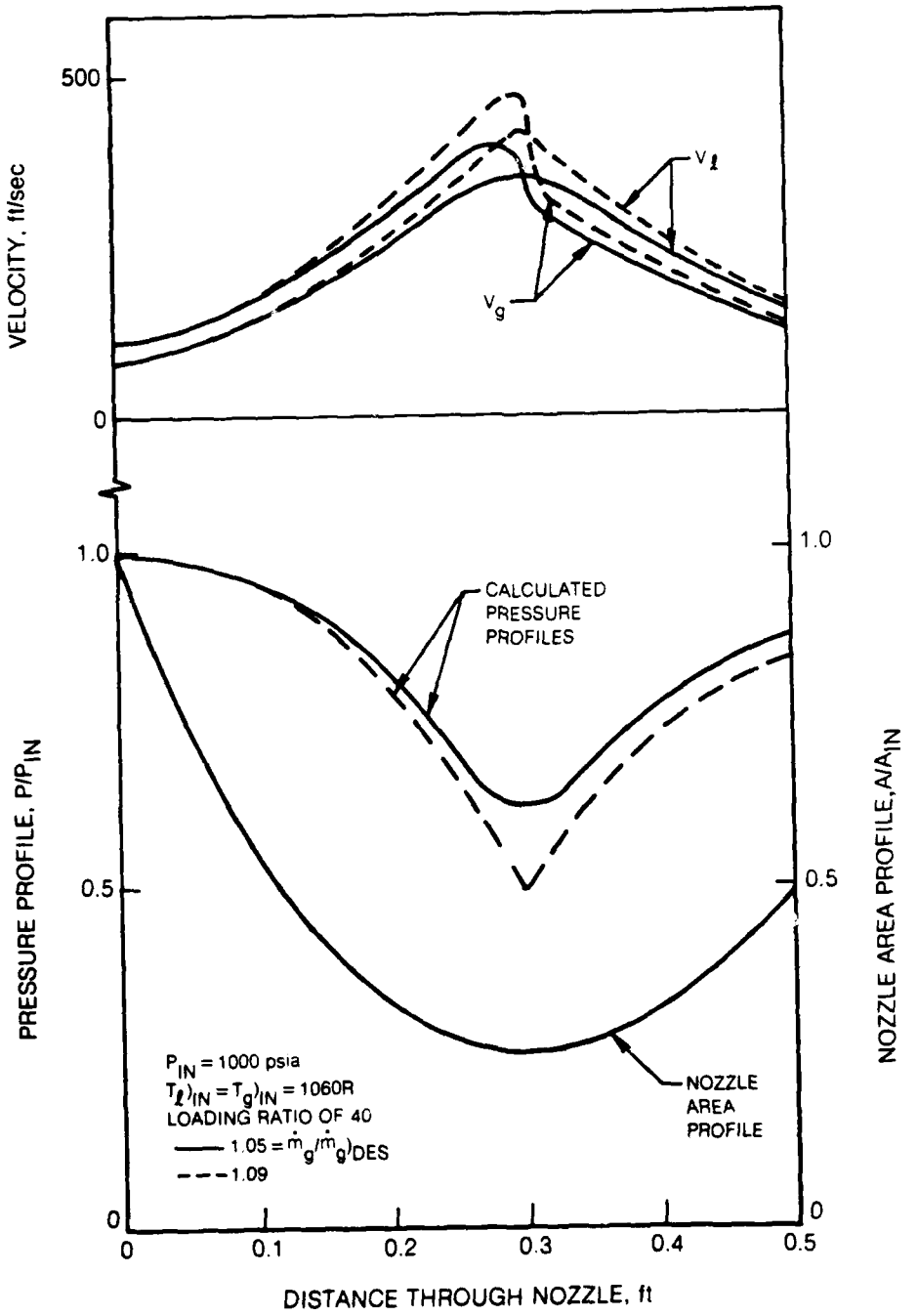

82-6-10-1

FIG. III.2

ALL-GAS OFF-DESIGN PERFORMANCE MODEL WITH DROPLET HEAT TRANSFER

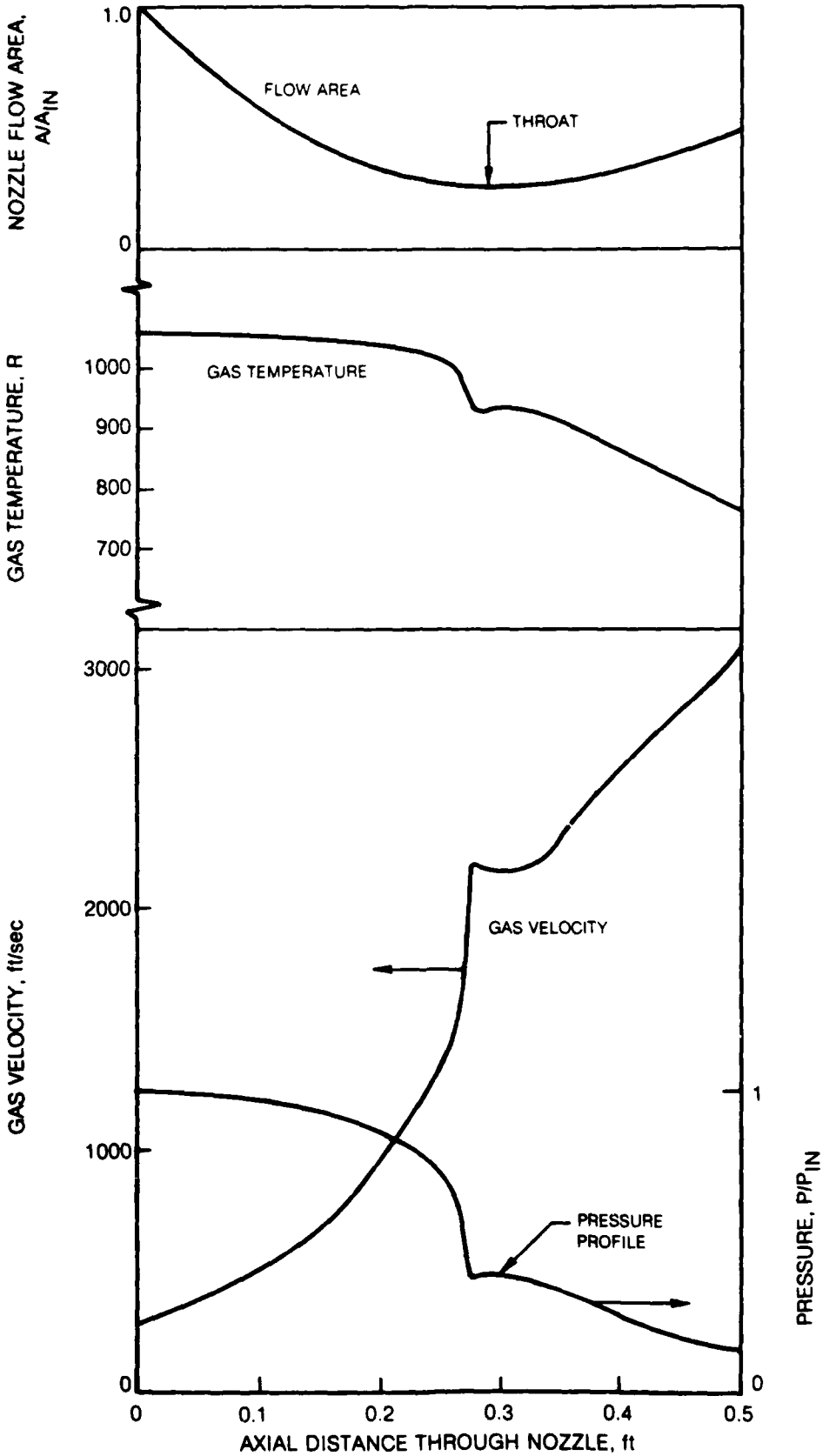

82-6-10-2

OFF-DESIGN PERFORMANCE OF TWO-PHASE NOZZLE

EFFECTS OF INLET PRESSURE AND PRESSURE RATIO

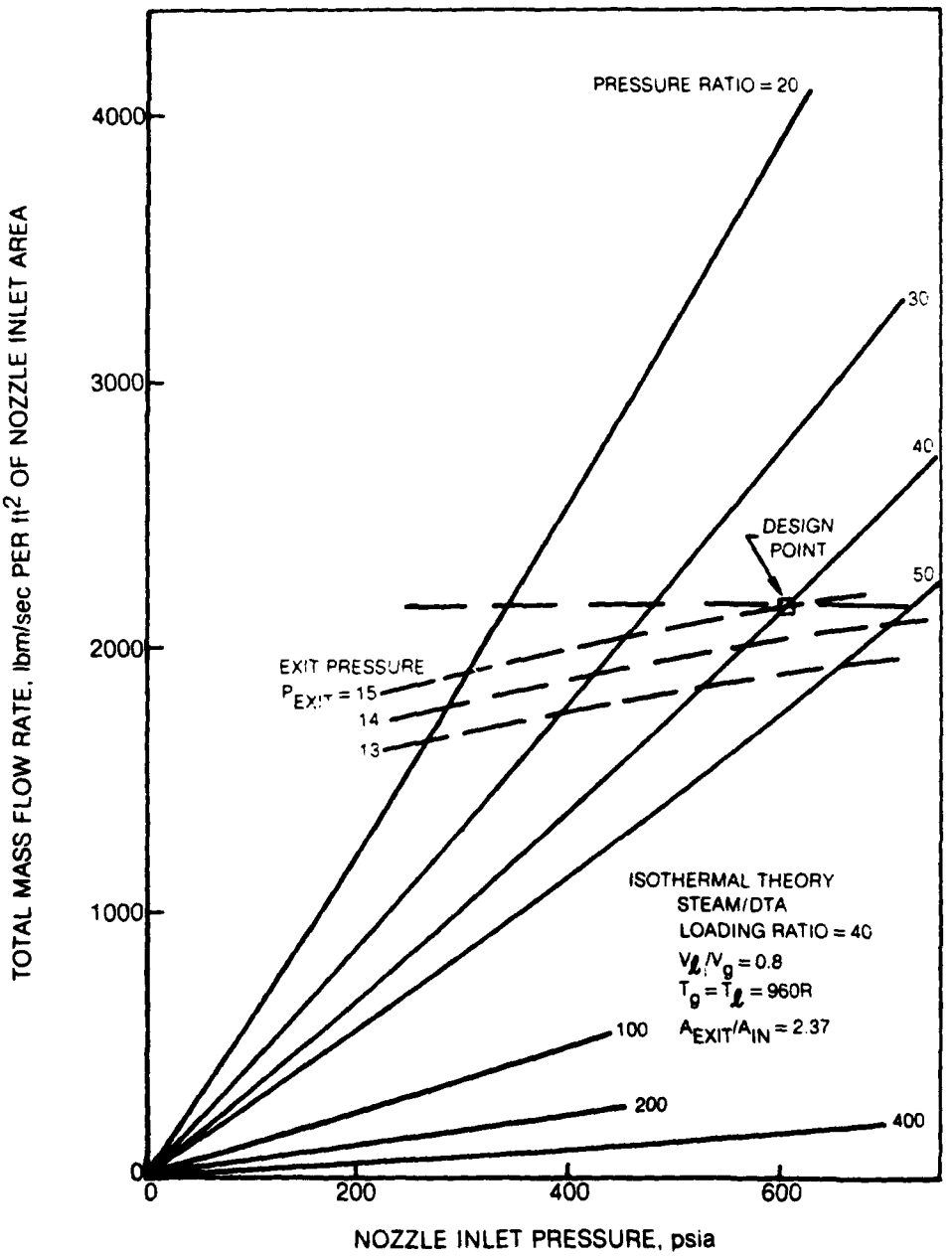

81-11-66-3

FIG. III.4

OFF-DESIGN PERFORMANCE OF TWO-PHASE NOZZLE

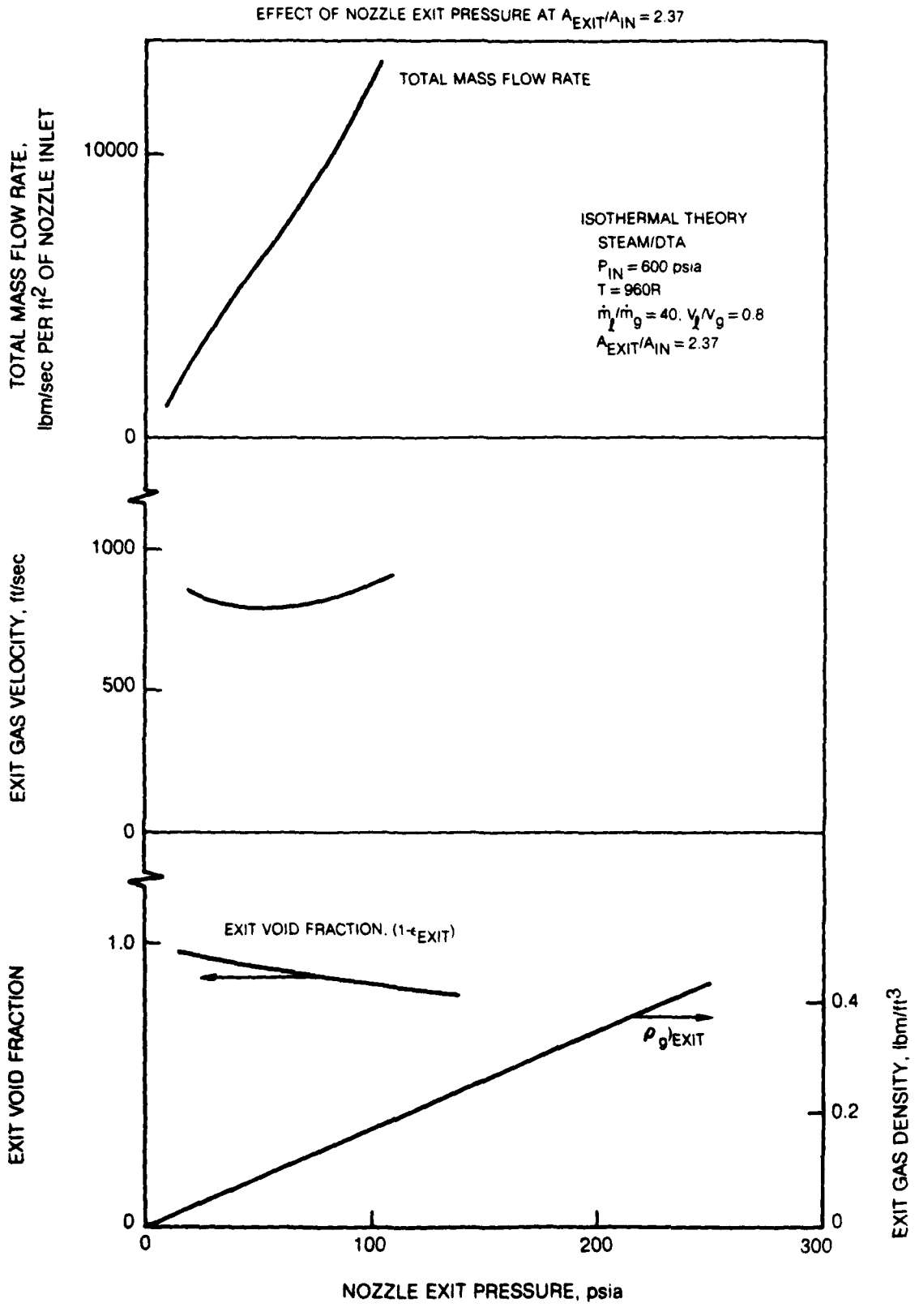

82-6-10-3

OFF-DESIGN PERFORMANCE OF TWO-PHASE NOZZLE

EFFECT OF NOZZLE EXIT PRESSURE

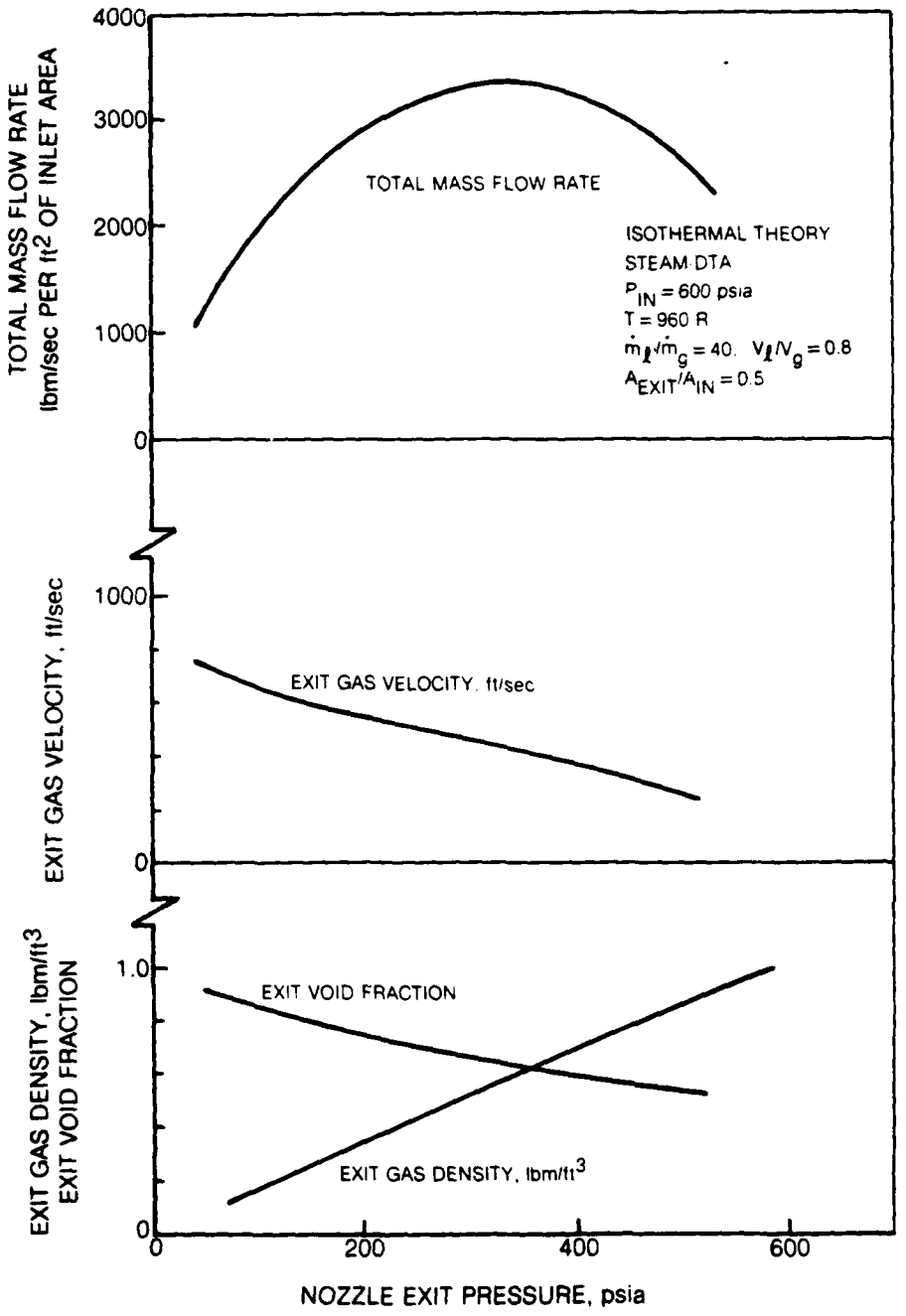

81-11-66-2

OFF-DESIGN NOZZLE EFFICIENCY

EFFECTS OF INLET PRESSURE AND PRESSURE RATIO

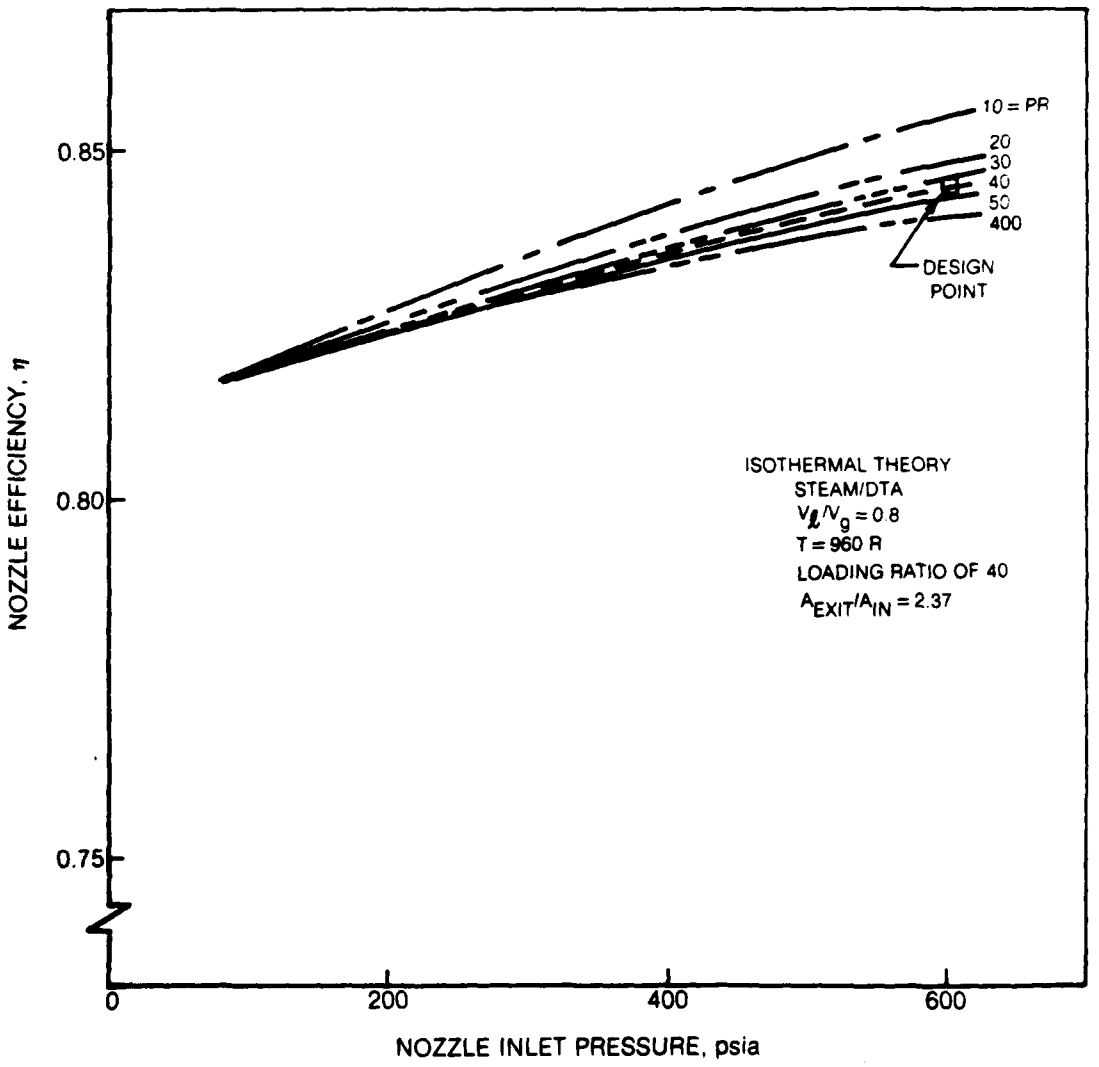

81-11-66-4

OFF-DESIGN NOZZLE PERFORMANCE

EFFECT OF LOADING RATIO

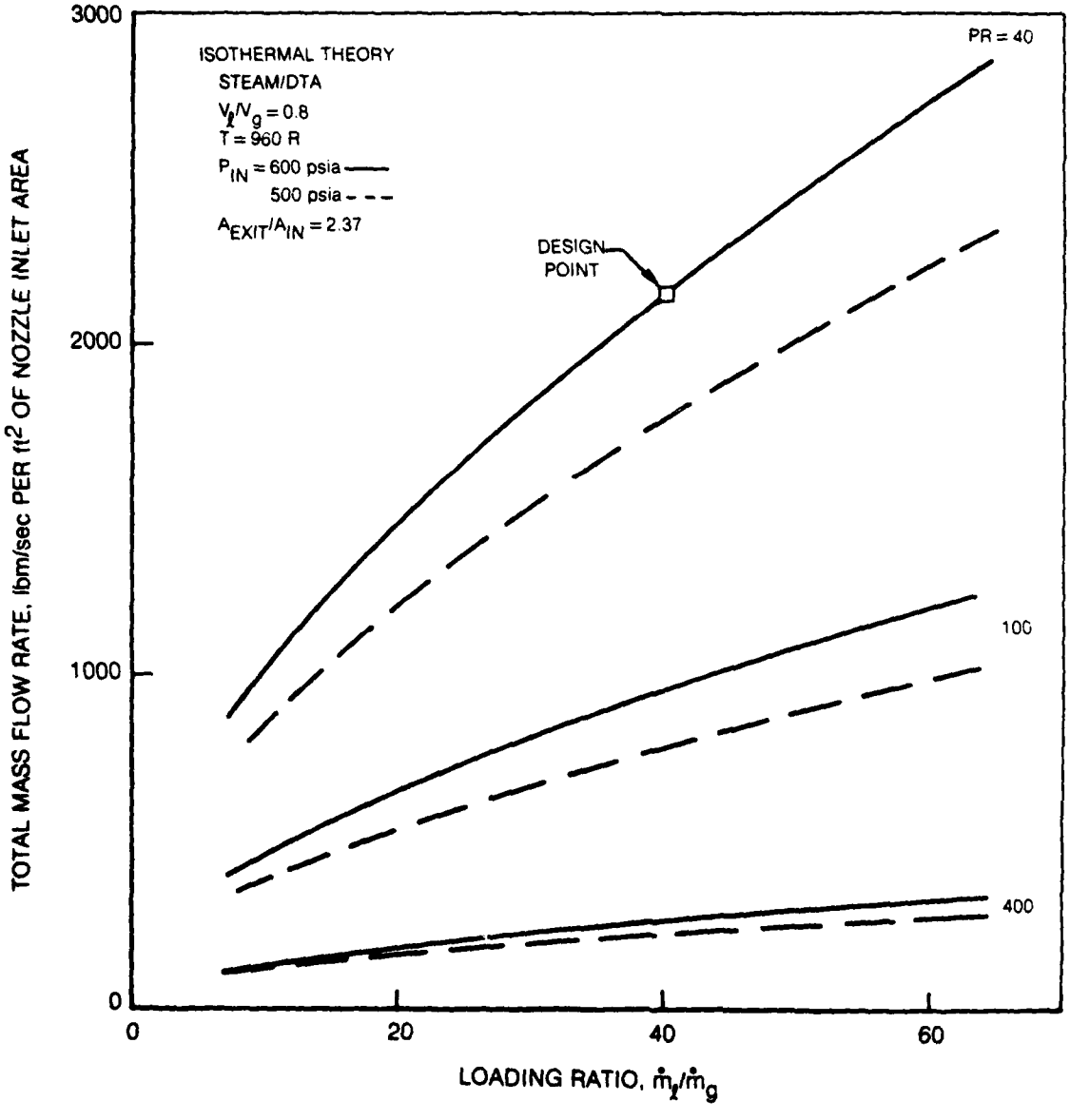

82-6-10-4

OFF-DESIGN NOZZLE EFFICIENCY

EFFECT OF LOADING RATIO

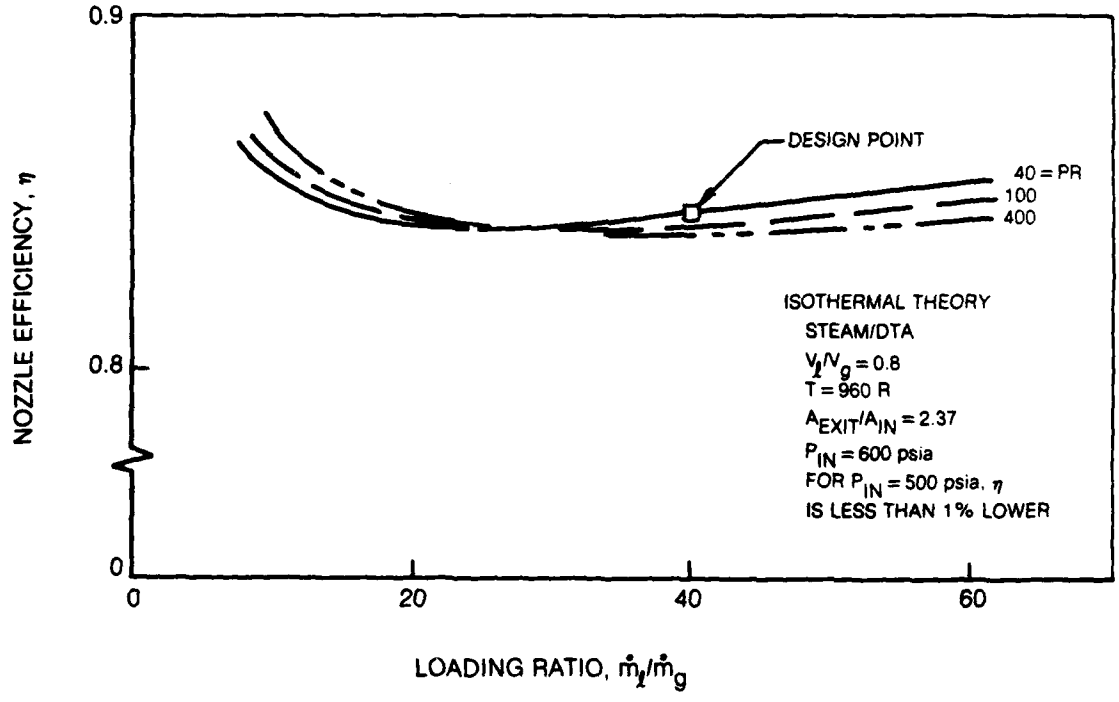

COMPARISON OF ISOTHERMAL OFF-DESIGN PREDICTION WITH AIR/WATER EXPERIMENTAL DATA

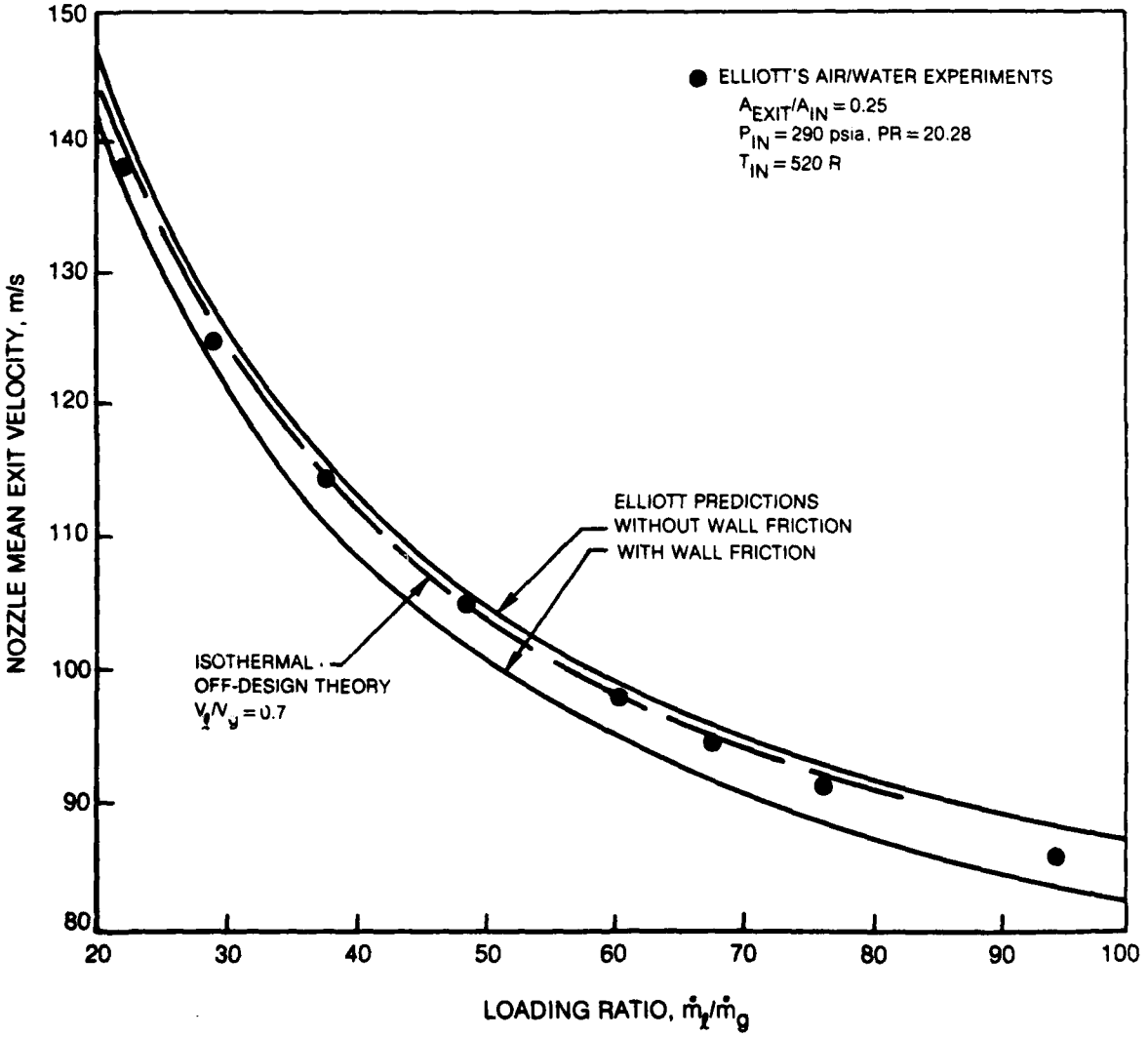

82-6-10-6

OFF-DESIGN PERFORMANCE

EFFECT OF INLET TEMPERATURE

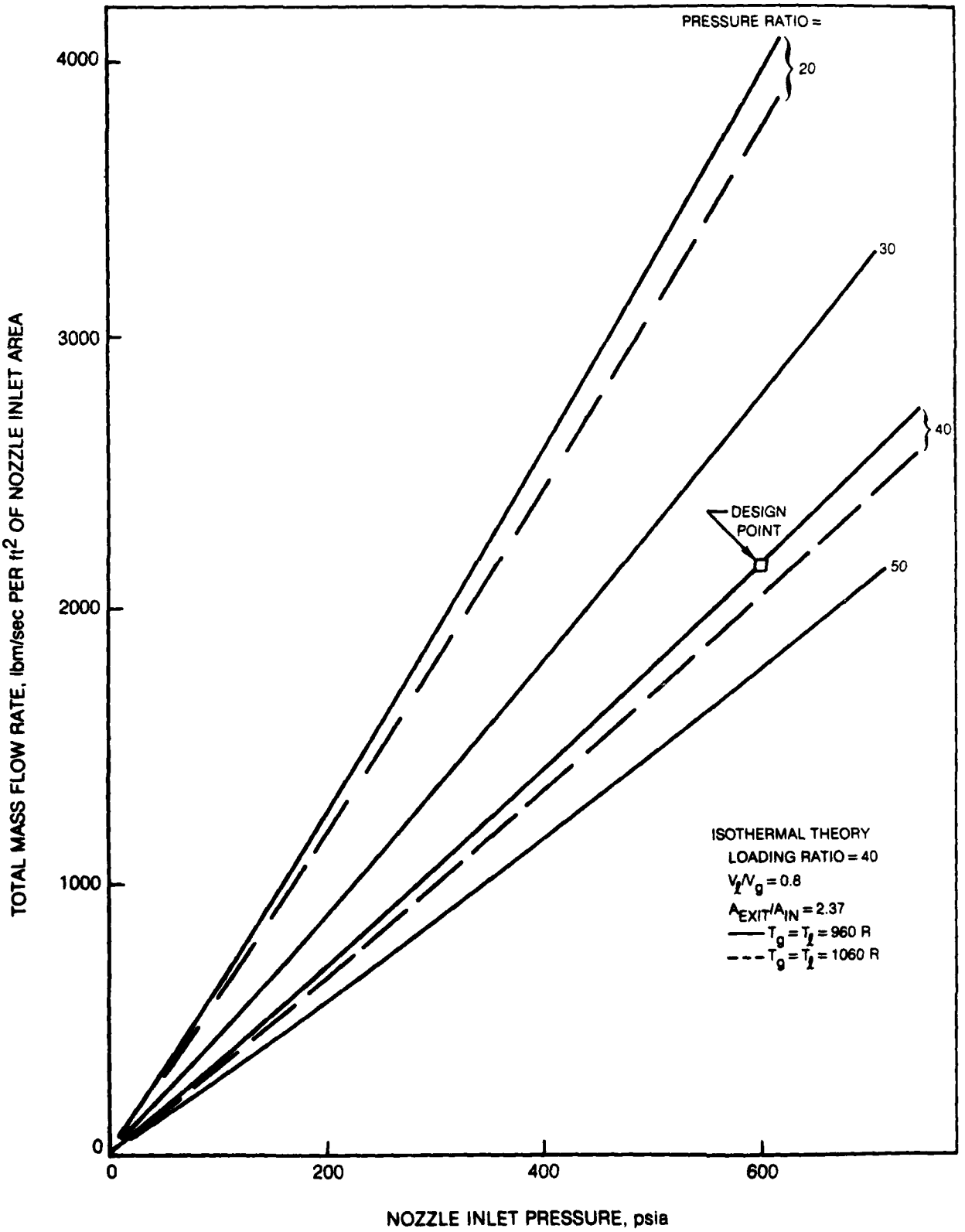

82-6-10-7

FIG. III.11

VELOCITY PARAMETER

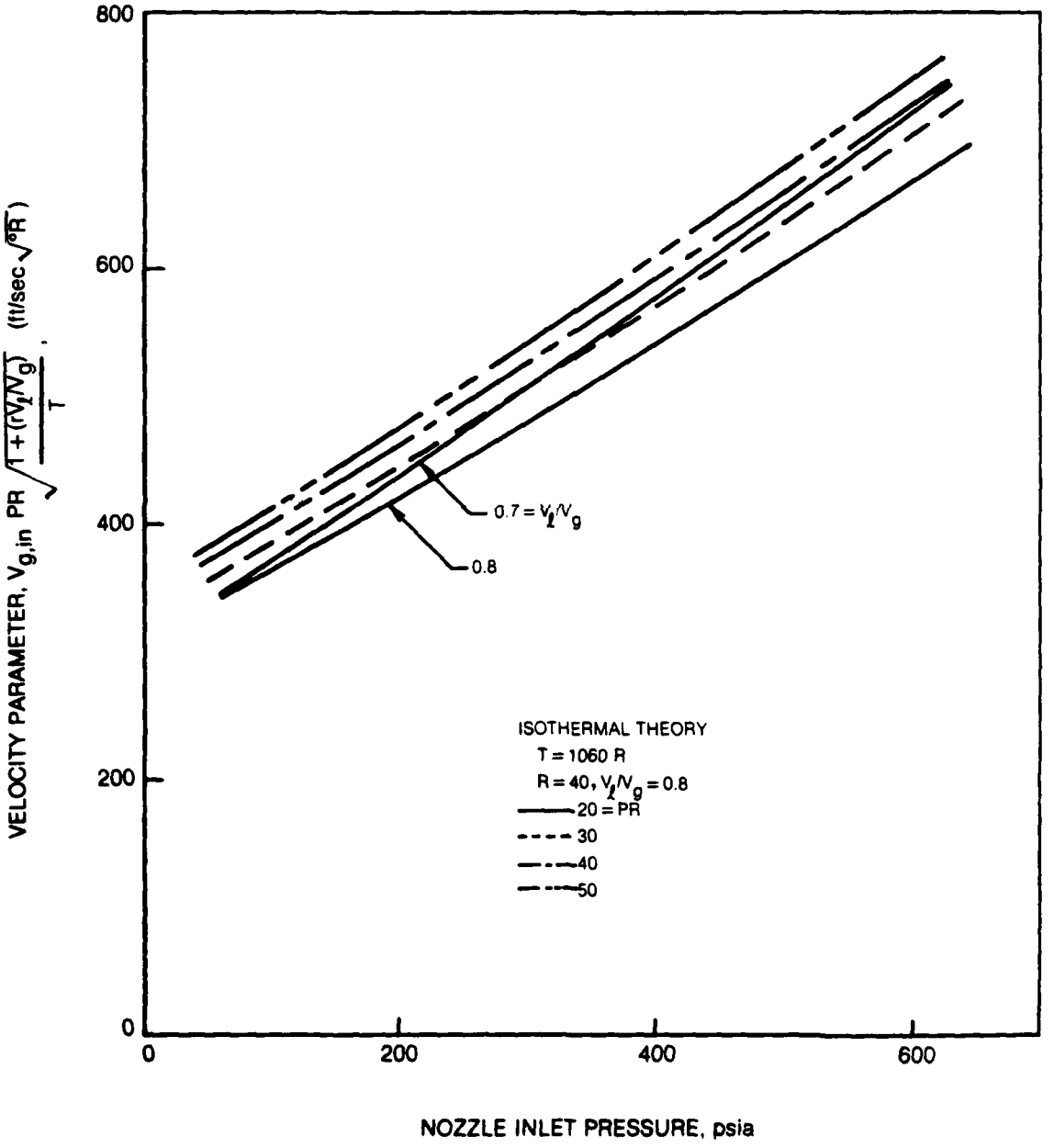

82-6-10-8

FIG. III 12

EFFECT OF DROPLET SIZE ON HEAT TRANSFER ENHANCEMENT

LOADING RATIO OF 10

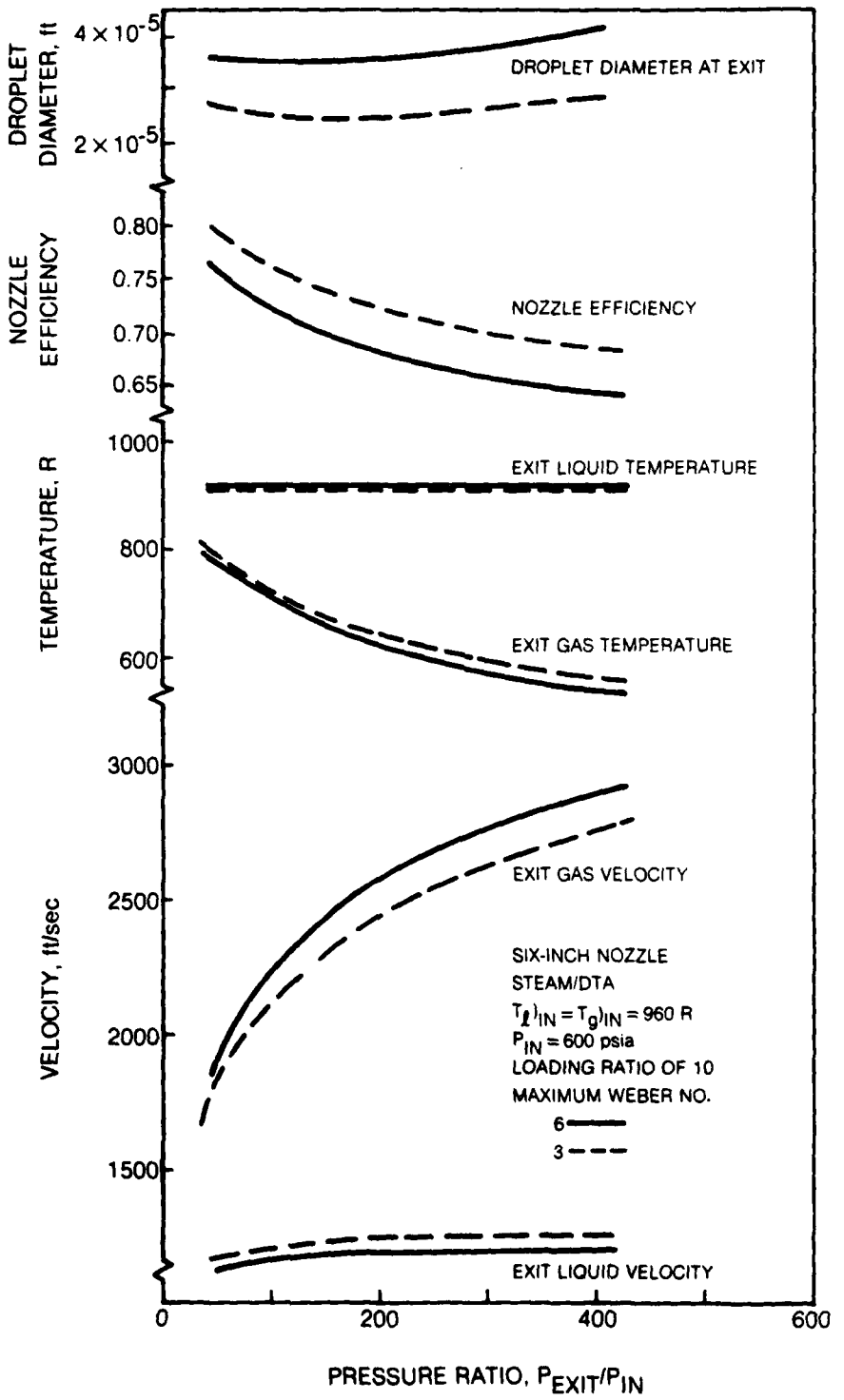

82-6-10-16

FIG. III.13

EFFECT OF DROPLET SIZE ON HEAT TRANSFER ENHANCEMENT

LOADING RATIO OF 40

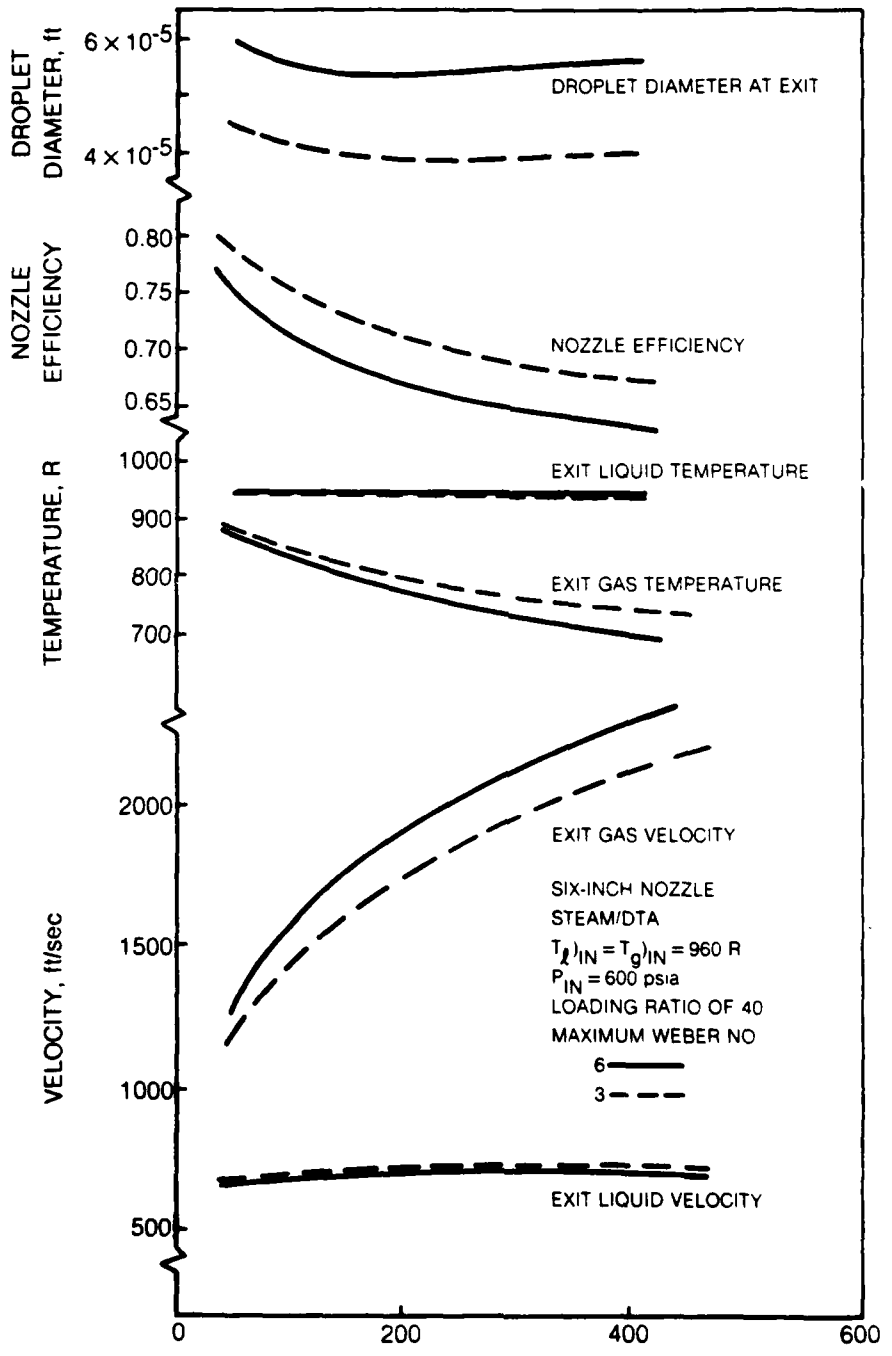

82-6-10-15

FIG. III.14

EFFECT OF DROPLET HEAT TRANSFER ENHANCEMENT ON NOZZLE PERFORMANCE

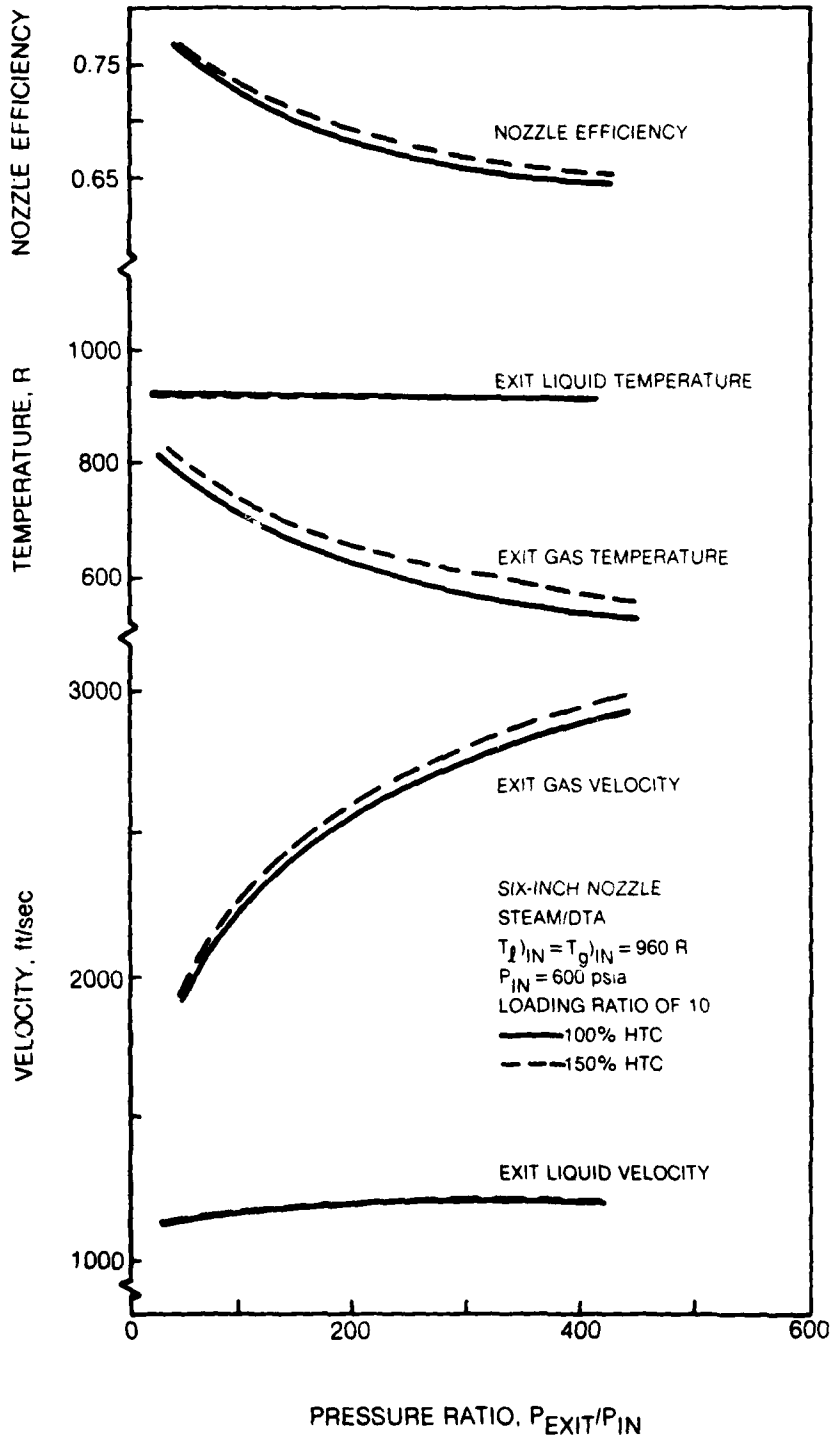

82-6-10-14

EFFECT OF ADIABATIC DROPLETS ON NOZZLE PERFORMANCE PREDICTIONS

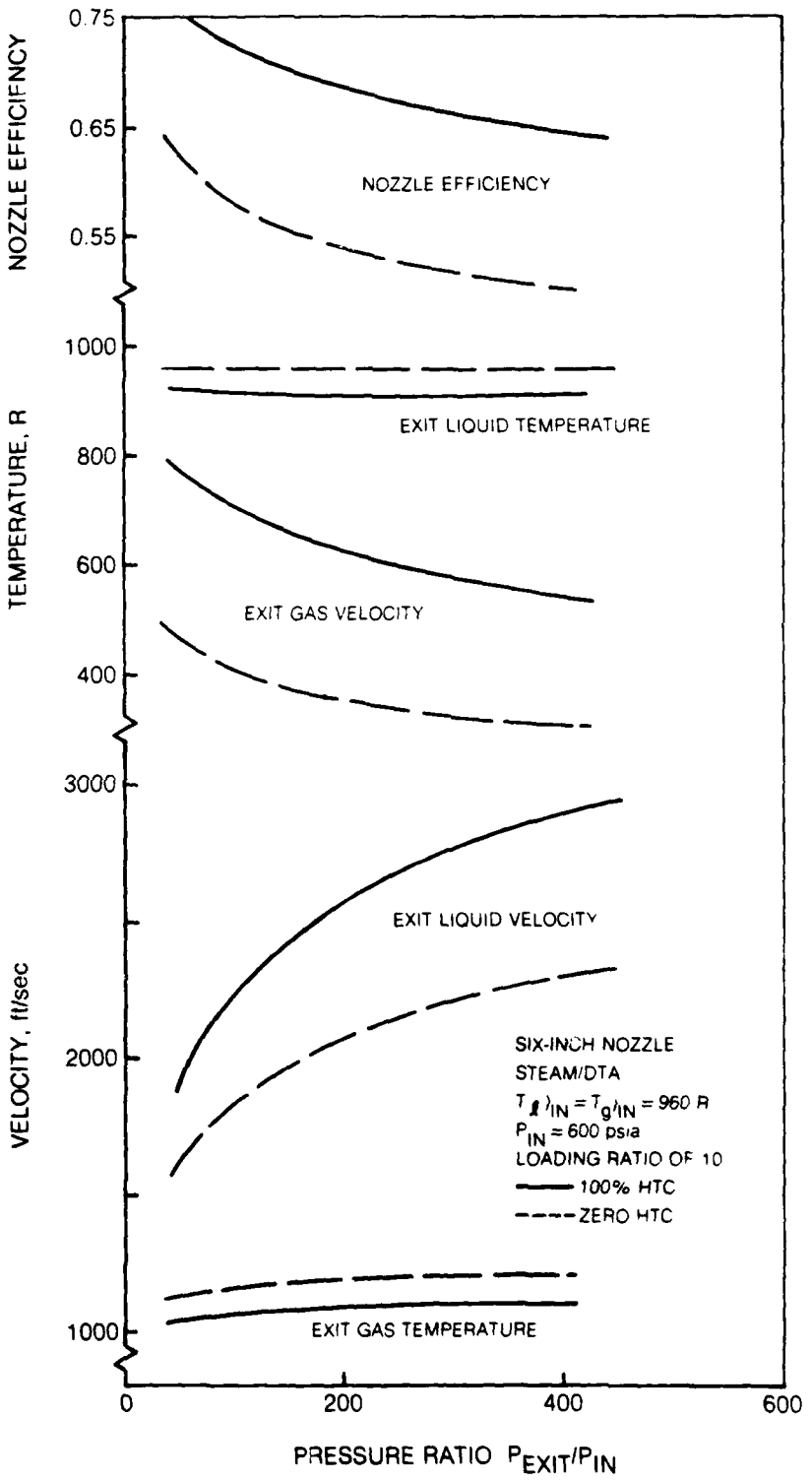

82-3-116-1

TEMPERATURE AND VELOCITY IN NOZZLE THROAT: r = 10

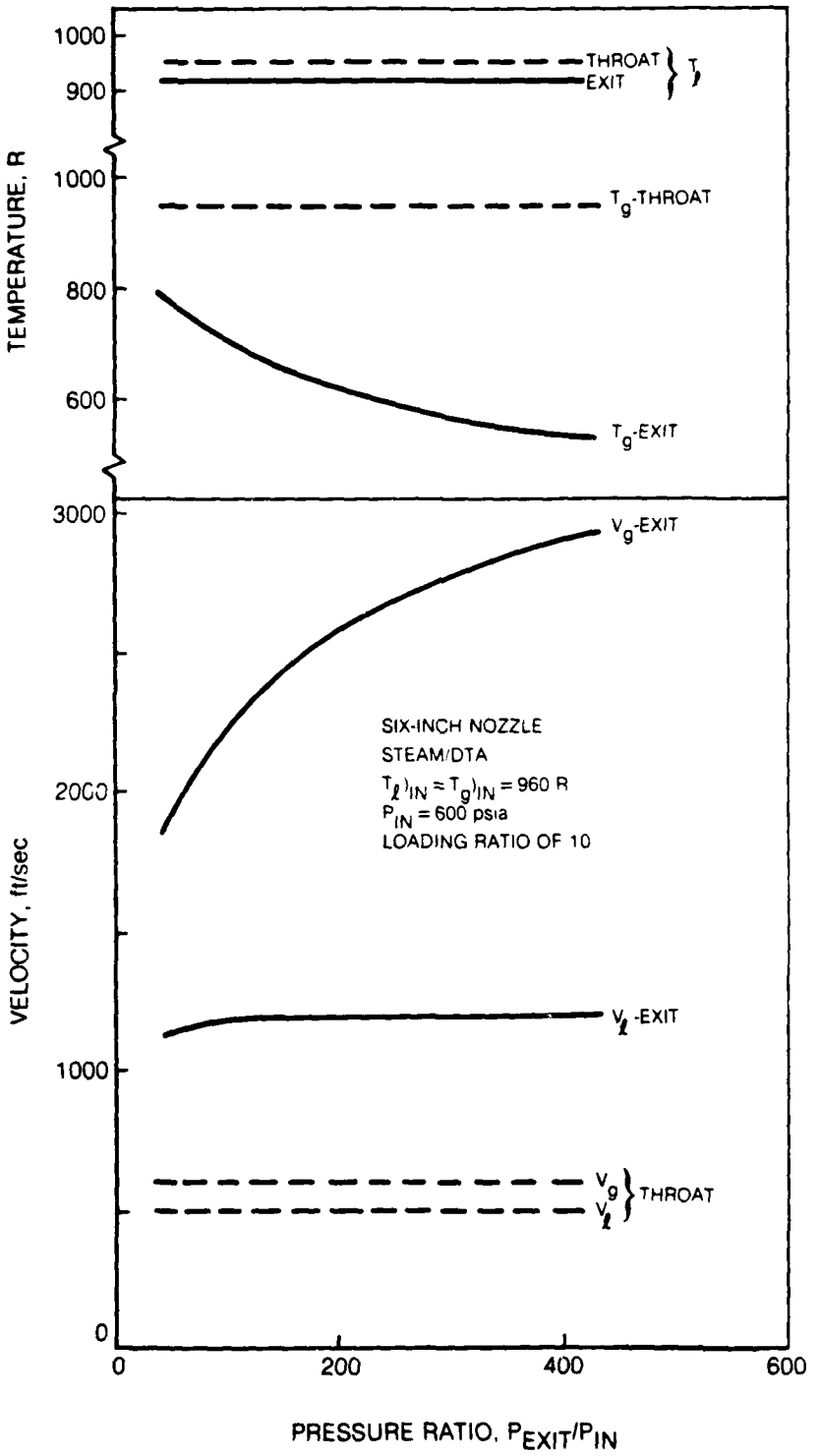

82-6-10-13

TEMPERATURE AND VELOCITY IN NOZZLE THROAT: $r = 40$

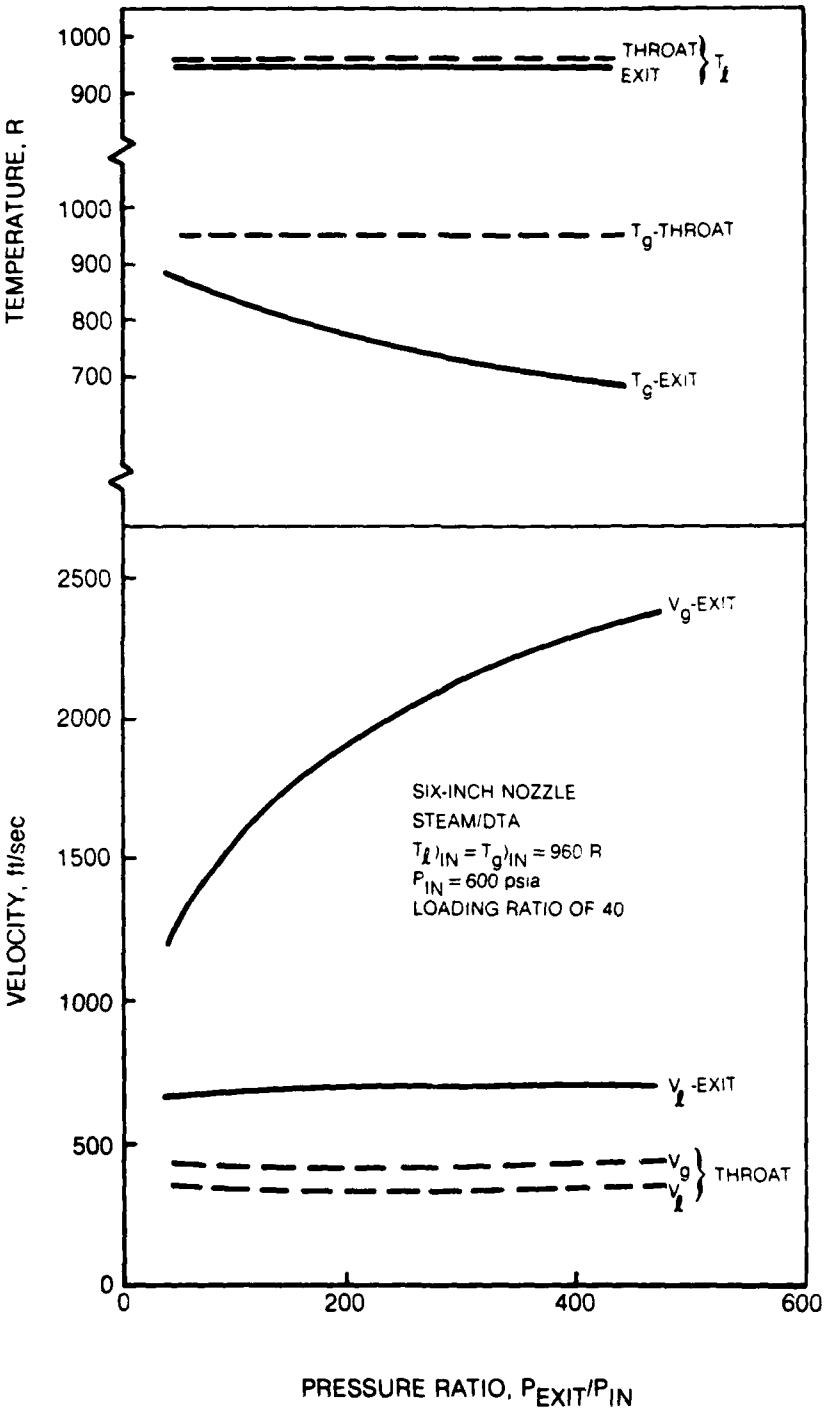

EXPONENTIAL PRESSURE PROFILE

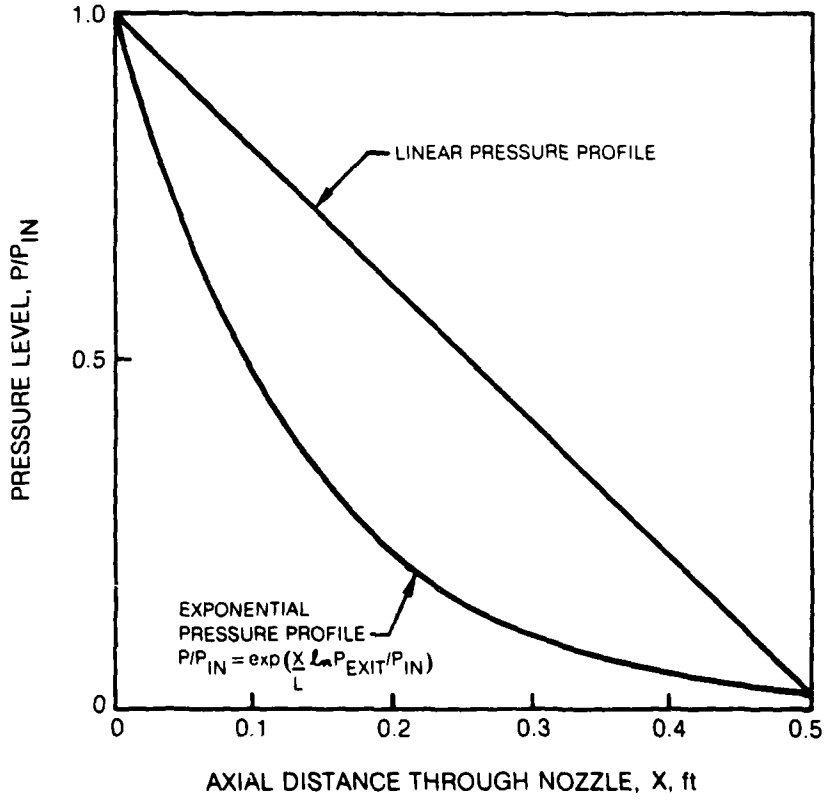

82-6-10-11

EFFECT OF PRESSURE PROFILE ON NOZZLE PERFORMANCE CHARACTERISTICS

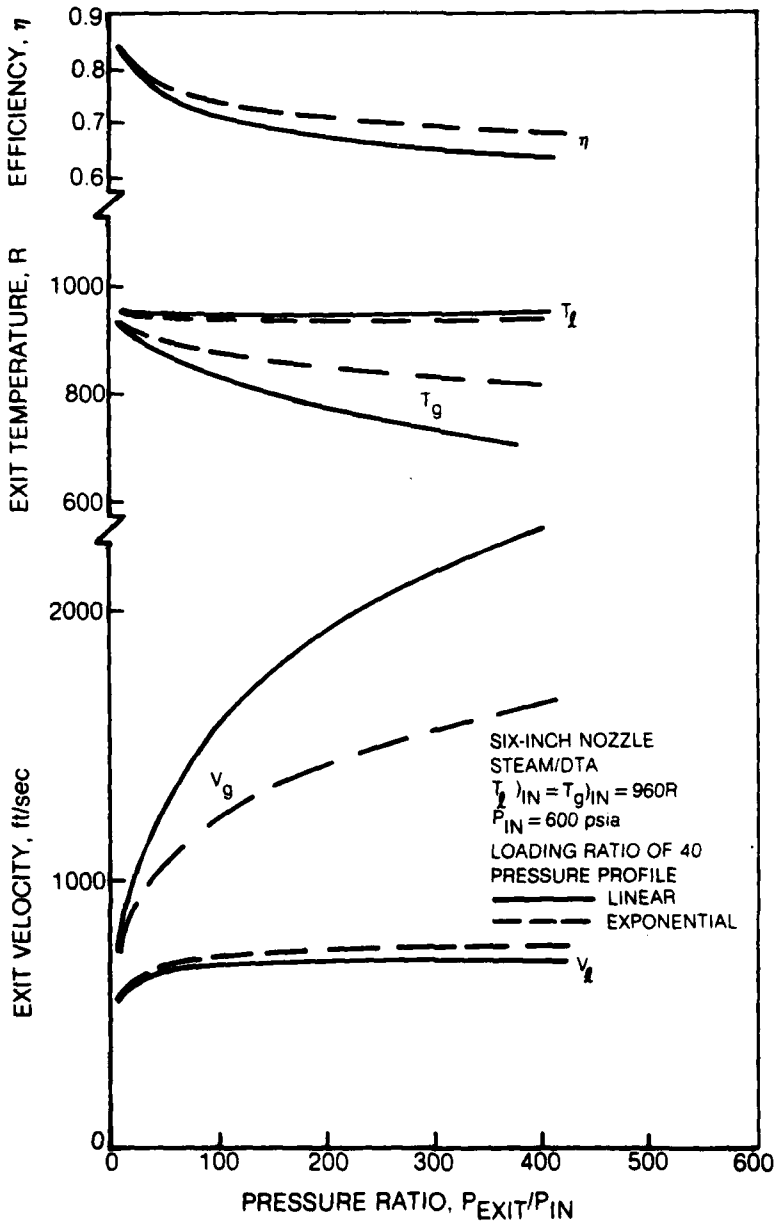

FIG. III.20

EFFECT OF PRESSURE PROFILE ON NOZZLE DIAMETER PROFILE

PRESSURE RATIO OF 50

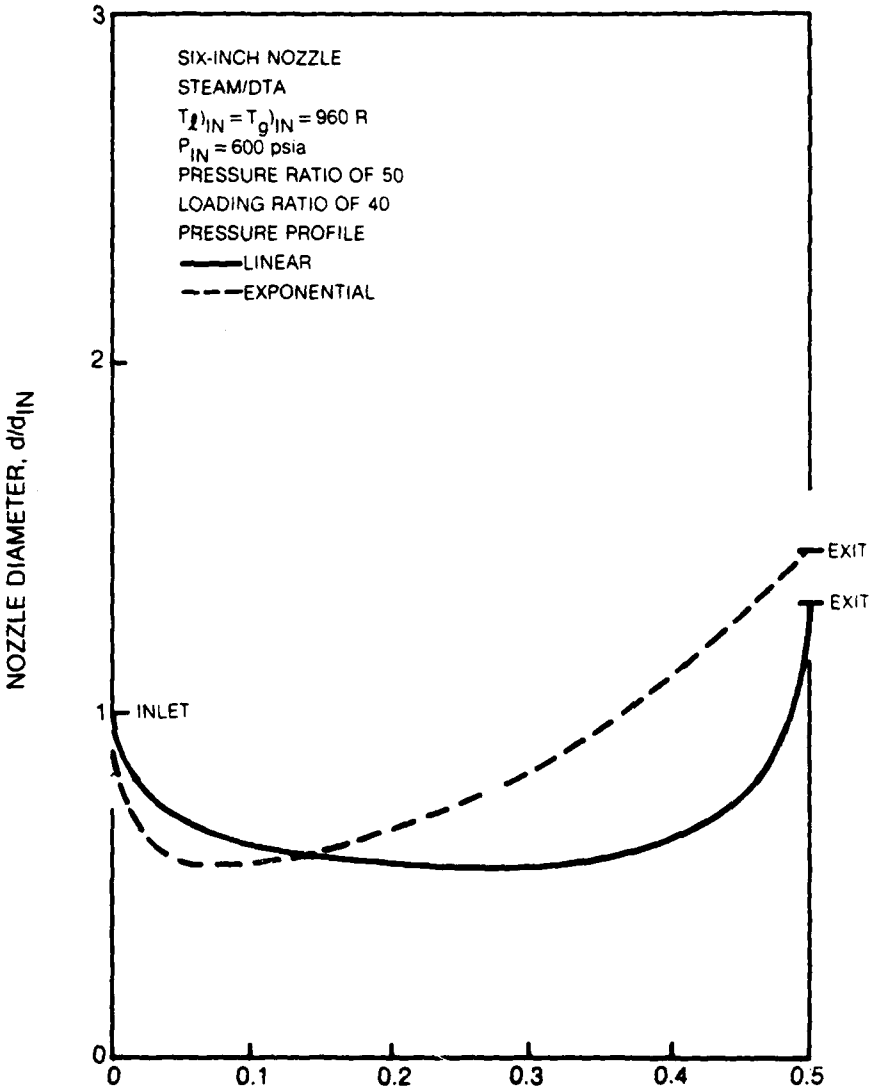

82-6-10-10

EFFECT OF PRESSURE PROFILE ON NOZZLE DIAMETER PROFILE

PRESSURE RATIO OF 400

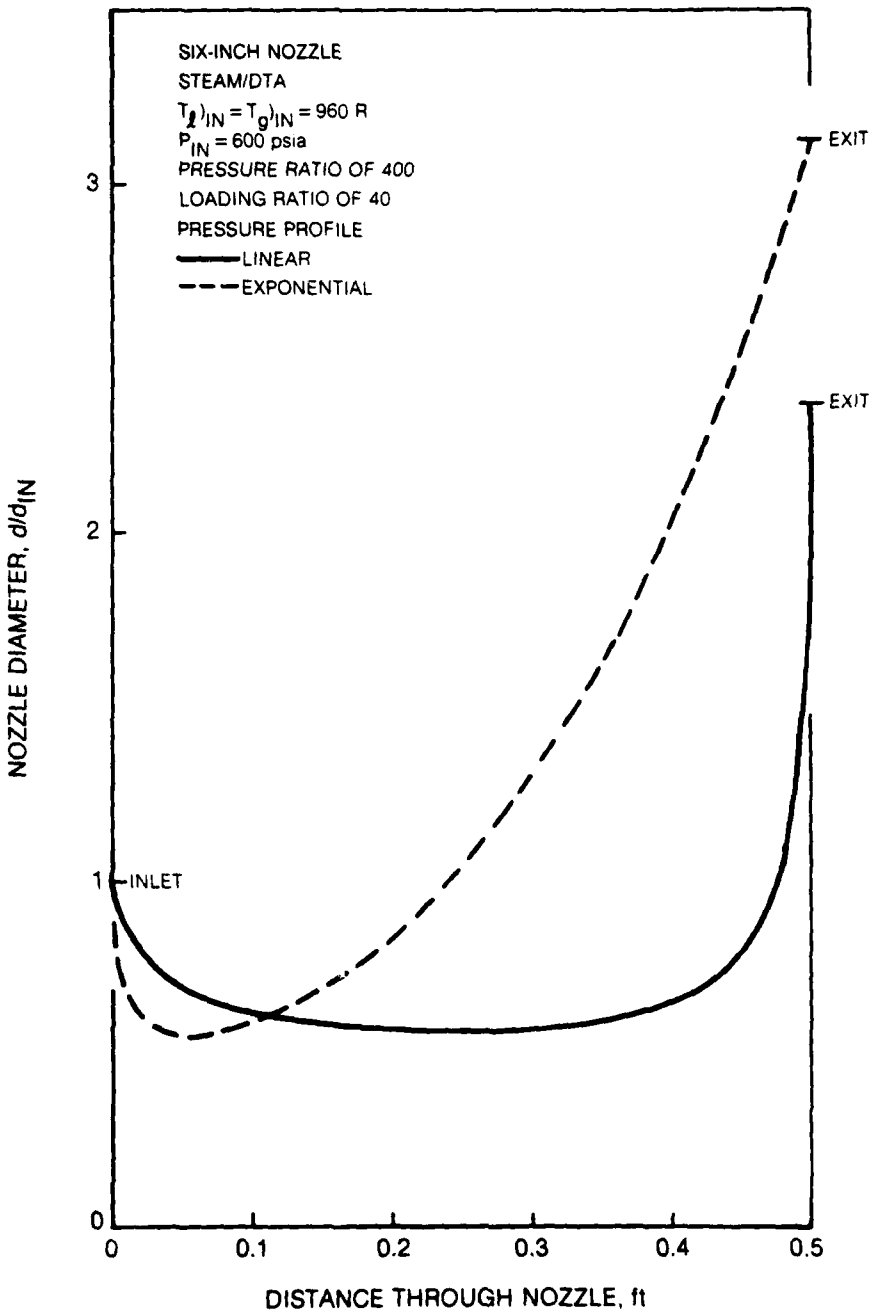

82-6-10-9

SONIC VELOCITY OF TWO-PHASE MIXTURES

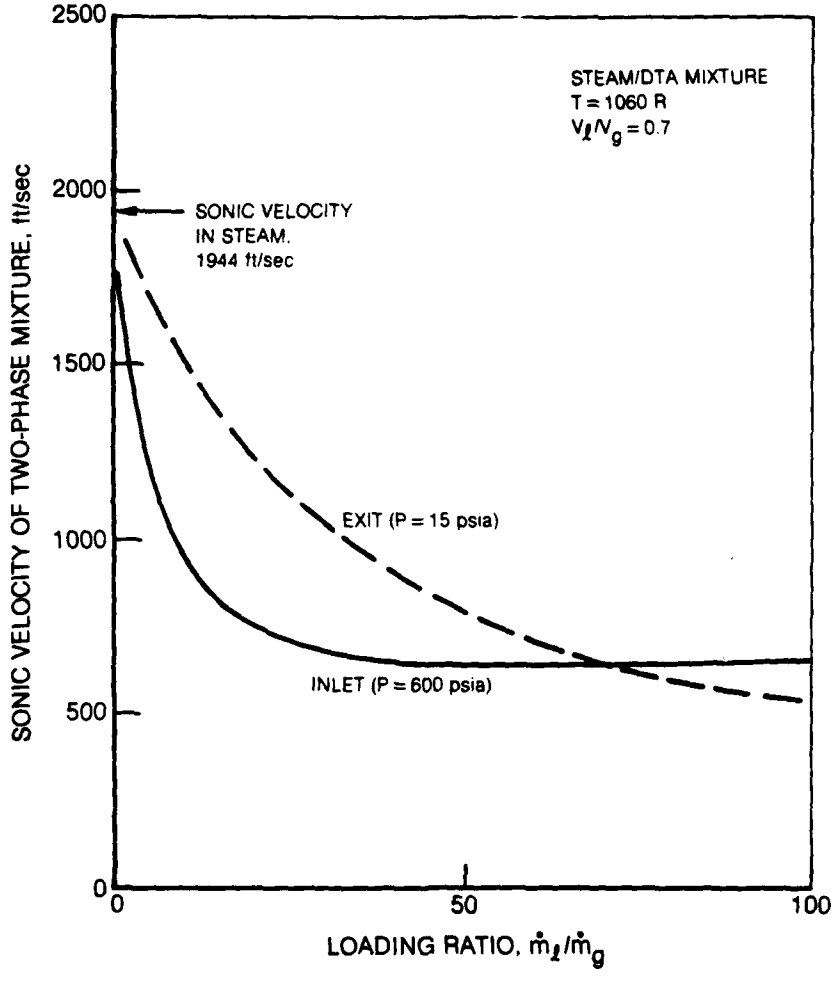

COMPARISON OF TWO-PHASE SONIC VELOCITIES

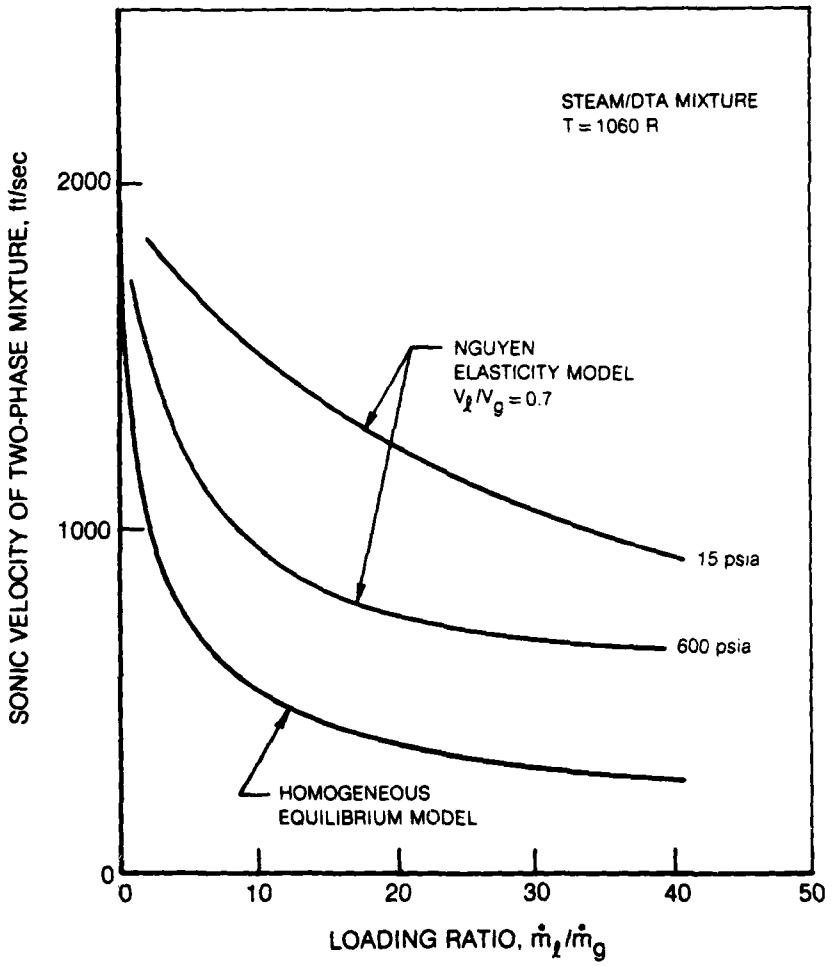

SONIC VELOCITY AND MACH NUMBER IN TWO-PHASE NOZZLE

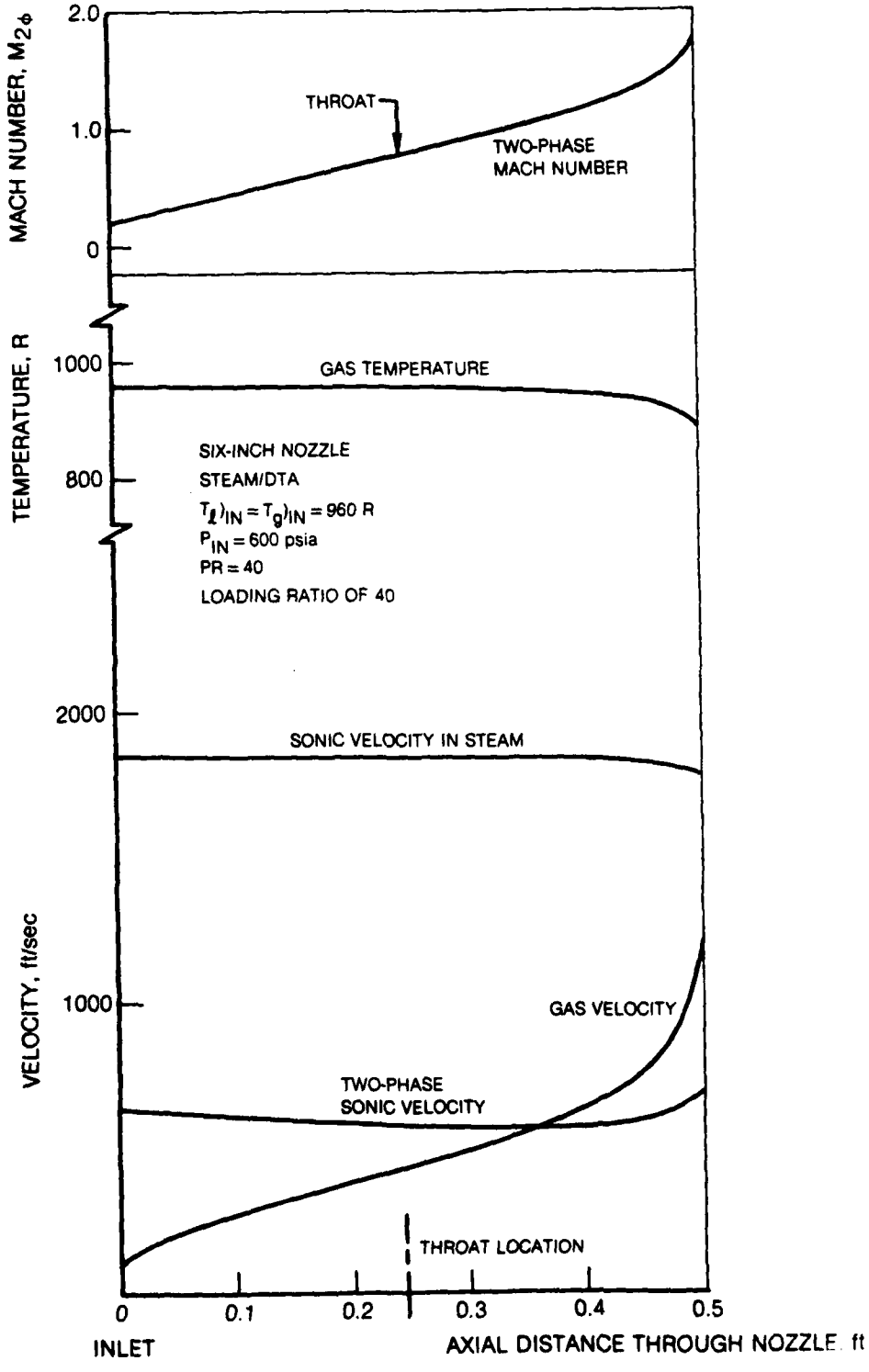

82-6-10-19

FIG. III. 25

LOCAL DROPLET SIZE AND VELOCITIES FOR PR = 40

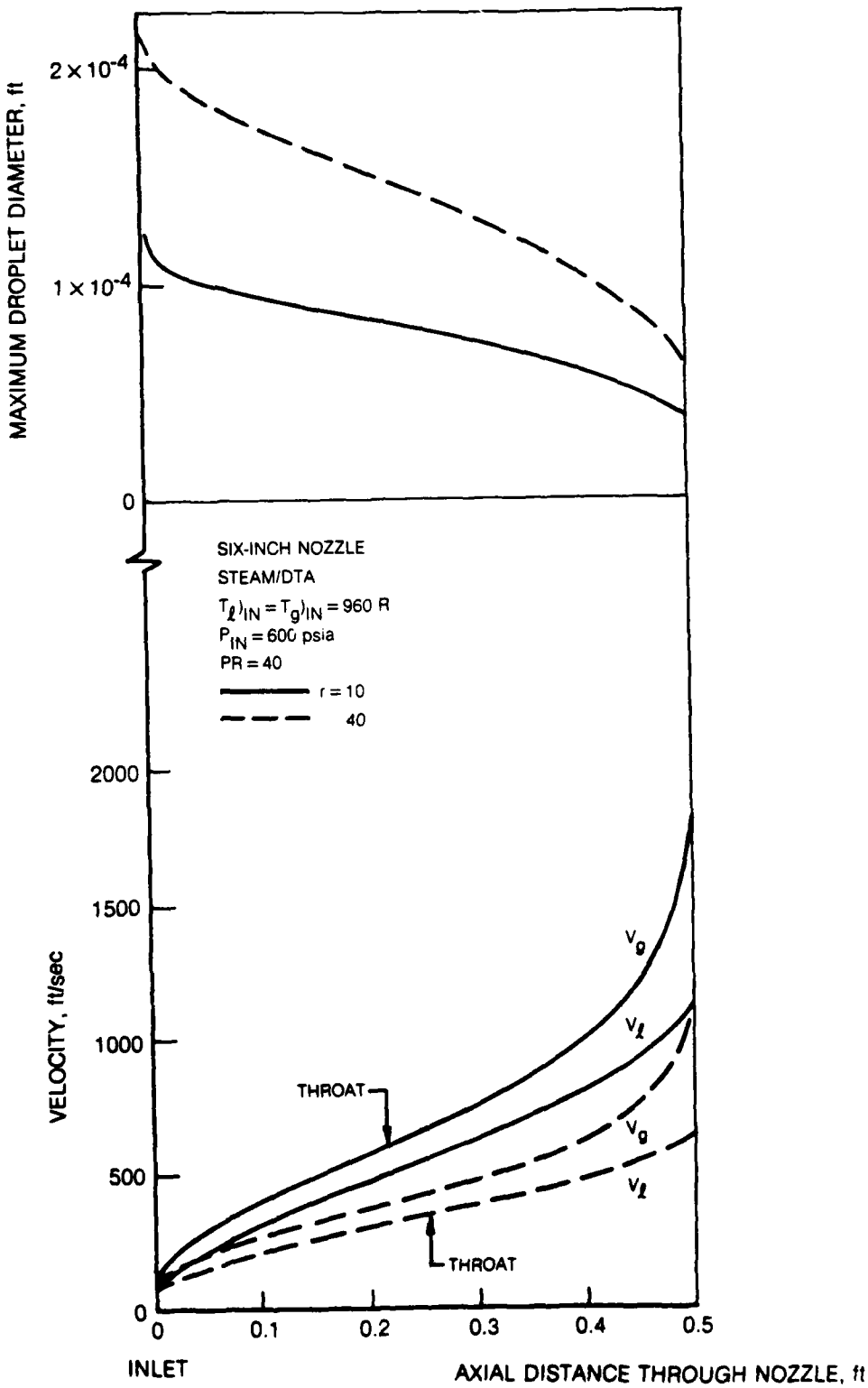

82-6-10-20

LOCAL DROPLET SIZE AND VELOCITIES FOR PR = 100

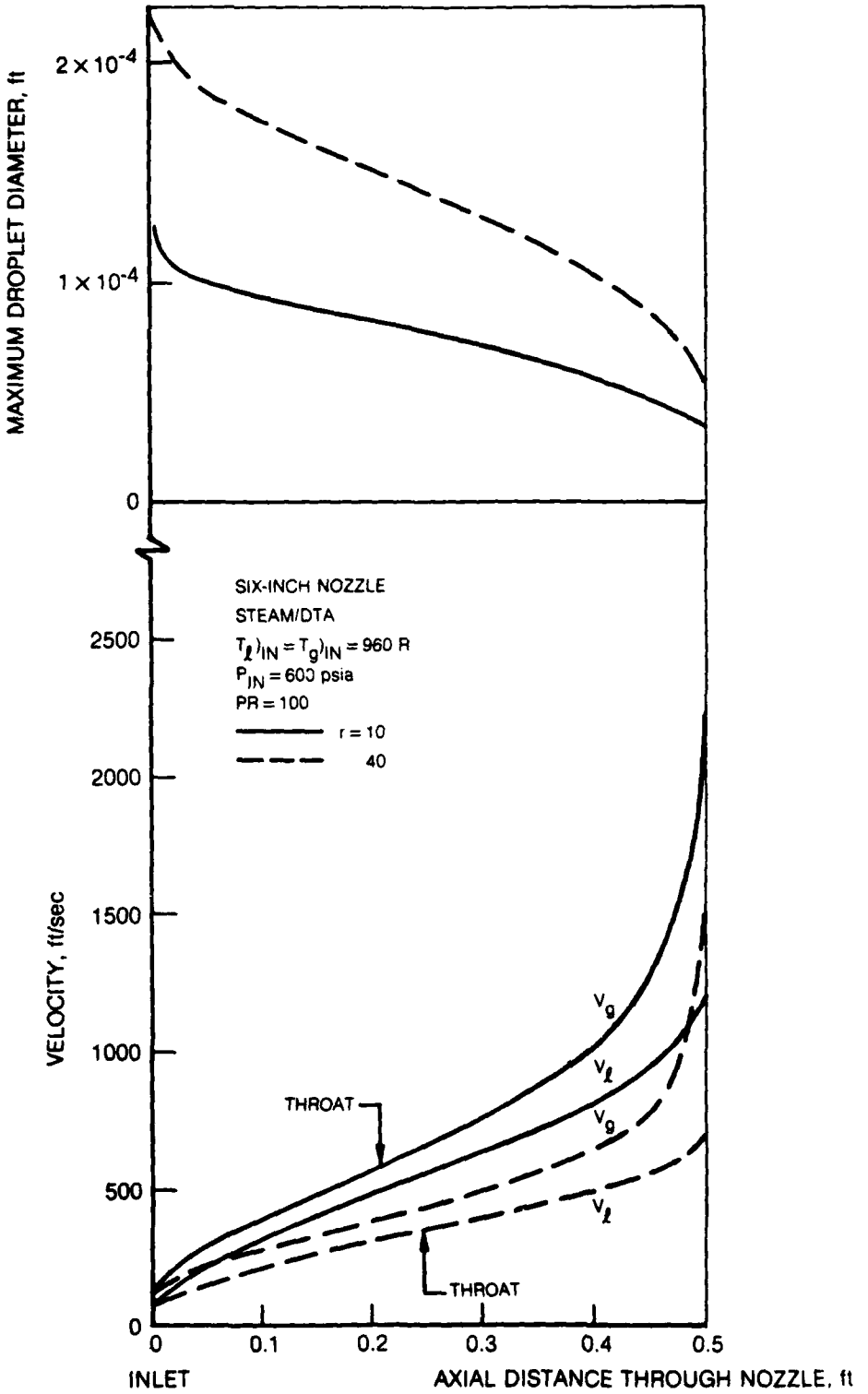

82-6-10-21

FOSSIL-FUEL-FIRED TWO-PHASE TURBINE SYSTEM

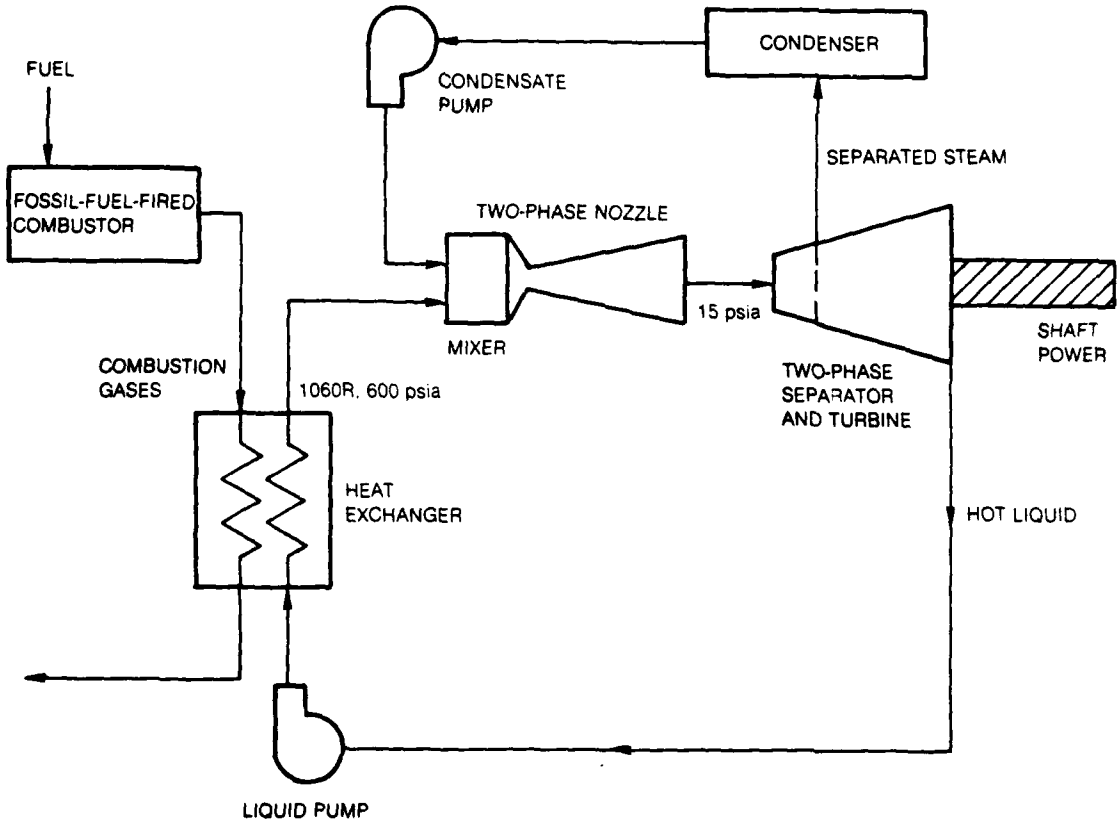

82-6-10-27

SOLAR-POWERED TWO-PHASE TURBINE SYSTEM

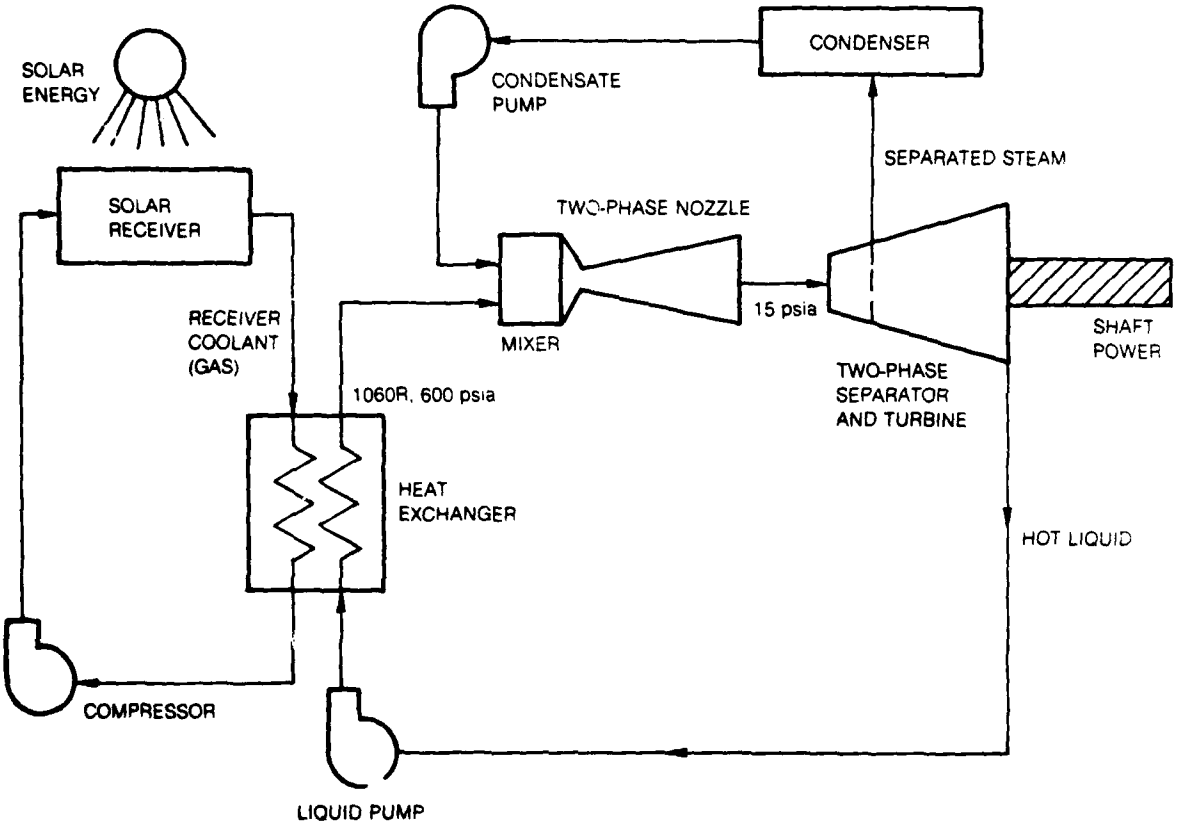

NUCLEAR-POWERED TWO-PHASE TURBINE SYSTEM

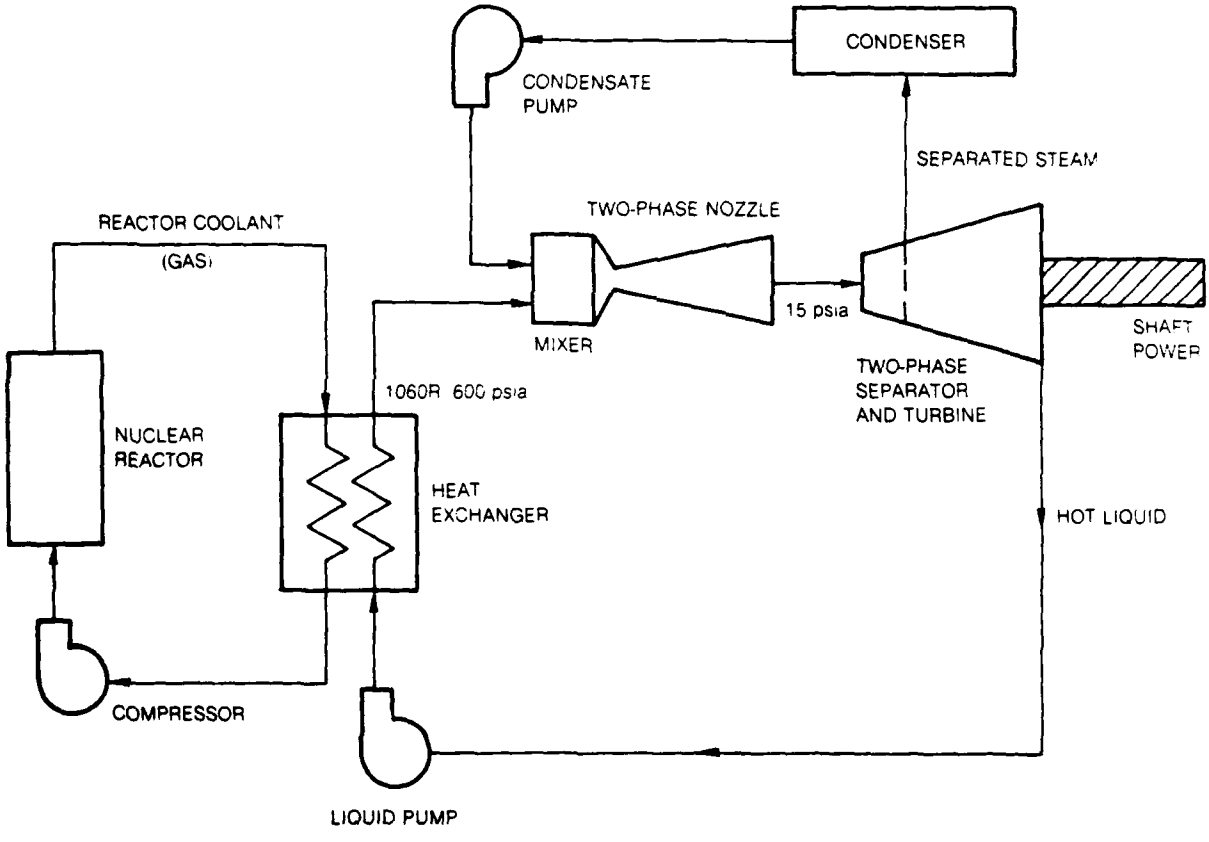

82-6-10-25

FIG. III.30

GEOTHERMAL TWO-PHASE TURBINE SYSTEM

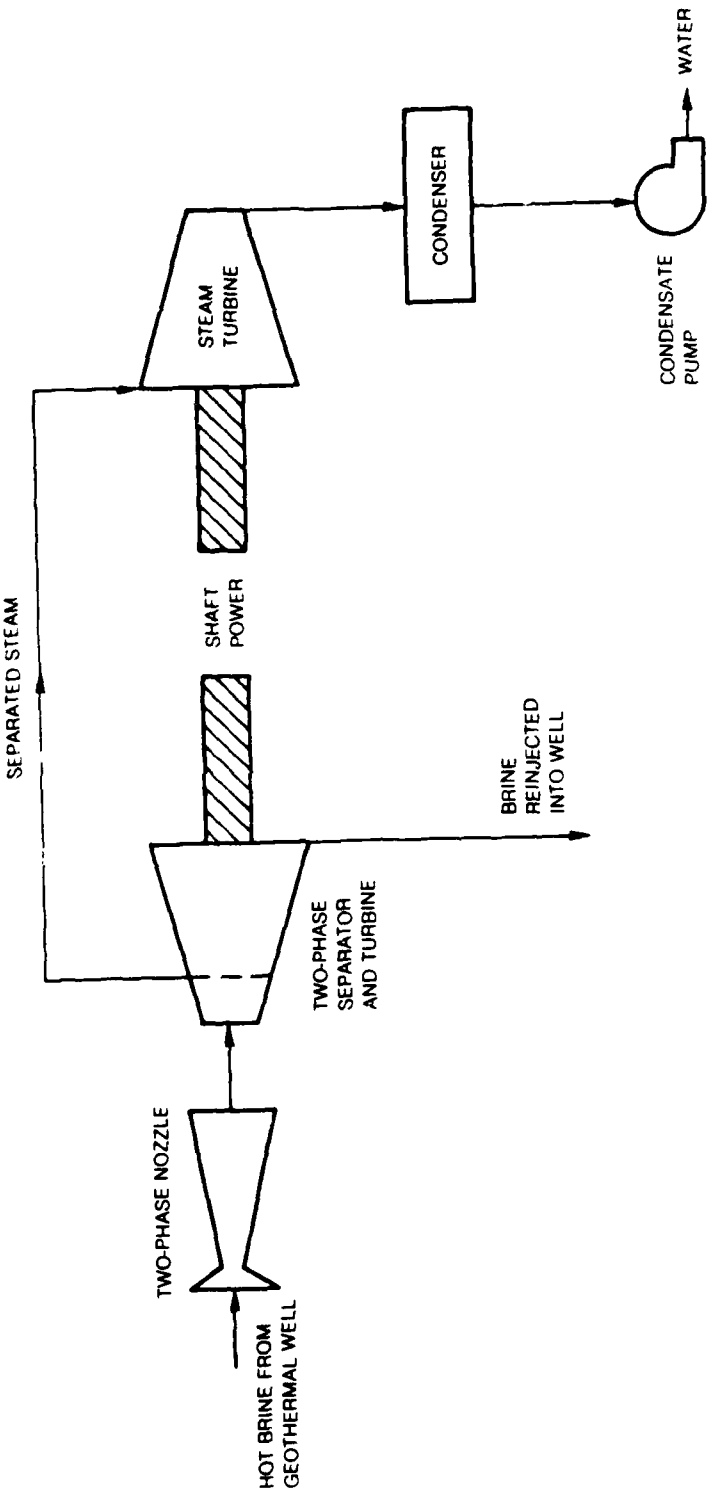

82-6-10-24

TWO-PHASE TURBINE SYSTEM FOR WASTE HEAT RECOVERY — TWO-COMPONENT SYSTEM

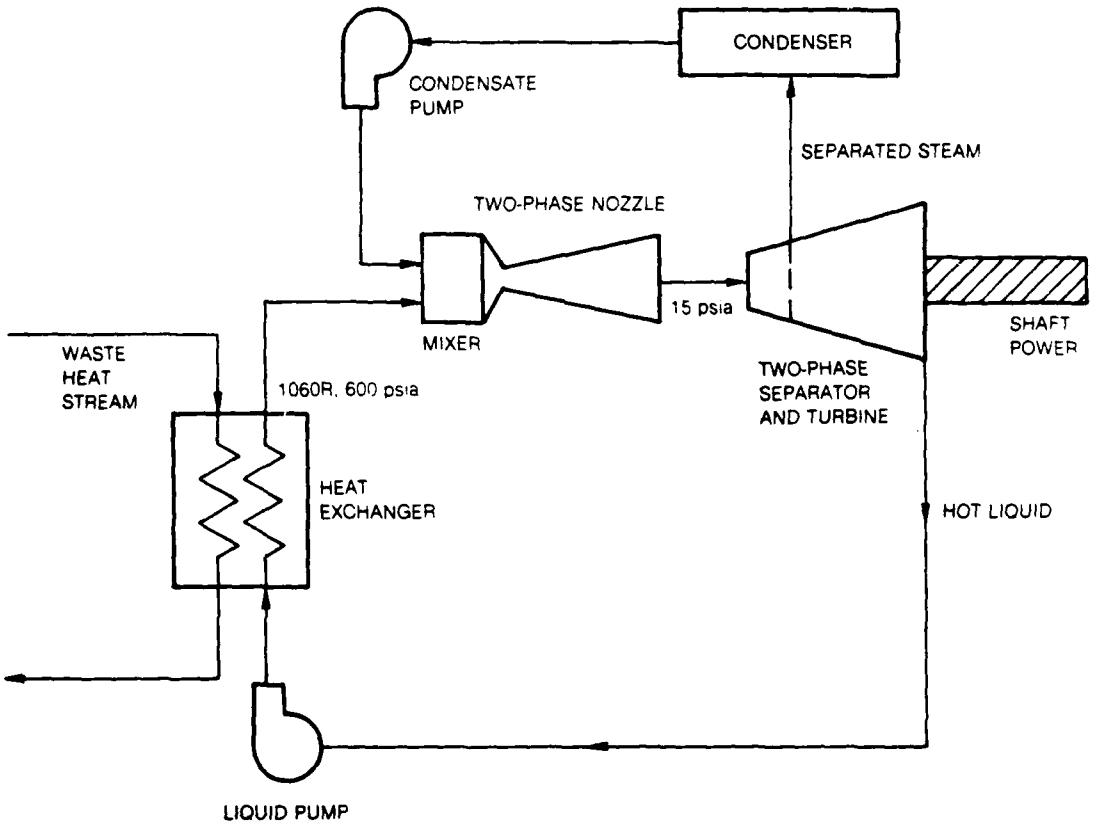

82-6-10-23

FIG. III.32

TWO-PHASE TURBINE SYSTEM FOR WASTE HEAT RECOVERY — ONE-COMPONENT SYSTEM

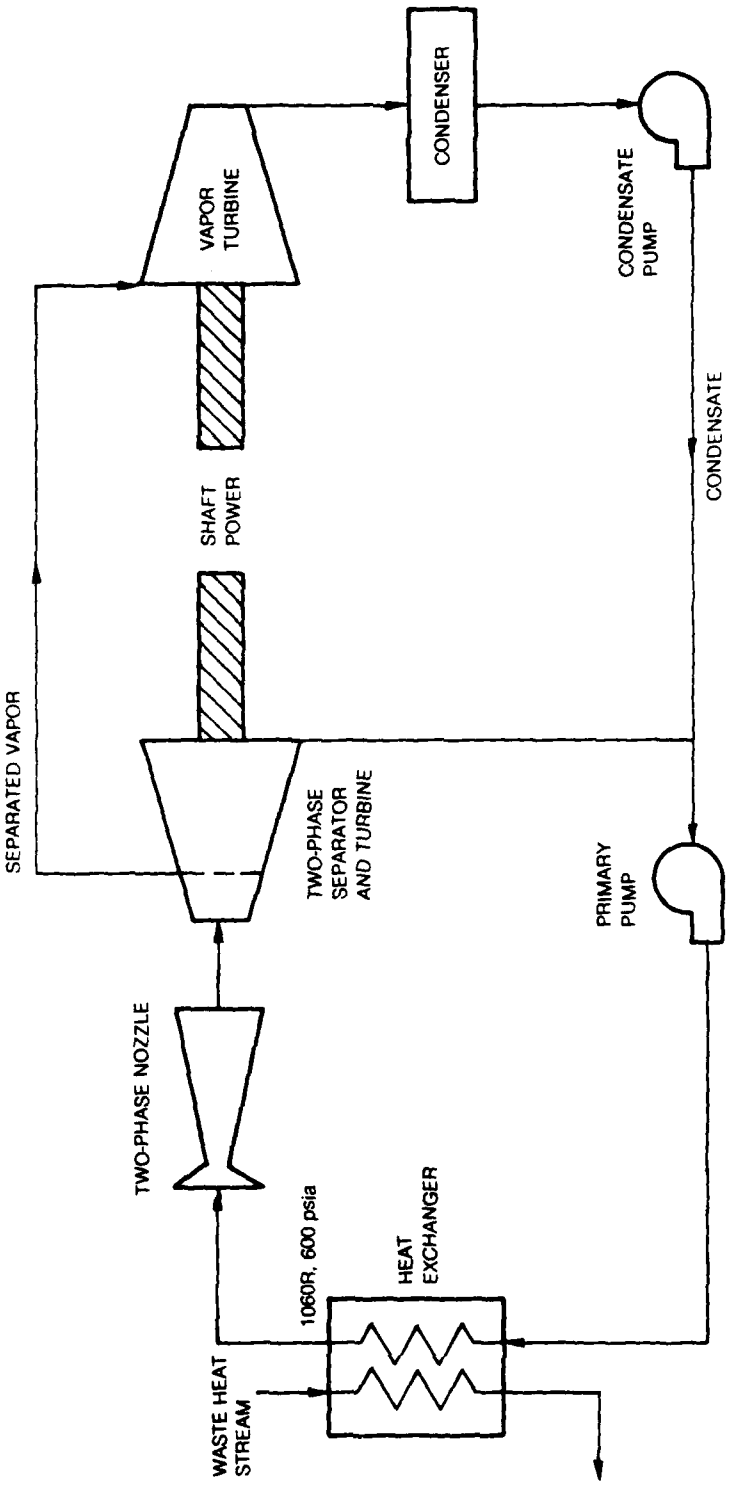

82-6-10-22

NOZZLE DESIGN FOR AIR/WATER EXPERIMENTS

DESIGN CONDITIONS

P_{IN} = 150 psia; PR = 10

$T_{\ell})_{IN} = T_{g})_{IN}$ = 520R

LOADING RATIO OF 40

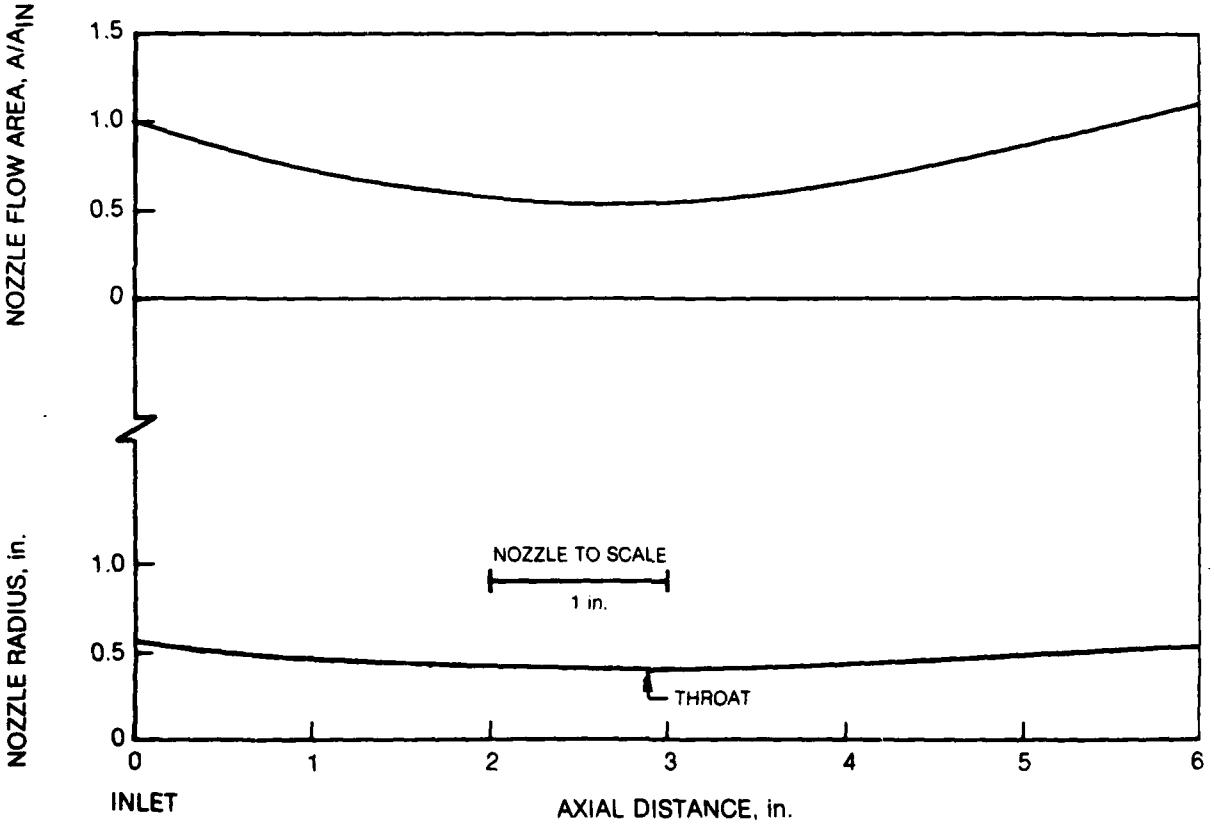

82-6-10-28

OFF-DESIGN PERFORMANCE OF AIR/WATER NOZZLE

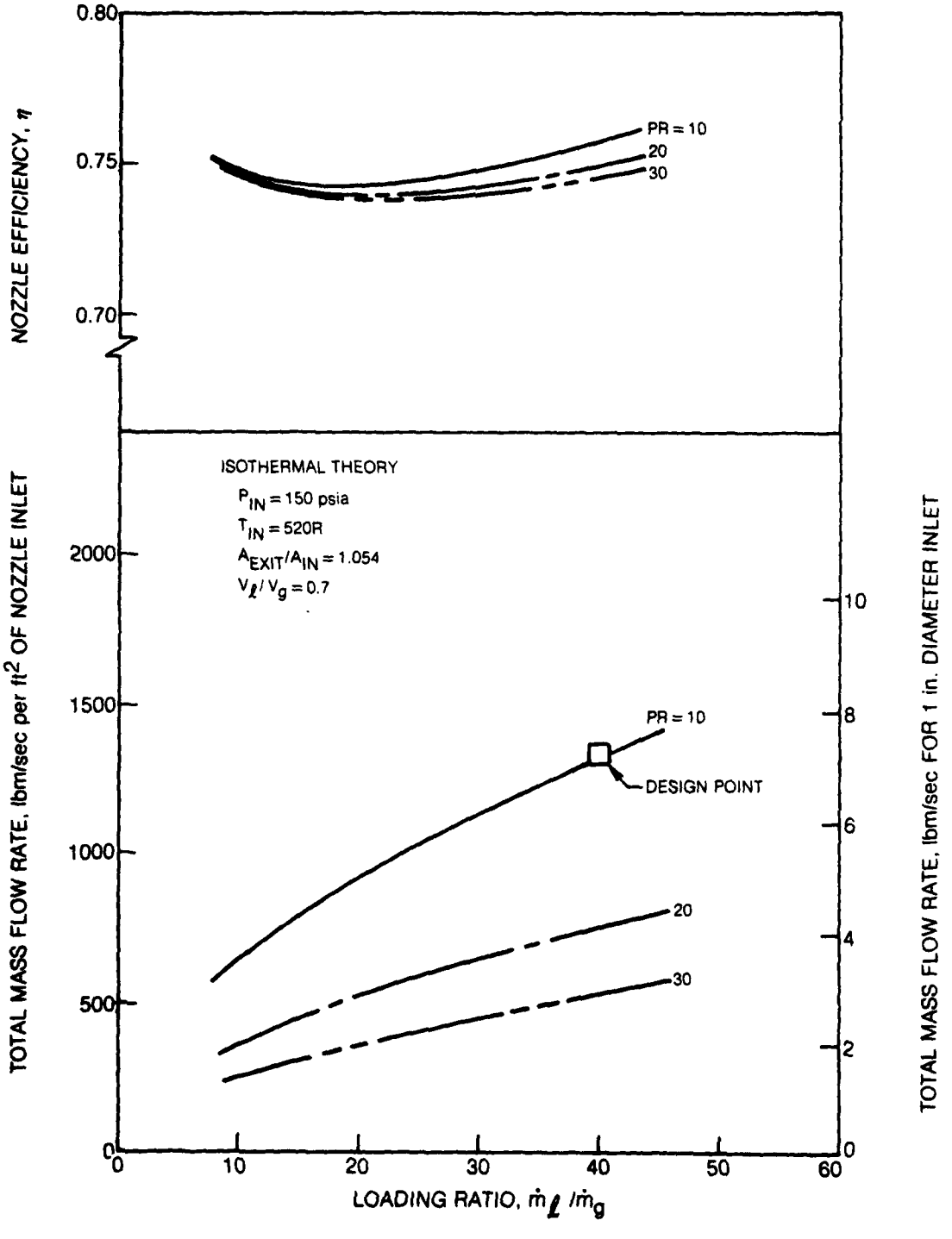

82-6-10-29

FIG. III.35

OFF-DESIGN NOZZLE PERFORMANCE AT CONSTANT EXIT PRESSURE

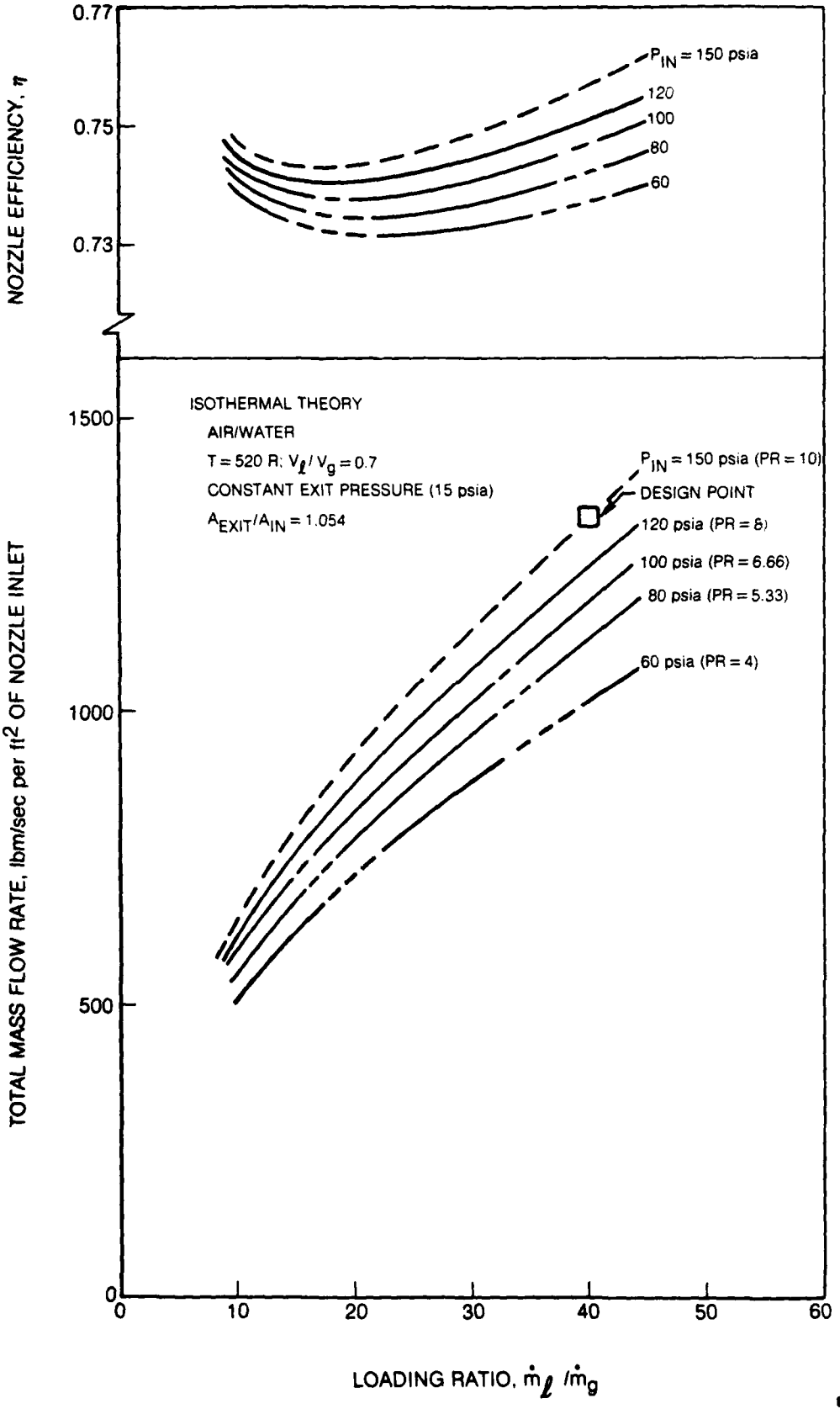

82-6-10-30

NOZZLE DESIGN FOR STEAM/DTA EXPERIMENTS

DESIGN CONDITIONS

P_{IN} = 600 psia; PR = 40

$T_{\ell})_{IN} = T_g)_{IN}$ = 960R

LOADING RATIO OF 40

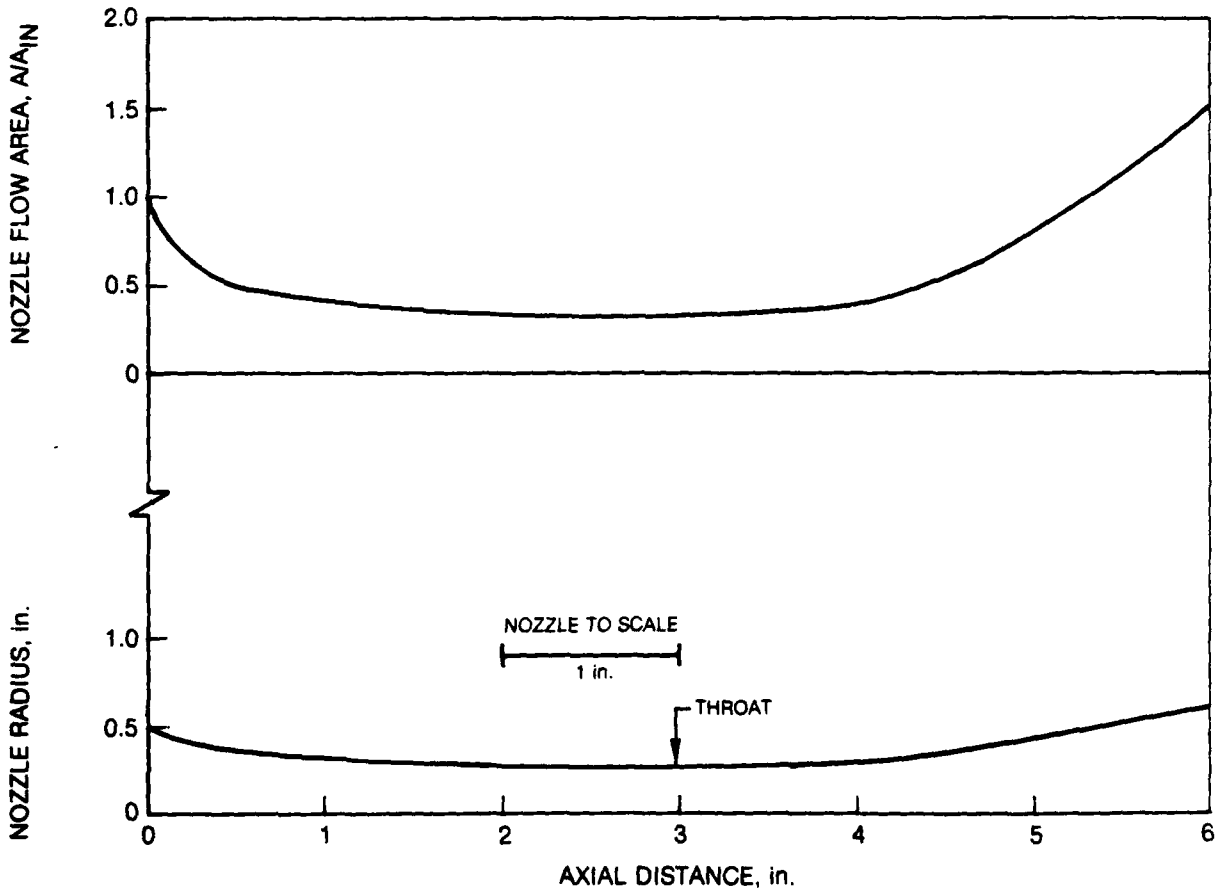

82-6-10-31

FIG. III.37

OFF-DESIGN PERFORMANCE OF STEAM/DTA NOZZLE

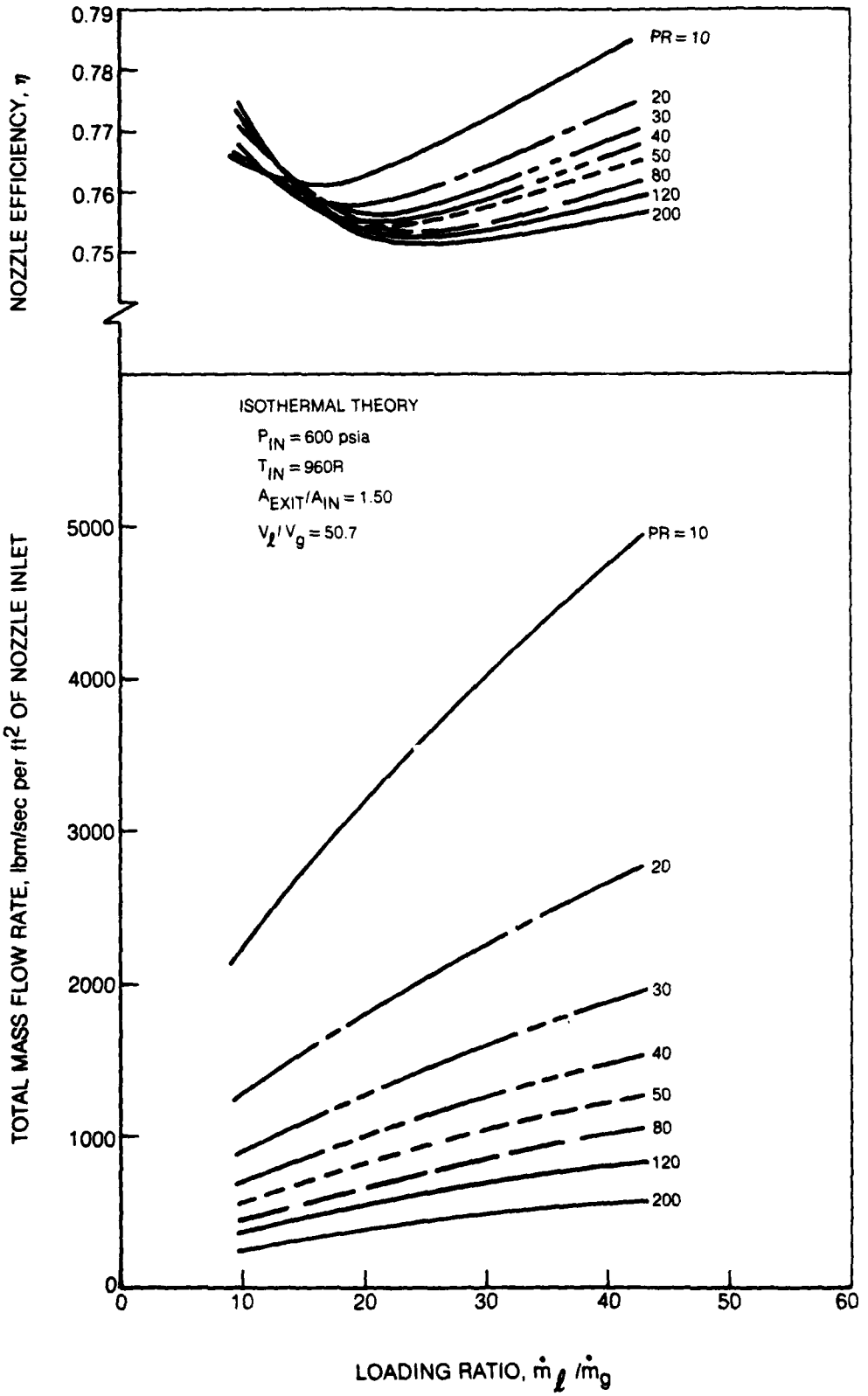

82-6-10-32

OFF-DESIGN PERFORMANCE OF STEAM/DTA NOZZLE

EFFECT OF INLET AND EXIT PRESSURES

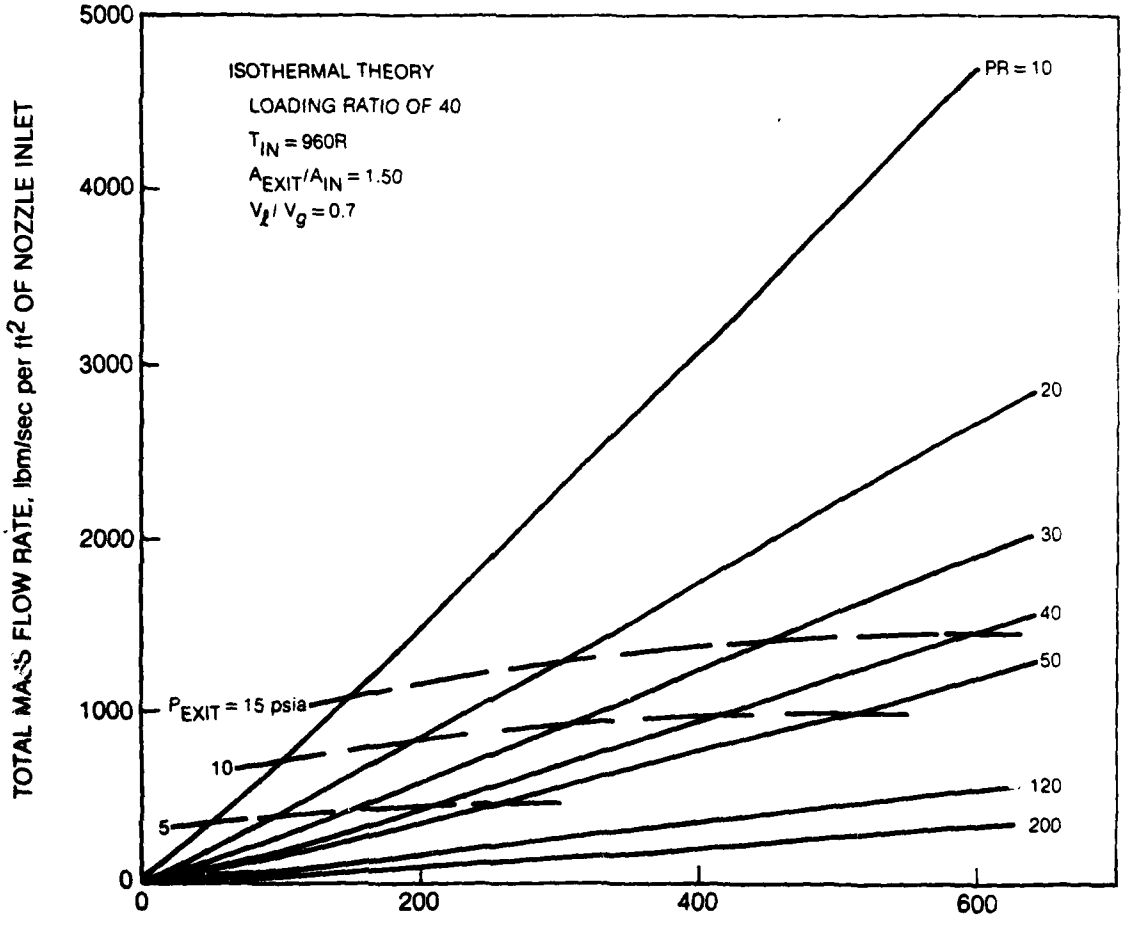

82-6-10-33

EFFECT OF NOZZLE EXIT PRESSURE ON GAS DENSITY AND VELOCITY

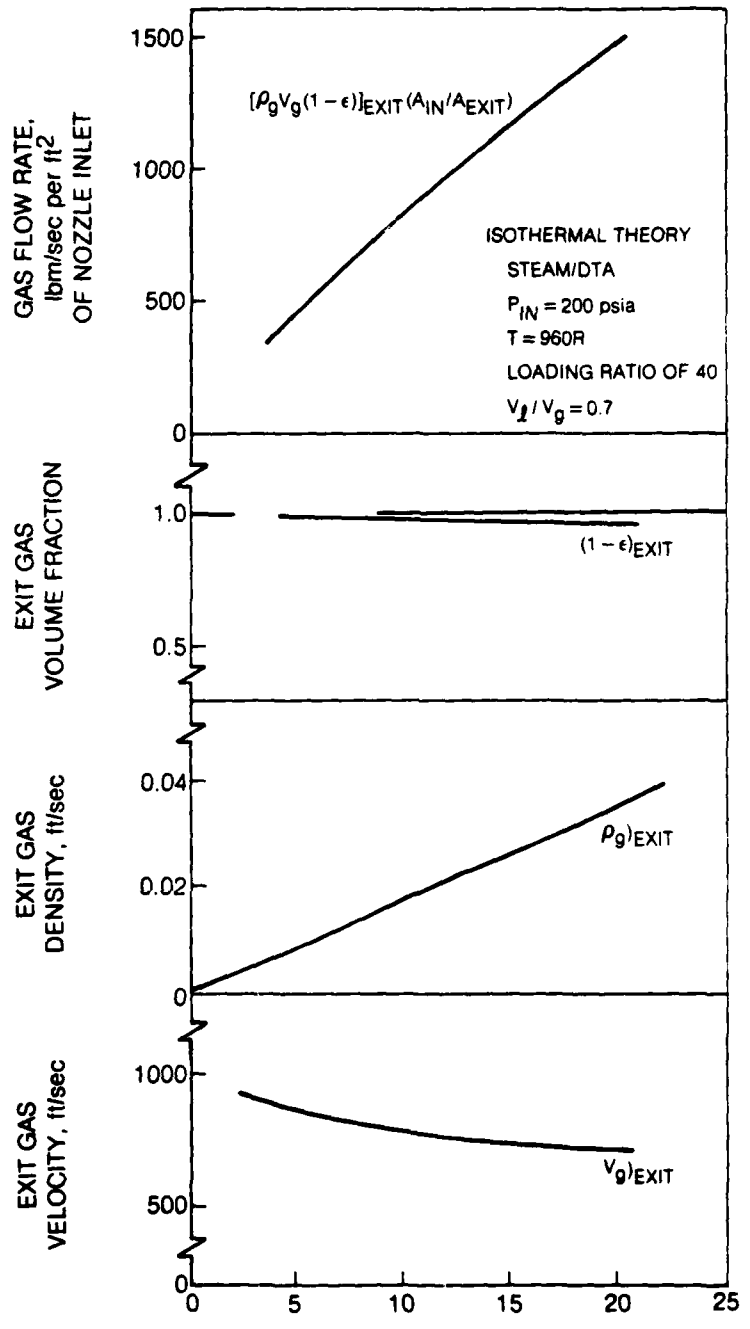

82-6-10-34

NOZZLE DESIGN FOR STEAM/DTA EXPERIMENTS

EXPONENTIAL PRESSURE PROFILE

DESIGN CONDITIONS

$P_{IN} = 600$ psia; PR = 40

$T_{\ell})_{IN} = T_{g})_{IN} = 960R$

LOADING RATIO OF 40

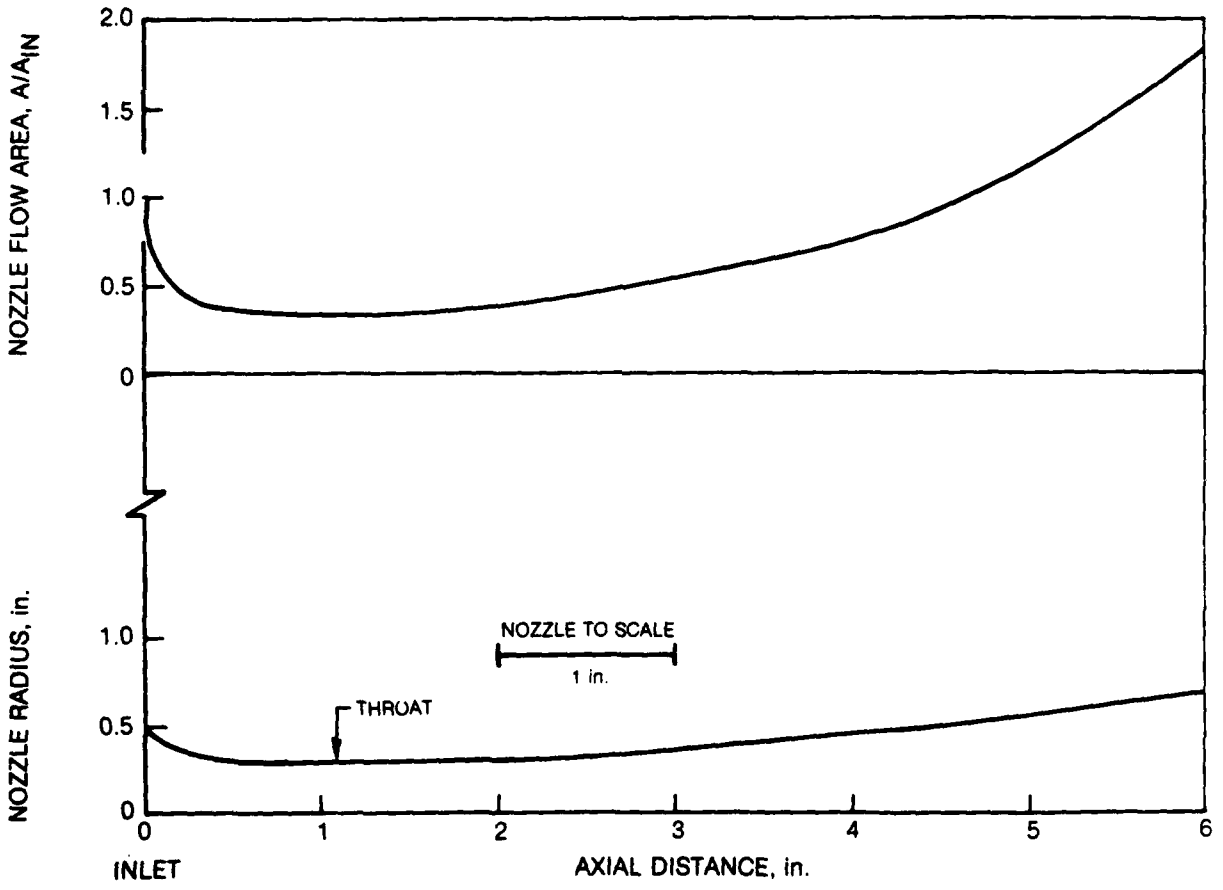

82-6-10-35

FIG. III.41

OFF-DESIGN PERFORMANCE OF EXPONENTIAL STEAM/DTA NOZZLE

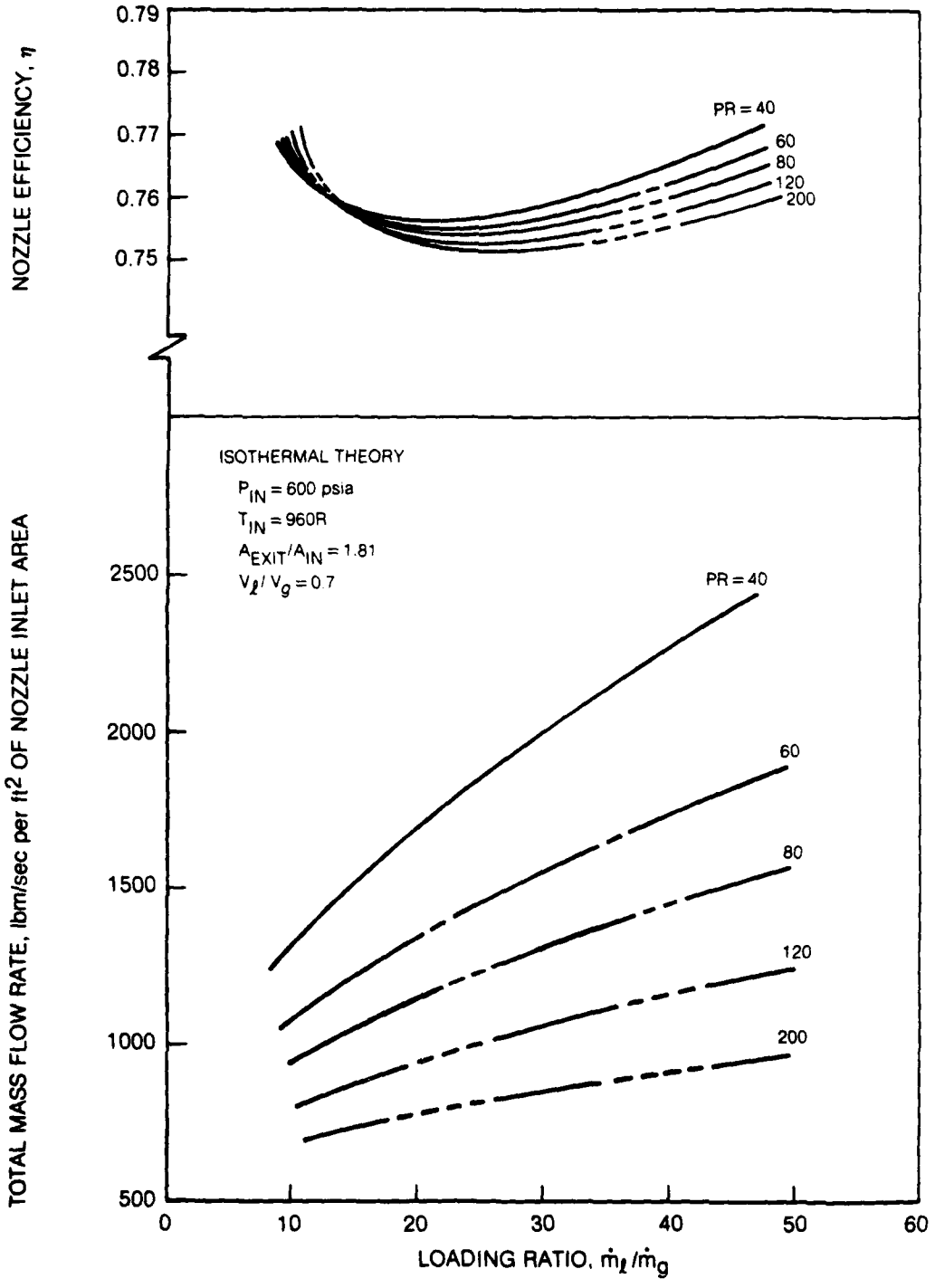

82-6-10-36

OFF-DESIGN PERFORMANCE OF EXPONENTIAL STEAM/DTA NOZZLE

EFFECT OF INLET AND EXIT PRESSURES

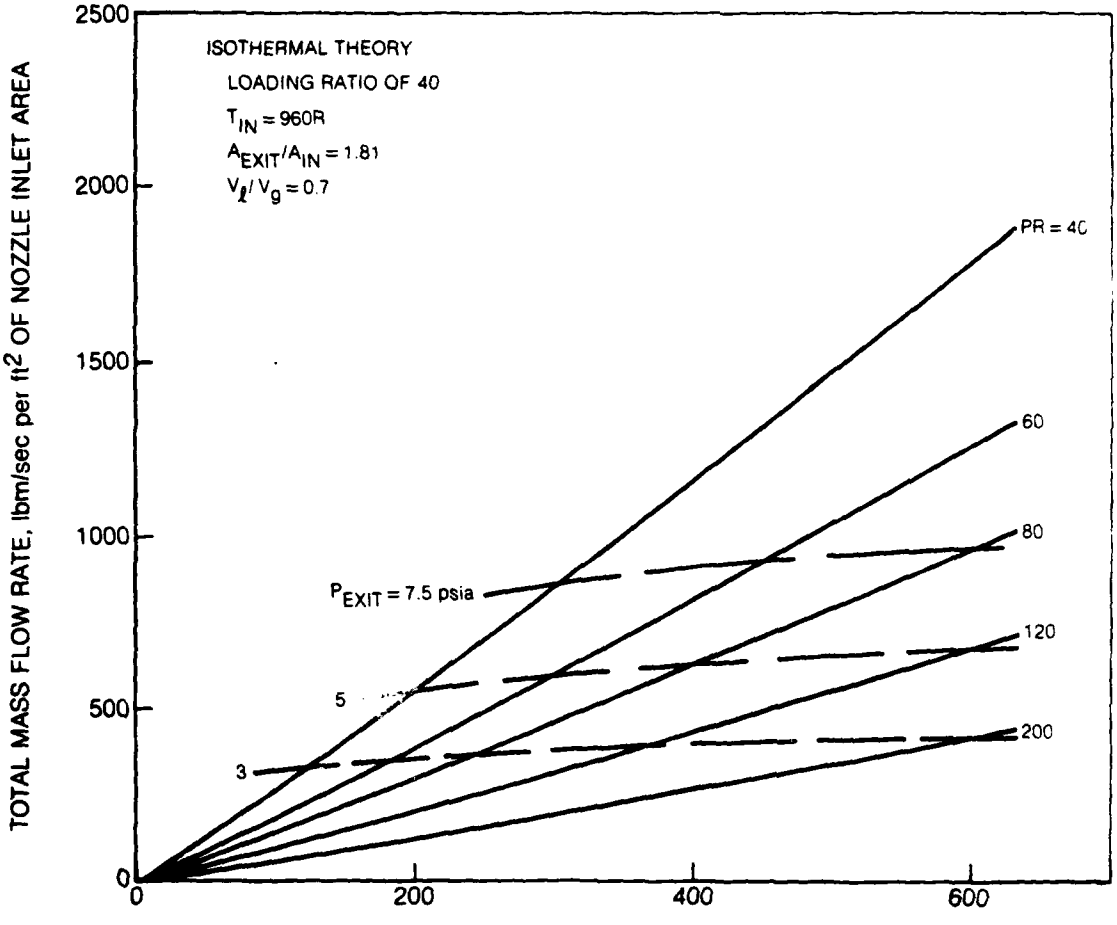

SCHEMATIC OF TEST RIG FOR AIR/WATER NOZZLE TESTS

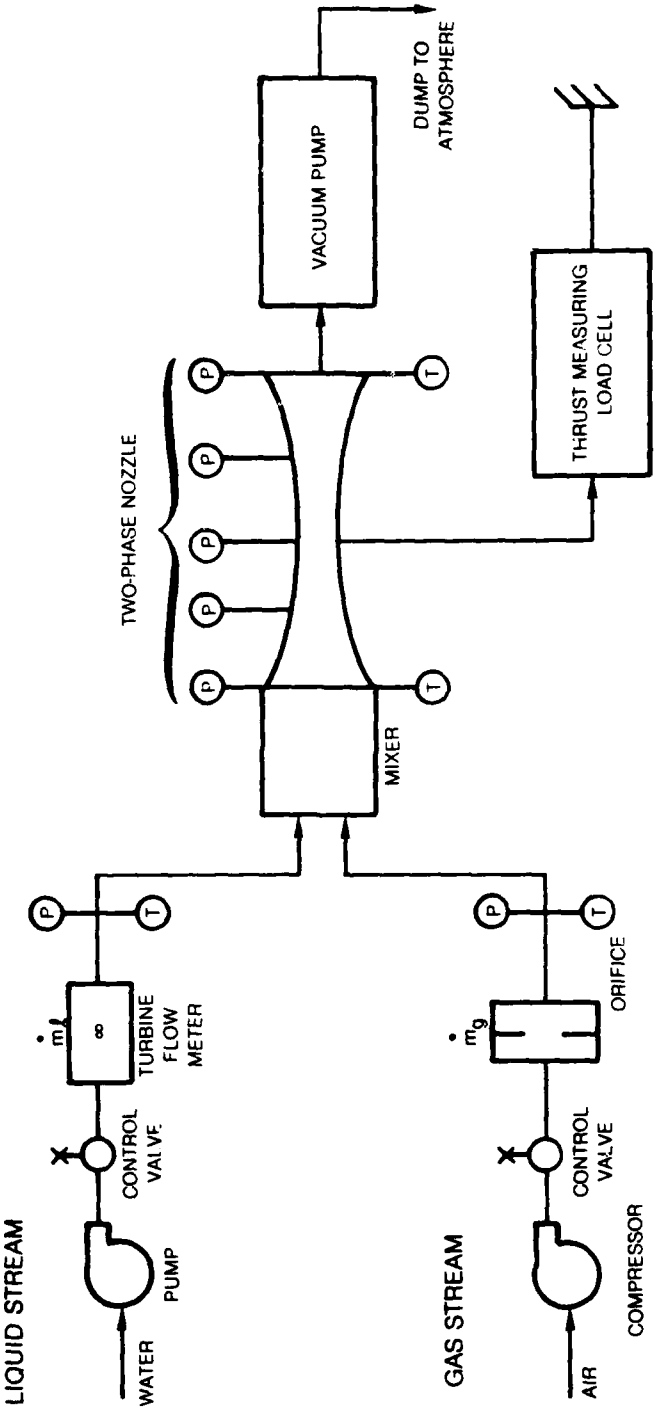

AD-A120 340 UNITED TECHNOLOGIES RESEARCH CENTER EAST HARTFORD CT F/G 13/10
TWO-PHASE NOZZLE THEORY AND PARAMETRIC ANALYSIS. PHASE III. OFF--ETC(U)
OCT 82 C W DEANE, S C KUO N00014-79-C-0344
UNCLASSIFIED UTRC/R82-955744-4 NL

2 OF 2
AD A
120340

END
DATE FILMED
11-82
DTIC

FIG. III.44

SCHEMATIC OF TEST RIG FOR STEAM/DTA NOZZLE TESTS

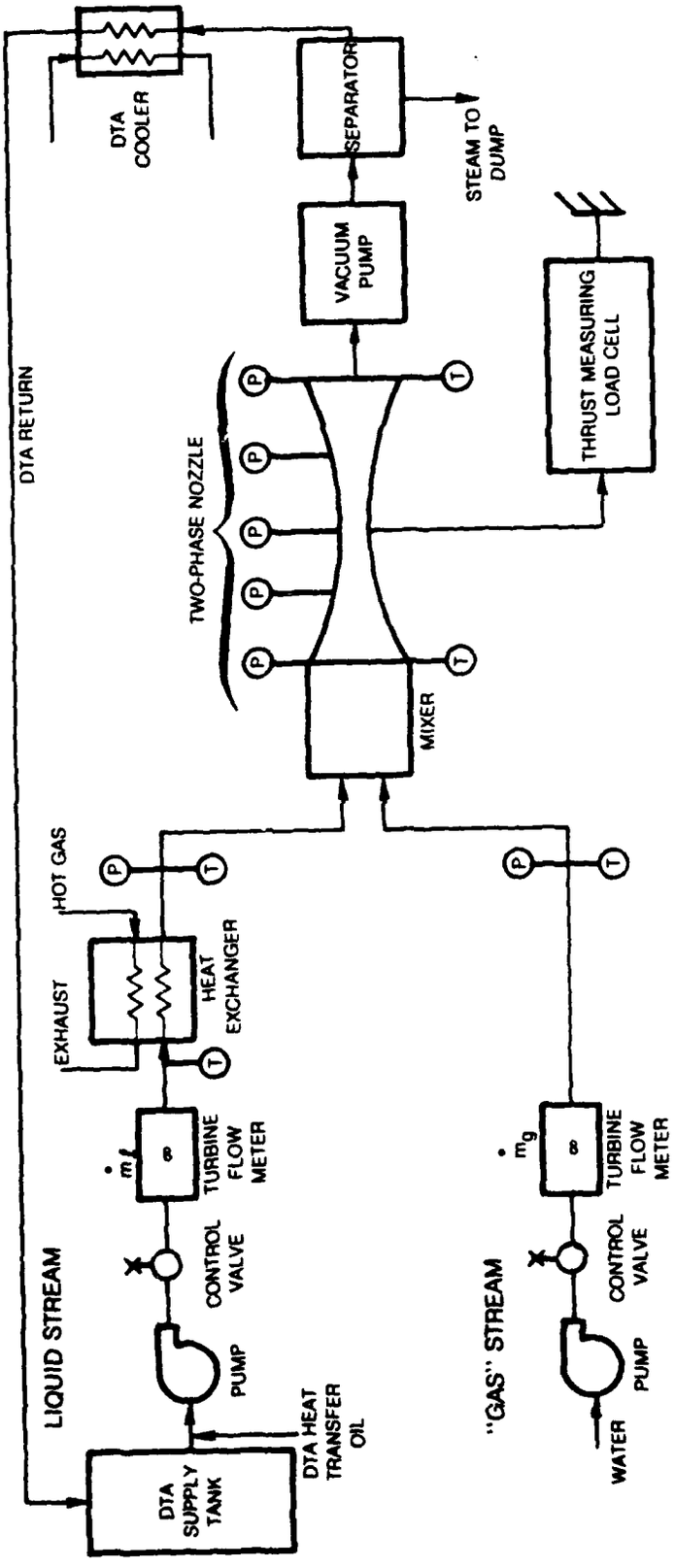

82-6-10-39

R82-955744-4

DISTRIBUTION LIST

TWO PHASE FLOW

	One copy except as noted
Mr. M. Keith Ellingsworth Power Program, Code 473 Office of Naval Research 800 N. Quincy Street Arlington, VA 22217	5
Defense Documentation Center Building 5, Cameron Station Alexandria, VA 22314	12
Technical Information Division Naval Research Laboratory 4555 Overlook Avenue SW Washington, DC 20375	6
Professor Paul Marto Department of Mechanical Engineering US Naval Post Graduate School Monterey, CA 93940	
Professor Bruce Rankin Naval Systems Engineering US Naval Academy Annapolis, MD 21402	
Dr. Al Wood Office of Naval Research Eastern/ Central Regional Office Bldg. 114, Section D 666 Summer Street Boston, Massachusetts 02210	
Mr. Mike Chaszeyka Office of Naval Research Branch Office 536 South Clark Street Chicago, Ill. 60605	

Mr. Charles Miller, Code 05R13
Crystal Plaza #6
Naval Sea Systems Command
Washington, DC 20362

Steam Turbines Branch, Code 5221
National Center #4
Naval Sea Systems Command
Washington, DC 20362

Mr. Ed Ruggiero, NAVSEA 08
National Center #2
Washington, DC 20362

Dr. Earl Quandt Jr., Code 272
David Taylor Ship R&D Center
Annapolis, MD 21402

Mr. Wayne Adamson, Code 2722
David Taylor Ship R&D Center
Annapolis, MD 21402

Dr. George Lea, Director
Fluid Mechanics Program
National Science Foundation
Washington, DC 20550

Mr. Michael Perlsweig
Department of Energy
Mail Station E-178
Washington, DC 20545

Professor J. A. C. Humphrey
Department of Mechanical Engineering
University of California, Berkeley
Berkeley, CA 94720

Professor Brian Launder
Thermodynamics and Fluid Mechanics Division
University of Manchester
Institute of Science & Technology
P088 Sackville Street
Manchester M601QD England

Professor Shi-Chune Yao
Department of Mechanical Engineering
Carnegie-Mellon University
Pittsburgh, PA 15213

Dr. Branko Leskovar
Electronics R&D Group
Lawrence Berkeley Laboratory
University of California
Berkeley, CA 94720

Dr. Ryszard Gajewski, Director
Division of Advanced Energy Projects
Office of Basic Energy Sciences
Department of Energy
Washington, DC 20545

Dr. David Elliot
NASA Jet Propulsion Laboratory
4800 Oak Grove Drive
Stop 67-201
Pasadena, CA 91103

Mr. Lance Hays, President
BiPhase Energy Systems
2800 Airport Blvd.
Santa Monica, CA 90405

Professor Paul A. Libby
Department of Applied Mechanics and Engineering Sciences
University of California San Diego
P.O. Box 109
La Jolla, CA 92037

Professor C. Forbes Dewey Jr.
Fluid Mechanics Laboratory
Massachusetts Institute of Technology
Cambridge, Massachusetts 02139

Professor Warren Rohsenow
Mechanical Engineering Department
Massachusetts Institute of Technology
77 Massachusetts Avenue
Cambridge, Massachusetts 02139

Professor A. Louis London
Mechanical Engineering Department
Bldg. 500, Room 501B
Stanford University
Stanford, CA 94305

Professor T. N. Veziroglu
Clean Energy Research Institute
University of Miami
Coral Gables, Florida 33124

Professor Daryl Metzger
Chairman, Mechanical and Energy
Systems Engineering
Arizona State University
Tempe, Arizona 85281

Professor T. H. Gawain
Department of Aeronautics
Naval Postgraduate School
Monterey, California 93940

Dr. J. E. Minardi
University of Dayton
Research Institute
Dayton, Ohio 45469

Professor Frank E. Marble
Mail Code 205-45
California Institute of Technology
Pasadena, California 91125

Dr. Oscar Manley
Div. of Engineering, Math., & Geo-Sciences
US Department of Energy
Washington, DC 20545


MEL
8